Imperial College London

Department of Bioengineering

Neuroepithelial signalling of tactile stimulus in the human hair follicle

Julià Agramunt

Supervised by Claire A. Higgins and Andrei S. Kozlov

Submitted in part fulfilment of the requirements
for the degree of Doctor of Philosophy at
Imperial College London, January 2022

I hereby declare that this thesis and the work reported herein was composed by and originated entirely from me. Information derived from the published and unpublished work of others has been acknowledged in the text and references are given in the list of sources.

Julià Agramunt (2022)

The copyright of this thesis rests with the author and is made available under a Creative Commons Attribution Non-Commercial No Derivatives licence. Researchers are free to copy, distribute or transmit the thesis on the condition that they attribute it, that they do not use it for commercial purposes and that they do not alter, transform or build upon it. For any reuse or redistribution, researchers must make clear to others the licence terms of this work

Abstract

Touch relies upon the most intimate of our senses. It enables us to feel our surroundings, to feel pleasure or pain and to interact with our loved ones. The hair follicle (HF) is an important mediator of touch perception innervated by low-threshold mechanoreceptors (LTMRs), a diverse group of tactile sensory neurons forming lanceolate and circumferential endings around the follicle. In this thesis I used a combination of immunofluorescent and microscopy approaches, combined with electroanalytical methods to evaluate the role of the HF epithelium in touch perception. I found that terminal human HFs are innervated by 5 different types of these neurons in the outer root sheath (ORS) where the HF epithelium has its stem cell niche. HF epithelial cells are capable to respond to tactile-like stimulus by activation of mechanosensitive ion channel, once activated, ORS cells are able to send signalling molecules such as ATP, serotonin and histamine to surrounding LTMRs. Using pharmacology to block specific histamine and serotonin receptors, LTMRs diminishes their response, suggesting that ORS cells can activate neurons using these neurotransmitters after tactile-like stimulus. Comparing to skin keratinocytes, both cell types can release histamine but interestingly, only ORS cells release serotonin. These results suggest that the HF epithelium is a special niche in the way it responds to tactile-like stimulus. Overall, these results are the first stone to investigate the relationship between ORS cells and LTMRs in touch perception.

Acknowledgements

Claire, thanks for your support and your advice all those years, for your patience with me. I was not the easiest student to supervise but you always trusted my abilities. I have grown professionally and personally at your side. Andrei thanks for your brilliant advice and your different, creative thinking in doing science, I learn from you that there's always different ways in doing things.

Thanks to Dr. Parry Hashemi and her lab members Melissa Hexter, Brenna Parke and Sergio Mena for their help and during FSCV experiments. It has been great experience to collaborate with you all.

Thanks to Leigh Knight, P&G and EPSRC who trusted in my project and fund it. Without your generosity the work I have done would not have been possible

Thanks for all Higgins and Kozlov lab member along these years. Specially thanks to you, Magda. What to say... All these years with you have been very special, thanks for the parties, the drinks, for the amazing life we had outside imperial. Thanks for being my companion in doing all these mad things we did together hehe. Our time together has shaped me as person.

Thanks to all the people I met along these 4 years and still on my side: Carmel, Melissa, Wayne, Will, Elena, Davide, Patri, Nacho, Jabi, Ismael, Filip, Olivia, Ben, Victor, Vivian, Gema, Ed, Lucia, Alice, Nuria, Davide, Emmalou, Alexandra, Fiona, Marta, James, Rita, Mike, Felix, Jack, Amber, Charlie, Shaun, Serena, Sihao... I truly love you all.

Per tota la meva família de Barcelona, Ja ho sabeu, estic aquí gràcies vosaltres: Carla, Manu, Rosa, Gispill, Ana, Faifa, Mike, Arantxa, Anna, Eva, Alexandra. La família es la família, us estimo. Per últim, I potser el mes important, gracies als meus pares per tot i a la meva àvia per confiar en mi I ajudar-me sempre que ha fer falta. Us estimo.

To everyone, to all of you I have met during my PhD,

I will keep something far bigger than knowledge after these years

xx

Contents

List of Abbreviations

1. General Introduction

1.1 Hairs and the HF: significance for biology and neuroscience…….12

1.2 HF morphology and cycling…….14

1.4 The somatosensory system……...16

1.4.1 Three levels of organization……..18

1.4.1.1 The periphery: LTMRs and HTMRs, first order neurons processing touch and pain……18

1.4.1.2 The Spinal Cord: the dorsal horn…….19

1.4.1.3 The Brain: the brainstem and the somatosensory cortex…….20

1.5 Touch and clinical considerations……..22

1.6 LTMRs: fibre diameter and cell bodies: fast, medium and slow conduction velocities….24

1.7 LTMRs and adaptation rates: slow and rapid……..25

1.8 LTMRs and end organs in the skin……...27

1.8.1 LTMR end organs in both hairy and non-hairy skin……...28

1.8.2 LTMRs and end organs non hairy skin ……28

1.8.3 LTMRs and end organs in hairy skin…….30

1.9 HTMRs, first order neurons processing pain with specific end-organs……...34

1.10 Identification of HF LTMRs and HTMRs……..36

1.11 HF neuronal interactions ……..37

1.11.1 Neurotrophic interactions in the HF bulge…….37

1.11.2 Bulge-structural support of HF innervation…….. 40

1.11.3 Neurotransmitter signalling in the HF bulge …….41

1.12 Mechanotransduction of touch sensation ……..42

1.12.1 Mechanosensitive ion channels in touch perception ……42

1.12.1.1 TRP channels in touch sensation ……..43

1.12.1.2 Piezo channels ……43

1.12.2 Ion channel activation mechanism ……44

1.13 Mechanotransduction in HF LTMRs ……..45

1.13.1 Mechanotransduction in the Merkel cell neurite complex ……..46

1.14 Mechanotransduction in the epidermis: keratinocytes as tactile receptors ……48

1.15 The human HF as a novel perspective for touch signalling..……50

1.16 Comparison between human and mouse hairy skin innervation…….. 51

1.17 Aims…….52

2. Experimental (Material and Methods)

2. 1 Samples…….53

2.1.1 Human samples……...……53

2.1.2 Animals……..53

2.2 Immunolabelling……53

2.3.1 Immunolabelling of tissue sections……53

2.3.2 Immunocytochemistry…….54

2.3.2 Immunocytochemistry…….54

2.3 Culture of primary cells……56

2.3.1 Keratinocytes……56

2.3.2 HF epithelial cells……...57

2.3.3 DRG and TG neurons extraction and culture……..58

2.3.4 Co-culture between human ORS cells and murine DRGs/TGs……...59

2.4 Calcium dynamics experiments ……59

2.4.1 Calcium transients after tactile-like stimulus with ORS cultures……..……59

2.4.2 Calcium dynamics experiments with ORS-DRG co-cultures……61

2.6 Fast-scan cyclic voltammetry with tactile stimulus in ORS cultures……..…….63

2.6.1 Experimental set-up and tactile stimulation……..62

2.6.1 Data acquisition……63

2.6.2 Current-concentration transformation……...63

2.7 qPCR…….64

2.8 Image analyses and data processing……...64

2.9 Statistical analyses…….65

3. Results

3.1 Humans have morphologically and molecularly distinct mechanoreceptors innervating terminal HFs. ……66

3.1.1 Revealing the morphology of LTMRs and HTMRs innervating human HFs……. 66

3.2 Human HFs are innervated by different types of LTMRs ……77

3.2.1 Circumferential Aβ-Field-LTMRs ……78

3.2.2 Merkel cell neurite complex ……...79

3.2.3 Longitudinal Aβ-RA-LTMR ……..…….80

3.2.4 Longitudinal Aδ-RA-LTMR ……80

3.2.5 Longitudinal C-LTMR ……..……..83

3.3 Human HFs are innervated by a type of HTMRs ……85

3.3.1 Circumferential Aδ-HTMRs ……85

3.4 Localization of LTMRs within the human HF…… 86

3.5 LTMRs innervate multiple follicles ……93

3.5 ORS cells are mechanosensory cells ……..94

3.6 Activated ORS cells transmit stimulus to LTMRs…… 101

3.6.1 Tactile activated ORS cells release an unknown molecule which activates LTMRs. ……..105

3.6.2 Tactile activated ORS cells employ ATP to activate LTMRs…….. 106

3.7 FSCV reveals that Tactile activated ORS cells release serotonin and histamine after tactile like stimulus ……..109

3.8 FSDV reveals skin keratinocytes show a different releasing profile after mechanical stimulus compared to ORS cells ……116

3.9 Mirtazapine incubation changes LTMRs responses after ORS cells activation…….. 118

4. Discussion

4.1 Human HF innervation ……122

4.2 ORS as a novel mechanosensitive cell in the human HF. ……123

4.3 Novel interaction between ORS-LTMRs for tactile stimuli ……124

4.4 Considerations for pleasant touch and serotonin release…….. 125

5. Future Directions ……..127

6. References ……128

7. Appendix ……145

List of Abbreviations

Aβ-RA-LTMR: Aβ rapid adapting low threshold mechanoreceptor

Aδ-RA-LTMR: Aδ rapid adapting low threshold mechanoreceptor

Aδ-HTMRs: Aδ high threshold mechanoreceptors

5HTR2: 5-Hydroxytryptamine (serotonin) 2A receptor

5HT2A: serotonin receptor 2A

5HTR3: 5-Hydroxytryptamine (serotonin) 3A receptor

5HT3A: serotonin receptor 2A

AMPA: α-amino-3-hydroxy-5-methyl-4-isoxazolepropionic acid

APM: arrector pili muscle

ASD: autism spectrum disorder

ATP: adenine triphosphate

ANOVA: analysis of variances

B2AR: beta 2 adrenergic receptor

BABB: denzyl alcohol/ Benzyl benzoate

C-LTMR: C low threshold mechanoreceptor

CGRP: calcitonin gene related product

Ch: cuticle of the hair shaft

Ci: cuticle

Co: cortex of the hair

Cp: companion layer

DEG/ENaC: degenerins and epithelial amiloride-sensitive Na+ channel

DMEM: Dulbecco's Modified Eagle Medium

DMSO: dimethyl sulfoxide

DNA: deoxyribonucleic acid

DP: derma papilla

DRG: dorsal root ganglion

ECM: extracellular matrix

EGFL6: EGF Like Domain Multiple 6

ER: endoplasmic reticulum

FSCV: fast scan cyclic voltammetry

GFP: green fluorescent protein

Gli1: GLI Family Zinc Finger 1

GluR1: glutamate receptor 1

H1: histamine receptor 1

HF: hair follicle

HBSS: Hans balances salt solution

HFSC: HF stem cells

HTMR: high threshold mechanoreceptor

IRS: inner root sheath

KO: knock out

LTMR: low threshold mechanoreceptor

MRGPDR: MAS Related GPR Family Member D

NA: noradrenaline

NFH: neurofilament heavy

NMDA: N-methyl-D-aspartate

NT: neurotrophin

NP: neuropathic pain

NT3: neurotrophin 3

NT4: neurotrophin 4

NTs: neurotrophins

ORS: outer root sheath

P1: purinergic 1 receptor

P2X: P2X purinergic receptor

P2X3: P2X2 purinergic receptor

PBS: phosphate buffered saline

PFA: paraformaldehyde

PLSR: partial least squares regression

RNA: ribonucleic acid

RT: room temperature

RT-PCR: real time polymerase chain reaction

SD: standard deviation

SEM: standard error of the mean

SERCA: sarco/endoplasmic reticulum Ca2+-ATPase,

siRNA: small interference RNA

SP: substance P

TG: trigeminal ganglion

TH: tyrosine hydroxylase

TrkA: tropomyosin receptor kinase A

TrkB: tropomyosin receptor kinase B

TrkC: tropomyosin receptor kinase C

TRP: transient receptor potential channel

TRPV1: transient receptor potential channel vanilloid 1

TSC: terminal Schwann cell

VPL: ventral posterolateral nucleus

1.General Introduction

1.1 Hairs and the HF: significance for biology and neuroscience.

The HF is a complex dynamic structure present in the skin of all mammals. The main function of the follicle is the production of hairs, that in humans, cover 90% of the body[1]. From a human perspective, hairs have become a cornerstone in cultural pertinence. Hairs are personal symbols associated to age, religion, and social status. Wherever a person is waxed, shaved or has a peculiar hairstyle, that expression of hair plays an important manifestation of this person as an individual in society[2]. From a more biological perspective, HFs have many functions, such as thermoregulation, sweat production and skin protection[3].

For example, the ability of some mammals such as polar bears or wolves to live in low temperature environments is possible because of their fur, which creates an isolated mass of air at viable temperatures[4]. In primates, vellus hairs are believed to have a protective function transmitting movements of ectoparasites and other potential undesired contacts through the body. In humans, eyelashes are important in protection of the eyes, keeping away sweat, dust and dirt. Eyebrows, also fulfil these functions and are important tools for non-verbal communication. Sadness and happiness can be inferred by eyebrow position and for deaf individuals, eyebrows movement is an important component of sign language[5]. Finally, hairs, and more importantly the HF itself, are key players in touch sensation[6]. Although the sensory capabilities of the HF have remained elusive for decades, recent research has started to show that HFs are important touch receptors and that their involvement in mediating social interactions is vast. Stimulation of hairs has been linked to sexual arousal and as a maternal bond mediator. Skin stroking reduces anxiety, improves breathing, and comfort us[7,8]. Stroking is most effective way to calm a new-born or to console a relative after a tragic event.

How does this happen? How are such heterogenous capabilities observed in such a small and relatively simple organ like the HF.

The common point of all these capabilities relies in that the HF is able to transduce and process the diverse tactile forces that mediate these behaviours. The sensitivity of hairs to tactile forces has been evident for ages, but it hasn't been until recently that this capacity has been justified scientifically. HFs are the most innervated structures in the human body[9]. Investigations with murine models has shown that HFs are highly innervated by a heterogeneous group of sensory neurons which form a complex neural network with designated morphology around the follicle. Up to now, several types of these neurons have been discovered. This heterogenous innervation has helped us to understand why the follicle is able to mediate all these different functions. However, this ability of process tactile stimulus has been always attributed to the sensory neurons but never to other HFs cells. Recently, the Merkel cell neurite complex, an association between an epithelial cell and a sensory neuron, has been shown to mediate some tactile functions. However, some investigations point out that other cells types in the follicle such as epithelial cells can also contribute processing of tactile stimulus[10].

Following up on these ideas and motivated by my strong interest in neuroscience and in skin biology, in this body of work I used a combination of immunolabeling, calcium dynamics, electroanalytical and molecular techniques on in vitro and ex vivo preparation of human HFs, to better understand which components of the follicle are involved in making the HF one of the most exquisite sensory receptors in the human body.

1.2 HF morphology and cycling

The human HF can be subdivided into different parts organized from the top surface of the skin until the deep layer connected to the dermis: infundibulum, isthmus, bulge, suprabulb and bulb respectively[11]. If we take as reference the concentric layers that compose the HF, it can be further subdivided into the hair shaft composed by the cortex hair cuticle and medulla and by the follicle composed by 2 differentiated clusters of cells; the inner root sheath (IRS) and the outer root sheath (ORS), separated by the companion layer **(Figure 1.1).**

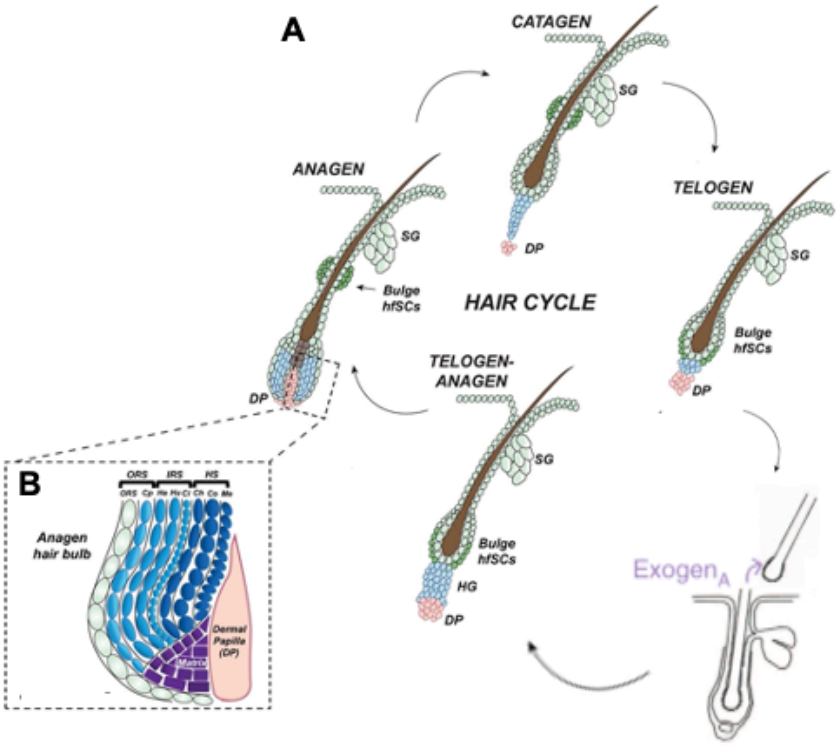


Figure 1.1. HF cycling stages and composition.
(A) In anagen, HF is in its growing phase. Signalling from the dermal papilla (pink) activate bulge HFSCs which promote HF and shaft growth. When the follicle enters catagen, the regression state, signalling from the DP stops and the hair stop growing and bulge HFSCs start to enter a quiescent state. Finally, in telogen, the hair enters the resting states where the bulge HFSCs remains dormant. After telogen, the hair shaft is ready to fall. In exogen, the hair fibre is actively released from the follicle. After the hair fibre has fallen, the hair cycle starts again in anagen, reactivating the DP and therefore the HFSCs which give rise to a new hair shaft (B) The HF is composed by different cell types organized in different layers. The outer root sheath (ORS) is composed by the ORS itself and the companion layer (Cp). The inner root sheath (IRS) is composed by the Henle's layer (He), the Huxley's layer (Hu) and the cuticle (Ci). Finally, the hair shaft is composed by the cuticle of the hair shaft (Ch), the cortex of the hair (Co) and the medulla (Me)[11].

A follicular region termed the bulge, which is found within the ORS, has been broadly investigated because of its composition in stem cells[12]. Molecular signalling from the dermal papilla located in the HF bulb stimulates HFSC permitting cellular proliferation and therefore hair growth[13,14]. There are 2 main stem cell types in the bulge region of the HF: melanocyte and epithelial stem cells. Melanocyte stem cells derive from the neuronal crest and their main physiological function is to give pigment to the hair shaft. During anagen, bulge resident melanocyte stem cells start to difference into melanocytes and move towards the hair matrix where they produce melanin to give pigmentation to the hair shaft[15]. On the other hand, epithelial stem cells or HF stem cells (HFSC) or bulge stem cells form an undifferentiated group of quiescent keratinocyte-like cells[11].

The HF cycle through different phases: anagen as the growing phase, catagen as the regression phase, telogen as the resting phase and finally exogen as the process when the hair fibre is released from the follicle.[4,16,17]. The main function of the hair cycle is to produce a new hair shaft, however, in this process, research in mice has also shown that while cycling, the follicle undergoes changes in its innervation patterns. While the isthmus and the bulge are the most innervated areas, those suffer dramatic change in the amount of innervating nerve fibres between HF cycling stages. Fibres increase in early anagen and peak in anagen. In telogen and catagen the amount of nerve fibres decrease therefore, anagen HFs are the most innervated[18–20].

Hairs have important functions, and their physiology is complex and dynamic. Among them, one of the most important functions of the follicle is mechanosensory perception. The nerves that are associated with the HF are part of the somatosensory system which gives the HF its sensory capabilities.

1.4 The somatosensory system

The somatosensory system -from the Greek *soma* (body)- gives organisms the ability to process physical, thermal and chemical changes inside and outside the limits of the body. It was the first sensory system to be studied experimentally and is the first sensory system to arise in mammalian development[21]. In humans, about 50 days after gestation, tactile receptors start to innervate lips and nose, and after 17 weeks, is it possible to find tactile receptors all over the unborn baby[22]. Somatosensation, however, is far broader than touch. The somatosensory system is involved in encoding several heterogeneous modalities: kinesthesis of the body, interoception of viscera and exteroception of the outer physical environment. This is possible because the receptors of the somatosensory system compose a highly heterogenous group of sensory neurons located in the trigeminal (TG) and dorsal root ganglion (DRG)[23]. Single-cell RNA transcription profiling in mouse DRG has identified 13 different types of sensory neurons with specific molecular origins **(Figure 1.2)**[24]. It is believed that 11 of them are involved in responding to touch, pain, or both. In this way, the mammalian sense of touch is the most heterogeneous and complex sensory system regarding its receptors.

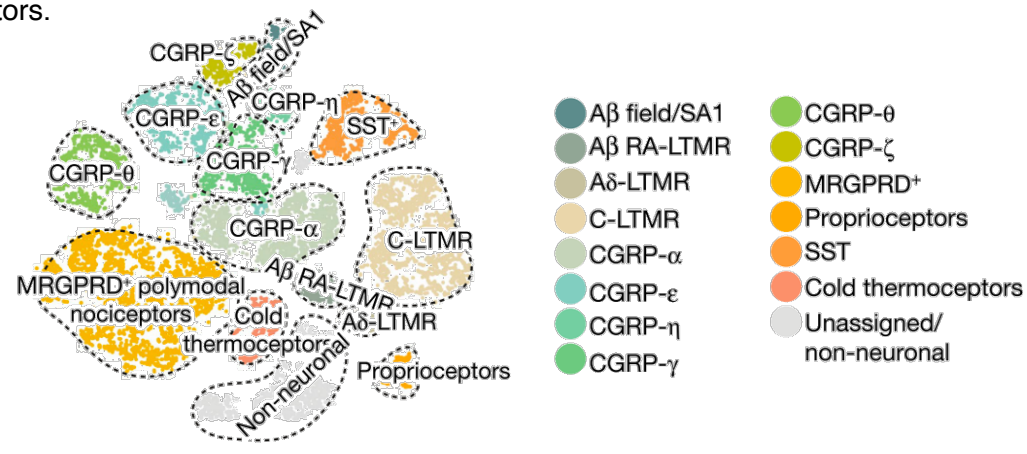


Figure 1.2. Distributed stochastic neighbour embedding of DRG single cell RNA sequencing data from mouse.
Different types of somatosensory neurons in the murine DRG: Aß field/SA1, Aß RA-LTMR, Aδ- LTMR and C-LTMR composing sensory neurons processing tactile information, CGRPs composing peptidergic nociceptors and MRGPRD+ composing polymodal nociceptors[23].

Because of the scope of this thesis, I will focus on describing the sensory neurons associated with the HF which are involved in processing light touch and mechanical pain. Decades of research have made it possible to depict the pathways within the somatosensory system which convey tactile and pain information from the periphery to the brain. The dorsal column medial lemniscal system conveys tactile stimulus whereas the anterolateral system conveys pain stimulus **(Figure 1.3)**[25]. In the next section I will deconstruct how the sense of touch is processed in the different compartments of this pathway, from the periphery to the brain.

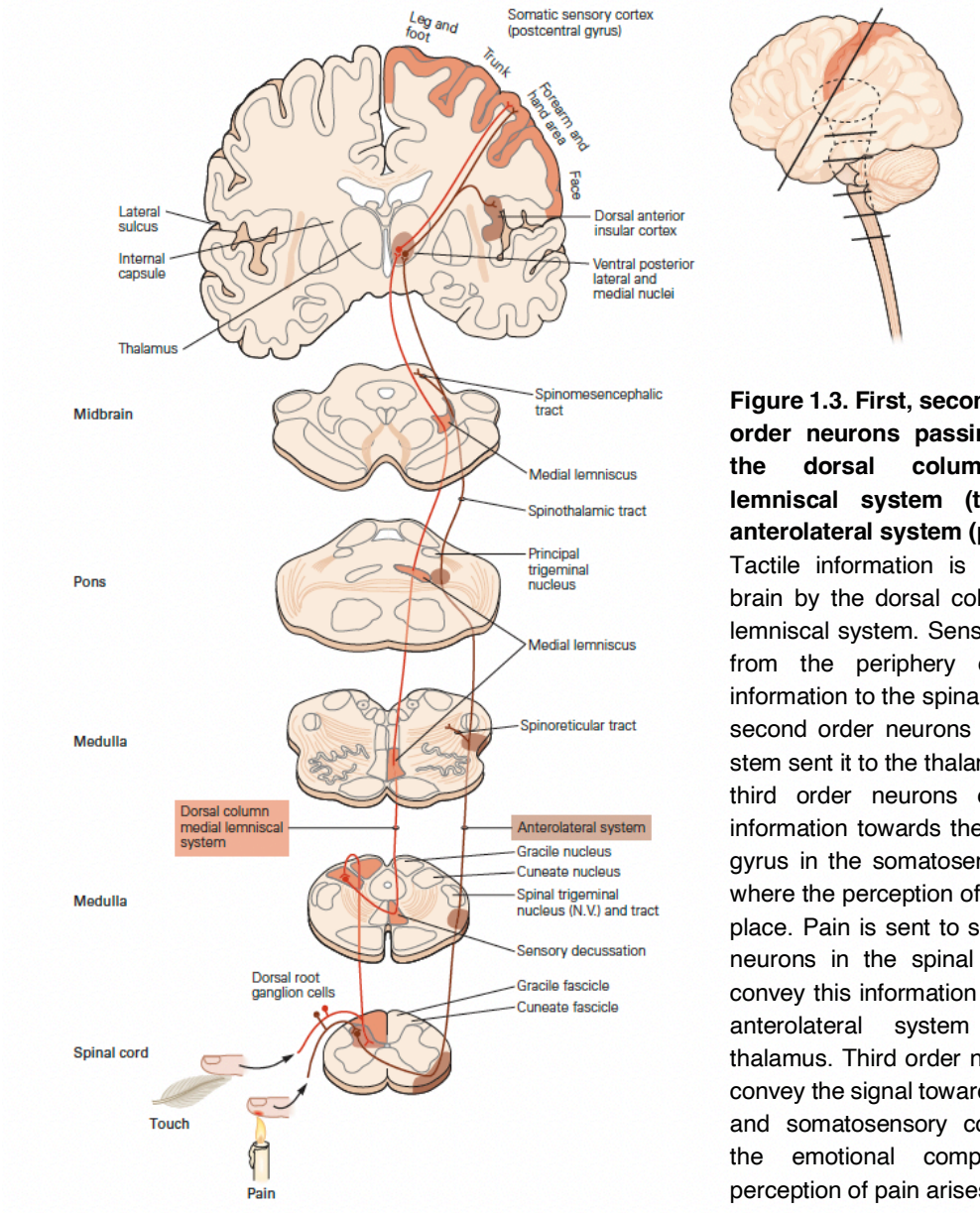


Figure 1.3. First, second and third order neurons passing through the dorsal column medial lemniscal system (touch) and anterolateral system (pain).
Tactile information is sent to the brain by the dorsal column medial lemniscal system. Sensory neurons from the periphery convey the information to the spinal cord where second order neurons in the brain stem sent it to the thalamus. Finally, third order neurons convey this information towards the postcentral gyrus in the somatosensory cortex where the perception of touch takes place. Pain is sent to second order neurons in the spinal cord which convey this information towards the anterolateral system until the thalamus. Third order neurons sent convey the signal towards the insula and somatosensory cortex where the emotional component and perception of pain arises[20].

1.4.1 Three levels of organization

Broadly, the nervous system is organized in 2 main parts: the central and the peripheral nervous systems. The central nervous system compromises the brain and the spinal cord and the peripheral nervous system the nerves and ganglia which innervate the body[21]. Across the dorsal column medial lemniscal system, from the periphery until the brain, input signals travel along 3 different neurons[26]. Therefore, the somatosensory system is organized in neurons based in specific locations: first, second and third order neurons[27]. Moreover, each of these neurons are believed to mediate different functions within the sensory pathway. First order neurons are located between the skin and the spinal cord. They compromise the first receptors that detect tactile stimulus and transmit the information to the spinal cord. Second order neurons are located between the spinal cord and the brainstem. These neurons send the information towards the thalamus and the brainstem. Third order neurons project the signal from the thalamus to the somatosensory cortex where the final representation of tactile stimulus occurs[28]. In the following section, I will go through the different somatosensory system compartments to understand how it is organized and how its information is processed.

1.4.1.1 The periphery: LTMRs and HTMRs, first order neurons processing touch and pain

Low threshold mechanoreceptors (LTMRs) and high threshold mechanoreceptors (HTMRs) are the first order neurons of the somatosensory system involved in processing touch and pain respecitvely[29]. These neurons are composed by 2 main parts: the peripheral axon, also called dendron, and the central axon **(Figure 1.4)**. The first one innervates receptor cells in the periphery allowing the processing of mechanical forces applied to the skin. The central axon goes into the spinal cord where it makes synapsis with interneurons then transmits the signal to the second order neurons in the dorsal column nuclei[21]. LTMRs and HTMRs are the sensory

neurons which conform the proper receptors for touch and pain converting mechanical and nociceptive stimulus into electrical impulses. Once LTMRs and HTMRs have been activated, its information is sent to the dorsal horn of the spinal where the second step of sensory processing occurs.

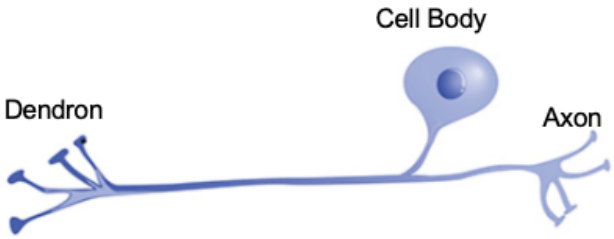


Figure 1.4. Example of pseudo-unipolar sensory neuron.
Sensory neurons have their cell body located in the trigeminal and dorsal root ganglia. These neurons send processes towards the periphery (dendron) and spinal cord (axons). The tactile information activates the dendron eliciting electrical impulses that travel along the axon toward the spinal cord.

1.4.1.2 The Spinal Cord: the dorsal horn

Recent research has shown that the dorsal horn of the spinal cord play an important role in processing the tactile stimulus encoded by peripheral LTMRs. Bourane and colleagues discovered a group of excitatory interneurons in the DRG expressing ROR alpha nuclear orphan receptor (RORα) which innervate LTMRs. After genetic ablation of RORα interneurons these knock out mice show a reduction in behavioural responses to light touch, suggesting that these interneurons play a role in signalling touch stimulus to higher centres[30]. More recent research has elucidated more interaction between LTMRs and interneurons in the dorsal horn. Taking advantage of mouse genetic tools, Abraira and colleagues discovered a novel group of interneurons with unique morphological and physiological properties. In the dorsal root, they identified the LTMR recipient zone (LTMR-RZ). The authors found a total of seven excitatory

and four inhibitory interneurons[31]. As suggested by previous research, LTMRs make synapses with these interneurons modulating the way LTMRs send the tactile information towards the second order neurons located in the medulla. Taking together, these results suggest that the spinal cord is an important part of tactile processing and that the perception of touch is created long before reaching the cortex. The next section will be about the last step of neuronal processing: the brain.

1.4.1.3 The Brain: the brainstem and the somatosensory cortex

Once the information is pre-processed in the dorsal horn, LTMRs send tactile information to the dorsal column nuclei in the brainstem where second order neurons reside[27]. The function of these second order neurons in the somatosensory pathway remains somewhat elusive but some research has suggested their involvement in tactile processing[32,33]. Experiments done with cats showed that second order somatosensory neurons in the cuneate nucleus of the dorsa column nuclei respond to different type of haptic stimuli suggesting that somatosensory stimulus are already processed in subcortical stages[33]. After somatosensory stimulus has reached the second order neurons, those transmit the somatosensory stimuli toward the ventroposterior lateral nucleus (VPL) in the thalamus via the medial lemniscus[34]. In the thalamus, the diverse information coming from different sensory systems become integrated in a single perception. Recent advances have postulated that sensory integration occurs far before associative areas in the neocortex and that the thalamus is an important subcortical region of tactile processing[35]. For example, Wahlborn and colleagues show that most thalamic neurons respond to tactile stimuli with specific firing patterns and that those patterns could be depicted to identify the type of tactile stimulus applied[36].In the last step of tactile sensory processing, third order thalamocortical neurons project tactile information towards the somatosensory cortex via the postcentral gyrus[37].

In humans, the somatosensory cortex sits in the parietal cortex, and it is subdivided in 3 main parts: the primary somatosensory cortex, the secondary somatosensory cortex and the posterior parietal cortex[21]. The neuronal organization between these areas shows an intrinsic level of complexity from primary to secondary areas. Although current models to explain how LTMRs contribute to cortical tactile representation have advanced in the last decades, these models are based in correlative experiments which lack a direct link between LTMRs response in the periphery and direct somatosensory cortex activation[38–40].

Interestingly, a recent investigation using transgenic mice with optogenetic stimulation have shown how somatosensory cortex activation is triggered by the activation of specific LTMRs types. For example, rapid adapting and slow adapting LTMRs activate different somatosensory cortex regions[41]. This data suggests that in the somatosensory cortex signals from LTMRs are integrated and computed to generate the entire cortical representation of touch.

In the somatosensory cortex, the receptive field of somatosensory neurons in the secondary somatosensory cortex are bigger than the ones in the primary somatosensory cortex[29,32,34]. For example, in the periphery LTMRs have the smallest receptive fields, like the end tip of the finger. In the brainstem the neurons will have larger receptive fields, composed by many LTMRs receptive fields, like the whole tip of the finger. In the primary somatosensory cortex, neurons will have larger receptive fields like the whole finger. Finally, in the secondary somatosensory cortex, neurons will have massive receptive fields expanding to 2 or 3 fingers or even the whole hand Taking into account the receptive field of HFs, this idea suggest that the number of follicles represented in the brain will increase from primary to tertiary areas

Finally, the somatosensory cortex is organize in a somatotopic fashion[42]. In 1950, Penfield and Rasmussen use electrical stimulation of the somatosensory cortex in patients undergoing brain surgery. From their studies it derives the idea that the human's homunculus represent a correlation between body parts and brain regions.[43]. In that model, the same regions of the skin represented by receptive fields are also computed in the somatosensory cortex following the same topographic fashion. For example, 2 receptive fields which will be located side by side in the fingertip will be process by 2 neurons located also side by side in the somatosensory cortex[32].

Until now, we have explained how our sense of touch is organized, from the first order neurons LTMRs in the periphery, passing towards the brainstem until reaching higher centres in the neocortex. In the next section, we will explain that like in all systems, aberrant processing of tactile information can lead to clinical problems.

1.5 Touch and clinical considerations

LTMRs and HTMRs disruption has important clinical implications affecting the health of millions of people worldwide[44]. In this section we will focus in the most prevalent ones and the ones believed to be more important to solve due to their prevalence and severity. One of the most prevalent and tactile related disorder is neuropathic pain (NP) or neuropathy. In the United Kingdom, NP is one of the most prevalent health conditions affecting between one third and one half of the total population which corresponds to around 28 million adults[45]. NP is defined as a pathology caused by injuries in the somatosensory pathways which process touch and pain[46]. NP has been linked to LTMRs and HTMRs damage caused by external cues such as traumatic injury or a drug-induced side effect.[47] Although the cause is multifactorial, it

is believed to arise after injury of the spinal cord or the brain producing at the same time imbalances between inhibitory and excitatory neuronal inputs and aberrant ion channel activation[48]. Two of the main symptoms of neuropathic pain are allodynia and hyperalgesia: allodynia is defined as the type of pain that occurs when a non-nociceptive stimulus is sensitized, such as the brush of a feather, produces pain whereas hyperalgesia happens when a nociceptive stimulus produced more pain that it should do[49]. It is believed that between 15-50% of people with neuropathic pain has these symptoms. The mechanism behind those definitions are not really clear but it is believed that LTMRs play an important role[50]. Theoretically hyperalgesia could be mediated by sensitization of HTMRs, and allodynia for the integration of LTMRs into the circuits that transmit pain. Several studies have shown that specific types of C-LTMRs and Aβ-LTMRs could be involved in mediating allodynia[51,52].

It is interesting to point that C-LTMRs have been linked to other touch related diseases. Autism spectrum disorder (ASD) is a devastating disease where the individual feels disconnected from the social world, that leads towards very self-restricted behaviour[53]. Interestingly, individuals with ASD also show abnormal tactile sensitivity. and although there is no gross differences in brain morphology, electrophysiological studies have shown some differences compared to control subjects[53]. Although the focus in trying to understand the ethology of ASD has been focused in the brain mostly, recent research has given attention to peripherals LTMRs as contributors of the syndrome[54]. Recent studies have shown that individual with ASD have mutations in *Mecp2* and *Badrd3* genes. Deleting these genes in mice leads to LTMRs hypersensitivity, social interaction deficits and anxiety-like behaviours[55]. A more recent study has also shown that KO mice lacking C-LTMRs from birth show a pronounced social isolation and reduced tactile interactions. Interestingly, stimulation of C-LTMR in wild type adults promoted touch seeking, pro-social behaviours and positive effects in group dynamics[56].

These findings support the idea that C-LTMRs are an important mediator of social behaviour. This idea has been proposed since a long time and studies with humans as shown that C-LTMRs are also involved in mediated tactile pleasure stimulus[8,57].

Up to now, I have covered how the different sensory neurons and brain regions are involved in process touch and pain and also the problems that arise when there's an aberrant activation or damage of these neurons. In the next sections, I will focus on how the first order neurons processing touch. I will focus in how LTMRs and HTMRs can be classified and organized in the skin and which activation mechanism leads to the touch coding in the periphery.

1.6 LTMRs: fibre diameter and cell bodies: fast, medium and slow conduction velocities.

Years of research have made it possible to build an LTMRs and HTMR classification system based on 5 main features: conduction velocities and cell body size, adaptation rates and receptive fields and finally end organs[6].

Perhaps the oldest way to classify LTMRs is based on how fast they transmit tactile stimulus from the periphery to the spinal cord. Pioneering work from Taub and Bishop in 1965 with cats showed for first time that the speeds of the signal transmitted from the DRG axons towards the spinocervical tract were heterogenous, suggesting the presence of different sensory neurons with a diverse type of conduction velocities[58]. Further research on LTMRs histology also showed that DRG were composed with 3 differentiated types of LTMRs depending on the cell body and axons diameter size: myelinated large and medium neurons and unmyelinated small neurons[59]. Interestingly, a relationship between LTMRs soma size and conduction velocities was made where larger neurons transmitting the stimulus quicker than smallest ones[60]. Therefore, there are 3 main different axonal conduction velocities which can be used

as classification: LTMRs with big soma sizes and capable to transmit the stimulus at speeds in the range of 16-100m/s are classified as Aß-LTMRs, LTMRs with medium soma sizes and able to transmit the stimulus at speed in the range of 5-30ms/ are classified as Aδ-LTMRs and lastly, LTMRs with small soma sizes and able to transmit tactile stimulus at speed ranging from 02-2m/s are classified at C-LTMRs[61].

1.7 LTMRs and adaptation rates: slow and rapid

Besides how quickly LTMRs are able to send tactile signals from the periphery to the brain, LTMRs can also be classified depend on their firing properties when a tactile stimulus is applied. Therefore, is it possible to classify LTMRs as a slow and fast adapting **(Figure 1.5)**. Slow adapting LTMRs (SA-LTMRs) are tactile receptors which exhibit sustained firing during the whole duration of the stimulus. SA-LTMRs can also be further divided in two subtypes: SA type I (SAI-LTMRs) and SA type II LTMRs (SAII-LTMRs) depend on specific firing patterns and stimulus selectivity. SAI-LTMRs have small receptive fields that display preferences to respond to skin indentation with maximal firing for stimulus edges, points and contours[62,63]. The firing pattern is constant with irregular burst increasing as more stimulus force is applied. These receptors are believed to give information about velocity and stimulus position with high spatial resolution, encoding information about the shape and texture of the object, and are therefore the ones involved mostly in object recognition.

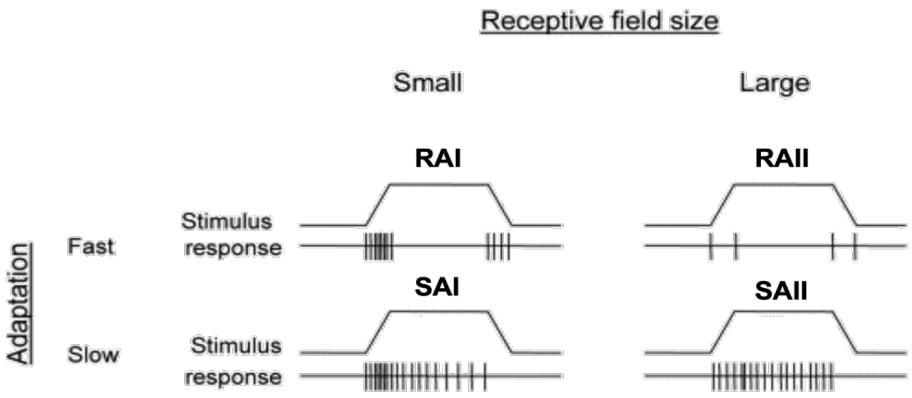


Figure 1.5. Firing patters of slow and rapid adapting LTMRs in relationship with their receptive field size. The firing patters of the different LTRMs are dependent on their receptive fields and adaptation rates. RAI LTRMs are composed by small receptive with fast adaption rates which leads to a high frequency firing pattern at the start-end point of the stimulus. RAII LTRMs are composed by large receptive with fast adaption rates which leads to a low frequency firing pattern at the start-end point of the stimulus. SAI LTRMs are composed by small receptive with slow adaption rates which leads to a high frequency firing pattern at the start point of the stimulus. SAII LTRMs are composed by large receptive with slow adaption rates which leads to a low frequency firing pattern at the start point of the stimulus.

SAII-LTMRs have large receptive fields show preference for skin stretch of larger areas. Different from SAI-LTMRs, this type II shows a more uniform firing pattern with less irregular burst. These receptors are involved in detecting texture of larger objects. Overall, there is consensus that both SAI and SAII LTMRs are the sensory neurons involved in object recognition[34].

Rapid adapting LTMRs (RA-LTMRs) fire action potentials just when the stimulus is moving or changing force. Therefore, these receptors will stop firing once the stimulus is stable and does not change location or intensity. It is evident that this type of LTMRs are the ones involved in detecting when an object is moving along our body. Similarly, as SA-LTMRs, RA-LTMRs can also be sub classified in type I and type II. Type I RA-LTMRs (RAI-LTMRs), have small receptive fields and show firing patterns at a maximal frequency of 1-10Hz, therefore are involved in process low frequency vibrations. It is believed that this type of receptors are involved in detecting slow motion in the skin therefore are involved in grip adjustment once we are holding an object or when we tap a keyword[64,65]. Type II RA-LTMRs (RAII-LTMRs) show large receptive fields and conform the most sensitive LTMRs in the skin and are able to adapt their firing rate to frequencies up to 300Hz. These receptors are involved in transmitting the movements of object held in our hand, like when we are moving the steering **w**heel or while writing[66].

1.8 LTMRs and end organs in the skin

LTMRs are the most heterogeneous sensory receptors in the body. They show different conduction velocities, adaptation rates and specific receptive fields[67,68]. However, perhaps the most prominent features which differentiate them is their end organs in the skin. In the extreme periphery of the nervous system, the dendron form specific structural endings with preference to specific stimulus such as speed, shape, force, location[34]. In mammalian skin, LTMRs will display different end organ structures depending on a crucial factor - the presence or absence of HFs[10].

Consequently, hairy and glabrous skin show different end organs. In glabrous skin, these end organs are composed by Merkel cells, Ruffini endings, Pacinian and Meissner corpuscles. On the other hand, in hairy skin these end organs also form lanceolate complexes and circumferential endings wrapping around HFs[67].

In the next section we will cover the most prominent features of the different LTMRs and HTMRs innervation glabrous and hairy skin.

1.8.1 LTMR end organs in both hairy and non-hairy skin

Aß SAI-LTMRs and Merkel cells forming the Merkel cell neurite complex are in real terms the intrinsic association between an LTMR and an epithelial cell **(Figure 1.6A).** Back in 1875, Merkel was the first anatomist to describe a cluster of cells closely associated with afferent fibres. Merkel cells are enriched in highly sensitive zones such as the palm of the hand[69,70]. Merkel cells and their SAI-LTMRs are among the most sensitive and important touch receptors. The Merkel cell neurite complex is involved in a wide range of tactile function such as pressure, position and static touch detection[71].

Having in mind its firing properties in sustained firing once the tactile stimulus is present, is it believe that Merkel cells are the main receptors capable to process textures and shapes, making them the crucial complex for object recognition. Aß RAI-LTMRs Pacinian corpuscle has also been widely study due to its easy access and, because of its location deep into the dermis, it is also present in hairy skin **(Figure 1.6B).** Therefore, Pacinian corpuscles show a unique feature since there are widely present in both hairy and non-hairy skin[34]. As RA-LTMRs, these receptors respond vigorously when the stimulus changes frequency or force, however, what makes Pacinian corpuscles special is the large receptive field they have: some Pacinian corpuscles can have a receptive field up to 15cm^2. The receptor is composed by a S100 lamellar structure formed by lamellar and Schwann cells. Recent research has shown that the lamellar sheath acts a sensory receptors modulating the properties of its associated LTMR[72]. Due to their deep location on the skin, Pacinian corpuscles and their afferents are involved in processing deep pressure of larger areas.

1.8.2 LTMRs and end organs non hairy skin

Aß RAI-LTMRs Meissner corpuscles are LTMRs located close to the dermal-epidermal junction, and they account for the most superficial tactile receptors. These are composed by LTMRs axons in the centre wrapped but a lamellar like structure of S100 myelin **(Figure 1.6C).** These receptors are highly sensitive to skin deformation and are able to detect changes in stimulus location up to 2µm[61]. Therefore, it is believed its function is to permit grip control and fine tune manipulation of objects.



Figure 1.6. Confocal microscopy images of different end organs in glabrous and hairy skin.
(A) Merkel cell neurite complexes are touch receptors composed by an afferent LTMR (cyan) and cluster of Merkel cells (pink).
(B) Pacinian corpuscle formed but the lamellar sheath (green) and the LTMR afferent (red)[189].
(C) Meissner corpuscle showing the LTMR afferent (yellow) and the lamellar corpuscle composed by myelin (red)[190].

Interestingly, recent research has shown a peculiar feature of this tactile receptors. After genetic labelling of specific types of DRG LTMRs, the authors were able to reveal that Meissner corpuscles are indeed innervated by 2 different types of LTMRs: a LTMRs expressing TrkB and another one expressing Ret. Further electrophysiological studies shows that each of these neurons innervating Meissner corpuscles display different tunning properties and adaptation rates. TrkB are highly sensitive to skin indentation able to detect force variations up to 1mN whereas Ret afferents were more prone to respond to a more heterogenous stimulus and with less level of sensitivity[73]. Overall, these results suggest a highly complex level of integration in glabrous skin where the same corpuscle is shared with 2 morphologically identical but physiologically different LTMRs tuned to different stimulus.

Aß SAII-LTMRs Ruffini endings are tactile receptor believed to be associated to a Aß SAII-LTMRs. Work by Chambers and colleagues in 1976 showed that this LTMRs are associated with Ruffini endings in cats[74], further studies have fail to identify the association between the Aß SAII-LTMRs responses and the location on the skin with Ruffini endings in racoons and humans[75,76]. Therefore, these are the least known LTMRs and are believed to be present in glabrous skin.

1.8.3 LTMRs and end organs in hairy skin

Up to now, the last sections explained how the diverse type of LTMRs form specialized end organs in glabrous skin. Although the classification regarding conduction velocities and adaptation rates is the same for all LTMRs independently if they innervate glabrous or hairy skin, the end organs, as mentioned, are different. Murine LTMRs innervate HFs form Merkel cells neurite complexes, longitudinal-lanceolate and circumferential endings[34]. In mice, hairy skin on the body is composed by mainly 4 different types of HFs: guard, awl/auchene and zigzag with a distribution of 1%, 23% and 76% respectively[63]. Interestingly, in mice hairy skin LTMRs innervate different types of hair dependent on their physiology[67].

It is known that in mice 5 different types of LTMRs make specialized end organs around HFs: Aβ SAI-LTMR Merkel cell neurite complexes, longitudinal-lanceolate Aβ RA-LTMRs, circumferential Aβ Field-LTMRs, longitudinal-lanceolate Aδ LTMRs and longitudinal-lanceolate C-LTMRs[68].

Longitudinal-lanceolate Aβ RA-LTMRs are associated with guard and awl/auchene HFs and express the molecular markers neurofilament heavy chain (NFH) and RET receptor (Ret). These LTMRs have high speed condition velocities and rapid adapting properties form a longitudinal and lanceolate collar structure around the HF[77] **(Figure 1.7).** The lanceolate axons are surrounded with specialized Schwann cell processes and are located close to HF epithelial cells[78]. Back in 1967, Brown and Iggo were the first scientists to unravel the exact physiology of the LTMRs innervating hairy skin. They found that in cats and rabbit that hair fibre deflection causes LTMRs firing response[34,79]. Therefore, suggesting that this LTMRs were associated with HFs.

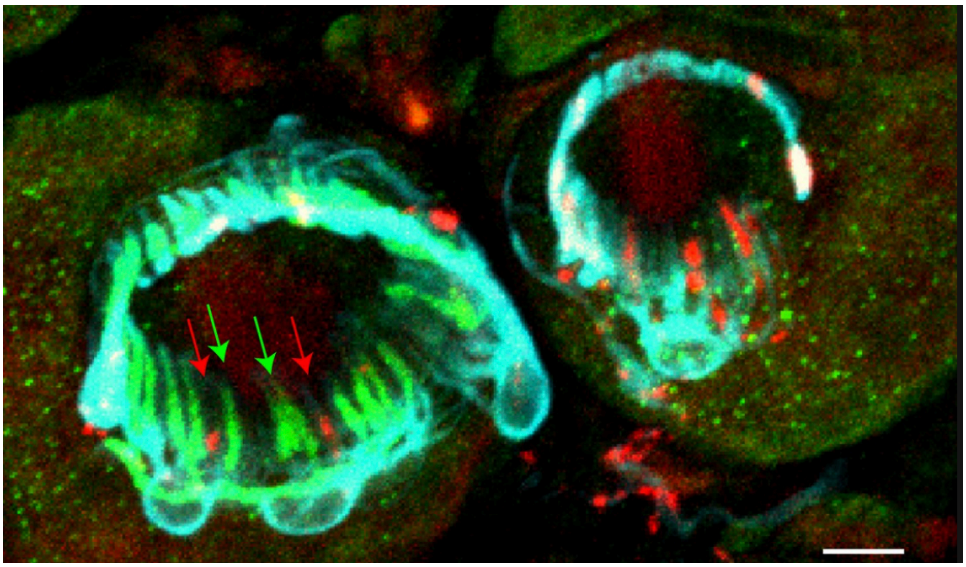


Figure 1.7 Longitudinal Aβ RA-LTMRs in murine skin
Whole-mount staining of mice hairy skin revealing the presence of longitudinal Aβ RA-LTMRs (green) around mouse HFs. The endings re wrapped by terminal Schwann cell processes (cyan)[77].

Circumferential Aβ Field-LTMRs and their physiology and morphology have remained elusive for long time. However, recent research by Bai and colleagues has been able to target this LTMRs to understand its function in touch perception. First, using retrograde labelling against tyrosine kinase receptor C (TrkC) the authors found that in mice these LTMRs are associated with guard, awl/auchene and zig-zag hairs, therefore innervating the whole of mouse hairy skin. These LTMRs also express NFH and Ret molecular markers as longitudinal-lanceolate Aβ RA-LTMRs. They also found that these LTMRs make circumferential endings around the follicle, therefore conforming a new end-organ structure around the follicle different from longitudinal-lanceolate Aβ RA-LTMRs (**Figure 1.8A**). Interestingly, the authors also found that the same LTMR is able to innervate many hairs, creating a field of innervated HFs and therefore a large receptive field (**Figure 1.8B**). Further electrophysiological studies shows that these type of LTMRs are insensitive to skin indentation but also to hair deflection but sensitive to gentle skin stroking. This finding reveals the unique and peculiar features of this LTMR giving this name as a field-LTMRs.

This LTMR associated with HFs is sensitive to gentle stroking of the skin but only when the stimulus in integrated between many of its circumferential endings[80].

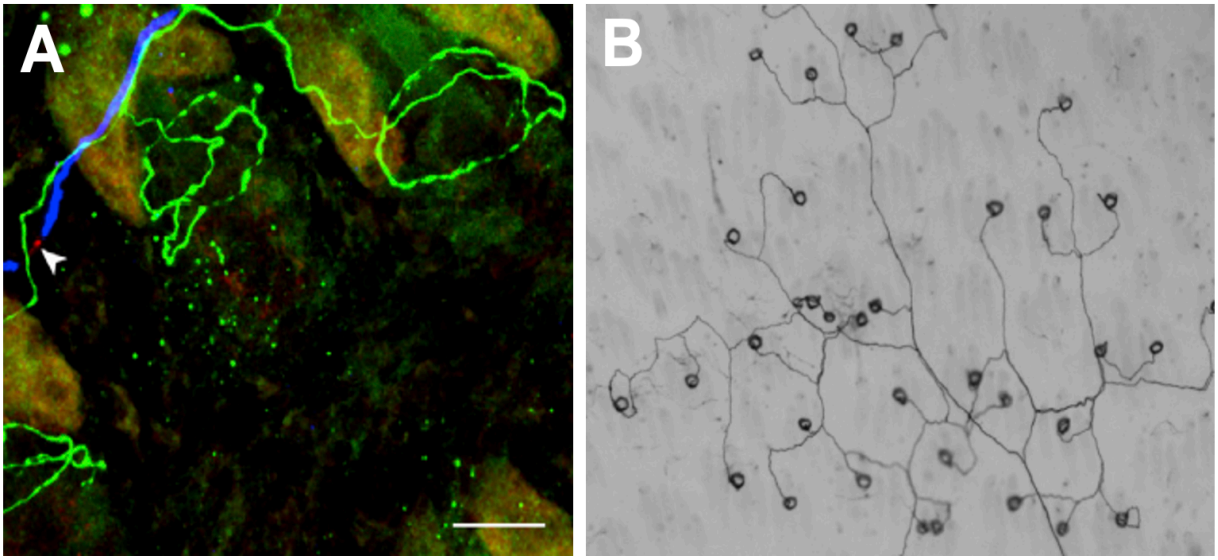


Figure 1.8 Circumferential Aβ Field-LTMRs
(A) Whole-mount staining of mice hairy skin revealing the presence of circumferential Aβ Field-LTMRs around mouse HFs.
(B) AP staining of mice hairy skin revealing the field pattern around many HFs originating from the same LTMR[79].

Longitudinal-lanceolate Aδ-LTMRs are the LTMRs associated with HFs with mid-range conductance velocities. These LTMRs express the molecular markers NFH and also tyrosine kinase receptor B (TrkB). In mice hairy skin these LTMRs innervate zigzag and awl/auchene HFs, but nor guard hairs. A special quality of this LTMR is that these LTMRs are tuned to respond to the direction of stimulus applied to the skin. Ruthin and colleagues found that in mice, this LTMRs respond when a tactile stimulus deflect the HF in the posterior to anterior direction.

Following this, they found LTMRs forming lanceolate endings which are more polarized towards to the anterior part of the animal, therefore explaining why these LTMRs are more prone to be activated towards posterior to anterior stimulus[67,81]. Finally, the authors ask the

molecular basis of this polarization and found that brain-derived neurotropic factor (BDNF) released from HF epithelial cells attracted longitudinal lanceolate complexes towards the posterior part (**Figure 1.9**)[81]. Overall, these findings reveal for first time how, like in all sensory systems, the sense of touch also has receptors which mediate direction-selectivity of stimulus.

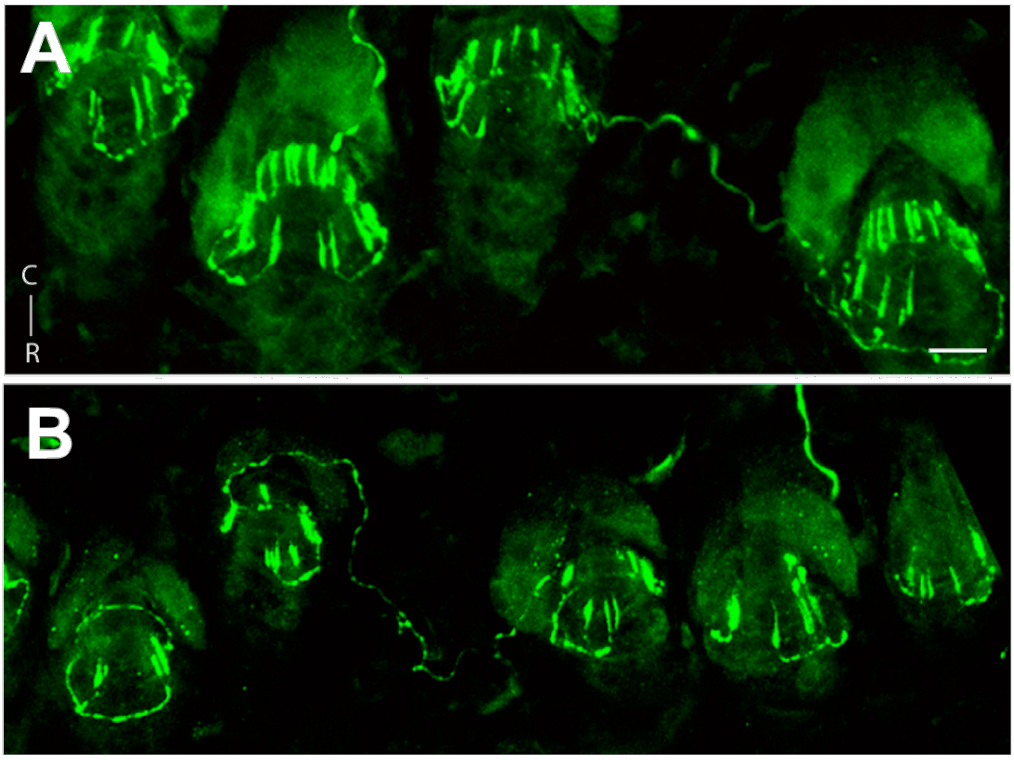


Figure 1.9 Confocal microscope image of longitudinal-lanceolate Aδ LTMRs around mouse zigzag follicles.
longitudinal-lanceolate Aδ-LTMRs are polarized in the caudal part of the follicle in wild type mice (A). KO mice lacking BDNF show a random pattern of innervation that lacks the caudal polarity of the axon[80].

Longitudinal-lanceolate C-LTMRs are the most studied LTMRs in humans. Thanks to non-invasive electromyographical studies it has been shown that human LTMRs have a slow-conductance velocities and that their activation is associated with pleasant sensation[57]. Unlike the other LTMRs associated with HFs, C-LTMRs have been studied extensively in humans[82]. C-LTMRs have been also linked to emotional touch and mechanical allodynia. However, there is no research in humans which has shown the morphology of C-LTMR in skin nor their

association within the follicle[57,65]. In mice, C-LTMRs are associated with awl/auchene and zig-zag hairs making lanceolate complexes around HFs and express the signature marker tyrosine hydroxylase (TH)[67] (**Figure 1.10**).

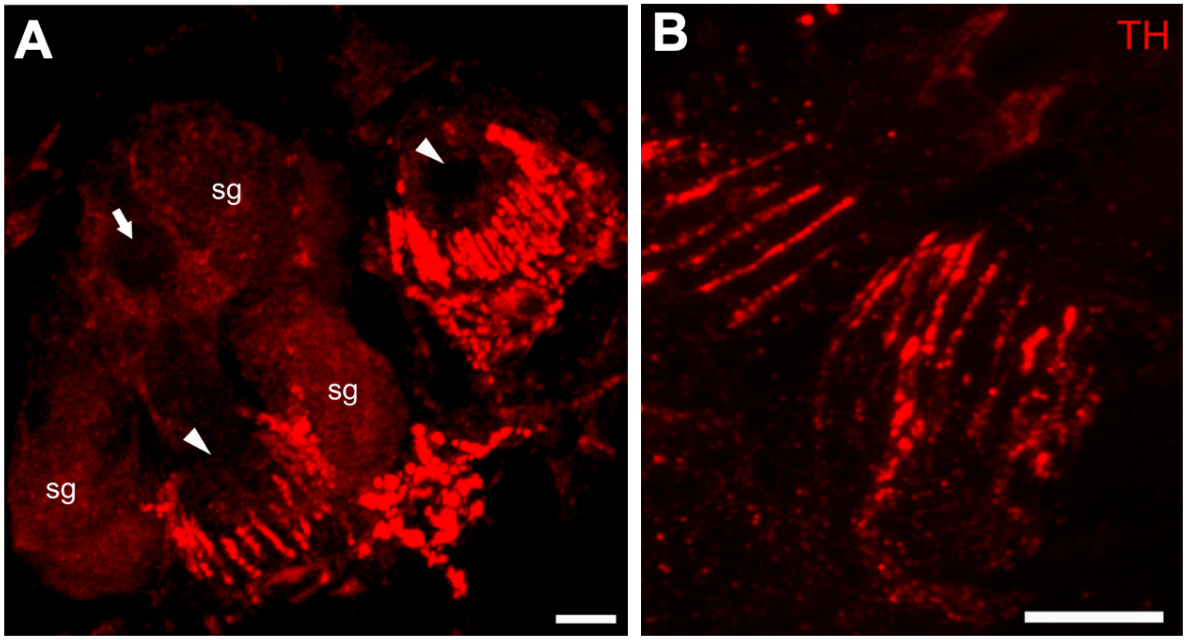


Figure 1.10. Confocal microscope image of longitudinal-lanceolate C-LTMRs around mouse HFs. Longitudinal-lanceolate C-LTMRs are the only LTMR in the HF expressing TH (A-B)[66]. Scale bars 10μm

1.9 HTMRs, first order neurons processing pain with specific end-organs

One of the most important differences between HTMR and LTMRs is their end organs. HTMRs in both glabrous and hairy skin make free nerve endings, so they are not associated with an end organ structure[34].

Some research thought have suggested that the morphology of the free nerve ending can be related to the type of HTMR and their function[83]. Nevertheless, this believe about free nerve ending only HTMRs was challenged recently. Ghitany and colleagues unravel a new type of murine Aδ HTMR making circumferential endings around HFs.

Circumferential Aδ-HTMRs are medium-fast conduction HTMRs that are activated after strong pull of a single hair, suggesting that this HTMRs are capable to respond to rapid and localized mechanical pain[84].

High threshold mechanoreceptors (HTMRs) or nociceptors process thermal, mechanical or chemical nociceptive stimulus, therefore they signal pain[57,85]. Some of them can be classified as polymodal nociceptors which respond to more than one single feature.

For example transient receptor potential vanilloid 1 (TRPV1) expressing HTMR response to both heat and mechanical pain[86–88]. HTMRs are classified as Aβ, Aδ and C, depend on their conduction velocities. Although the existence of Aβ HTMRs has been debated, nowadays there is consensus that Aβ HTMRs are fast conduction nociceptors which can be classified as hybrid receptor. Aβ HTMRs capable of responds to light touch and mechanical pain[51,89]. Aδ-HTMR are nociceptors with medium conductance velocities that respond to mechanical pain and also heat stimulus. This HTMRs are believe to mediate the first sharp pain[90]. Finally, C-HTMRs are unmyelinated nociceptors that mediate mostly mechanical pain and are belief to madidate the long lasting burning pain after stimulus injury[91]. C-HTMRs can be subdivided into peptidergic and nonpeptidergic nociceptors[92]. Peptidergic nociceptors express the markers calcitonin gene related product (CGRP) and or substance p (SP) and are believed to mediate pain localization and features whereas nonpeptidergic nociceptors express isolectin IB4 and the purinergic 2X3 receptors (P2X3) and are involved in mediate the emotional component of pain[93]

1.10 Identification of HF LTMRs and HTMRs.

The physiology and morphology of the diverse types of LTRMs and HTMRs associated with hairy and non-hairy mammalian skin. Because of the scope of this thesis, we will focus in the LTMRs and HTMRs associated with HFs. As explained before, the DRG is composed by highly heterogeneous group of neurons with different functions and innervation patterns. Therefore, one of the most important advances in the last decade that helped to unravel the morphology of these LTMRs has been its genetic labelling[67,94]. Using a battery of transgenic mice, several groups have been able to target molecularly most of the LTMRs and HTMRs innervating murine HFs. These experiments using genetic reporter mice with specific fluorescent markers such as dTomato and green fluorescent protein (GFP) have been used to label each type of LTMR and HTMR and its morphology (Table 1).

Neuron type	HF Sensory-end organ	Specific markers	Features
Aβ-RA	Longitudinal	Npyr2r[10], Early Ret[28], Maf[29], KCNQ4[30]	LTMR
Aβ-SA	Merkel-touch dome	NFH[10], Npy2r[10], TrkC[10, 27], DOR[31]	LTMR
Aβ-RA	Circumferential	NFH[10], TrkC[32], Ret[28], DOR[31]	LTMR/HTMR?
Aδ-RA	Longitudinal	NFH[10], TrkB[33]	LTMR
Aδ-SA	Circumferential	CGRP[11]	HTMR
C-SA	Longitudinal	Th[10], Vglut3[34]	LTMR

Table 1.1 Classification of mouse sensory DRG-neurons by conductance velocities, HF-associated sensory organ, specific molecular marker used in genetic labelling and stimulus-response features.

As a result of these advances, it was possible to depict how different HTMRs and HTMR form specialized longitudinal and circumferential endings around HFs, showing that in mice, a single follicle is innervated by more than one LTMR type. Overall, these advances confirmed that one of the main functions of HF is tactile perception[67,80,81,84].

1.11 HF-neuronal interactions

The HF is a highly innervated structure. As explained before, 7 different types of sensory neurons have been shown to innervate murine HFs[24]. Each of sensory neurons mediates specific and differentiated functions making the HF a complex receptor of tactile information[34]. For the 4 different types of murine hairs in their fur, different types of neurons innervate different hair types **(Figure 1.11).** However, LTMRs and HTMRs innervating HFs are not the single elements capable of processing tactile information[95]. Recent finding suggest that to understand the HF as a touch receptor, one needs to take into account the complex structure of the HF and the epithelial tissue that is colocalized within the LTMRs-HTMRs innervating the HF[96]. The main and most studied function of bulge HFSC is their involvement in generating new hair during the hair cycle and the development of the follicle in morphogenesis[97]. Interestingly, the different LTMRs and HTMRs that innervate the HF are localized in the bulge region where bulge HFSC reside[98]. Recent research has started to show that there is a wide range of epithelial-neuronal interaction in the bulge region where neurons regulate HF functions, and bulge epithelial cells regulate neuronal processes[98,99].

1.11.1 Neurotrophic interactions in the HF bulge

Neurotrophins (NTs) are a class of growth factors that are indispensable for the development of the nervous system. NTs serve to a wide range regulatory functions such as memory, weight control, cardiovascular function and therefore are involved in mediating a wide range of functions in different body systems[100]. The first discovered NT, nerve growth factor (NFG) by Rita Levi Montalcini in the 1950s was the first milestone that led to the discovering of its family composed by 4 different NTs and their receptors[101].

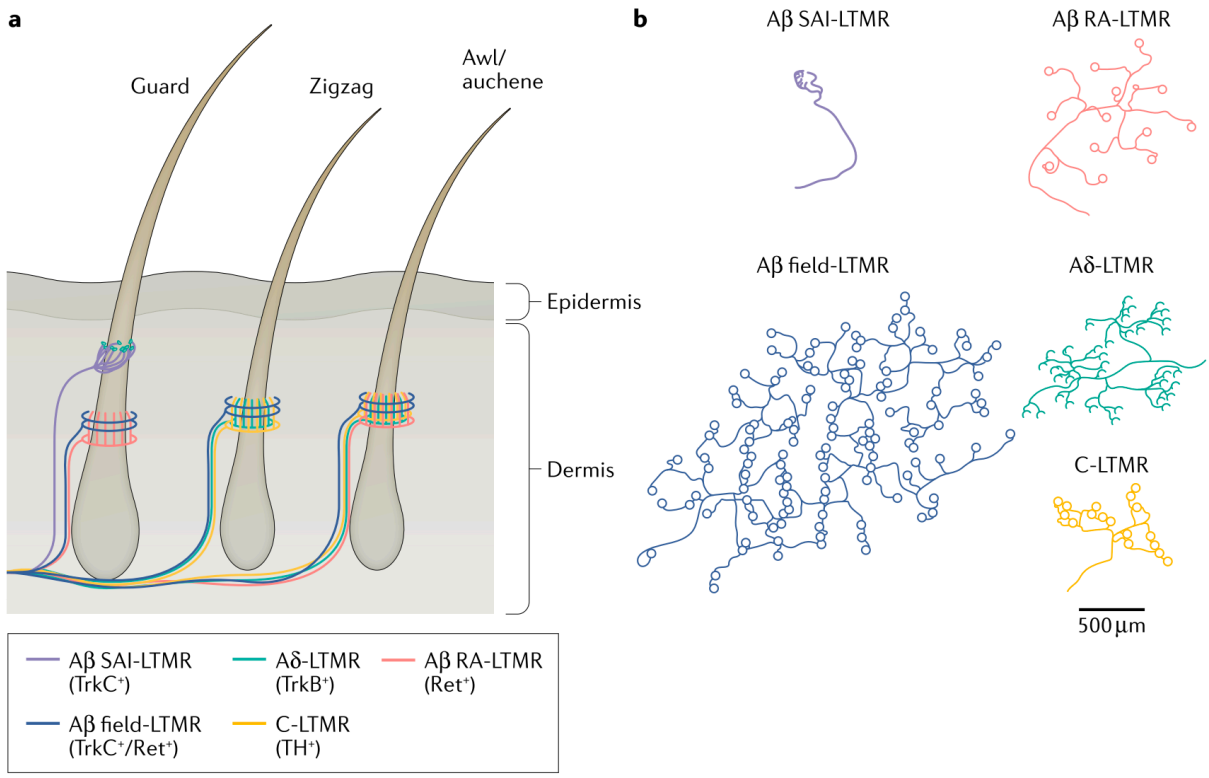


Figure 1.11. Murine hairy skin innervation and LTMRs receptive fields.

(A) Mouse have different hair types in their skin with different innervation patterns. Guard hairs are innervated by Merkel cell neurite complexes, lanceolate Ret+ Aβ RA-LTMR and circumferential TrkC+/Ret+ Aβ field-LTMR. Zigzag HFs are innervated by lanceolate TrkB+ Aδ-LTMRs and lanceolate Th+ C-LTMRs and circumferential TrkC+/Ret+ Aβ field-LTMR. Awl/auchene HFs are innervated by lanceolate Ret+ Aβ RA-LTMR, circumferential TrkC+/Ret+ Aβ field-LTMR, lanceolate Th+ C-LTMRs and lanceolate TrkB+ Aδ-LTMRs. Circumferential CGRP+ Aδ HTMR innervate all mouse HFs (not shown)[67].

NFG binds to the tyrosine kinase A receptor (TrkA), BDNF binds to the tyrosine kinase B receptors (TrkB), Neurotrophin 3 (NT3) binds to the tyrosine kinase C receptor (TrkC) and Neurotrophin 4 (NT4) bins to the TrkB receptor. Further, all NTs bind to the p75 receptors with low affinity **(Figure 1.12)**[100]. It has been suggested that neurotrophins (NTs) such as neurotrophin 3 (NT3) and neurotrophin 4 (NT4) and BDNF have the ability to regulate HF growth and cycling[102,103]. Other research showed that sensory neurons in the HF are also sensitive to different NTs. For example, Stucky and colleagues showed that NT4 is required for the presence of Aδ neurons associated with HFs[104]. Previous research also showed that BDNF is required for SA-LTMRs function. Mice lacking BDNF show impaired SA-LTMRs mechanosensitive function, that could be reversed after BDNF administration[105].

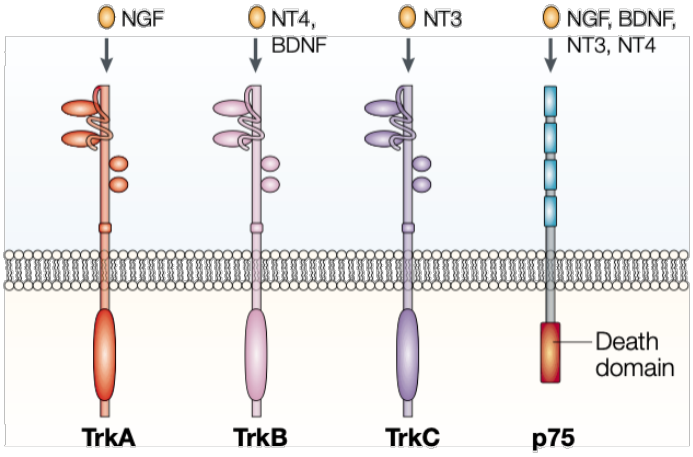


Figure 1.12. Neurotrophins and their binding receptors.
NTs bind to different receptors with low and high affinity. NGF, NT4, BDNF and NT3 bind with high affinity to TrkA. TrkB and TrkC respectively. All NTs bind to p75 with low affinity.

Although these studies suggest the role of neurotrophins in the normative function of the LTMRs innervating HFs, they to determine the origin of this neurotrophins which support neuronal function. Recently, Rutlin and colleagues showed that epithelial cells in the HF bulge were able to release BDNF which activate the TrkB receptor in longitudinal Aδ-LTMRs promoting axonal polarization and determining the function of the neurons to be direction selection of hair shaft deflection[81]. Overall, NTs are important molecules that control many functions both in bulge epithelial cells and HF associated sensory neurons. In the next section we will cover how epithelial cells in the HF also are important to support the structural integrity of HF lanceolate complexes

1.11.2 Bulge-structural support of HF innervation.

The bulge region of the follicle has been shown to be implicated in creating a scaffold matrix which supports HF regions. For example, upper-bulge cells release nephronectin (EGFL6) into the basement membrane of the HF to provide and anchor structure for the arrector pili muscle (APM) to insert and develop[106].

Further research in mouse has shown that Gli1+ bulge cells located in the upper bulge are able to release EGFL6 into the lanceolate endings promoting cell adhesion via α5 integrins. Mouse lacking Gli1+ cells lack EGFL6 which leads to aberrant lanceolate complex organization and impaired HF mediated touch sensation[98] (**Figure 1.13**). Therefore, cells in the bulge region of the follicle are not only involved in secreting NTs to regulate LTMR function but also to secrete matrix proteins to sustain LTMRs lanceolate complex organization. The HF bulge, however, it is also a target of neuronal signalling, so besides releasing molecules affecting neurons, cells in the bulge are also affected by substances released by neurons.

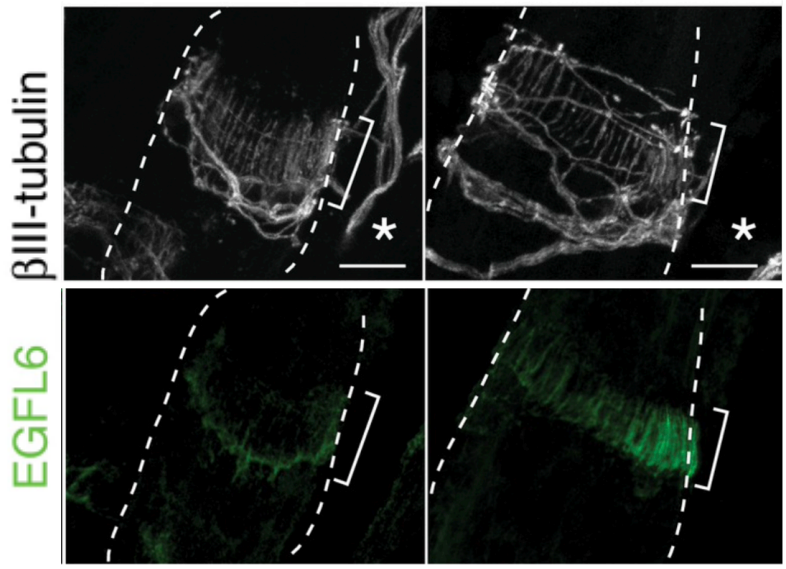


Figure 1.13. EGFL6 derived from Gli1+ HF epithelial cells are colocalized with lanceolate complexes
Co-localization of EGFL6 and lancelet complexes in the murine HF supports LTMRs integrity. Region of EGFL release by Gli1+ cells in the collar of longitudinal-lanceolate complexes (asterisk)[97]

1.11.3 Neurotransmitter signalling in the HF bulge

Recent research has been shown that neurons innervating the HF bulge can secrete neurotransmitters regulating the bulge cells fate and responses to the environment[107,108].

Although this communication is from the neurons towards the bulge and the neurons involve are not LTMRs, this is a relevant example to show the high level of interconnectivity between the HF bulge and the neurons which innervate the follicle.

Schwartz and colleagues shown that during piloerection or goosebumps the sympathetic nerves innervating the bulge region of the follicle via the arrector pili muscle (APM). Thus, in the event of a cold environment, the APM associated sympathetic nerves become stimulated by the contraction of the APM. Once stimulated, the sympathetic nerves release noradrenaline inhibiting the quiescent regulators *Foxp1* and *Fgf18* leading to bulge stem cell differentiation and hair growth[107].

On the other hand, research by the same authors show for first time how stress can promote hair greying. In the event of a stressful situation, the sympathetic nerves innervating the bulge region release adrenaline which binds to the beta-2 adrenergic receptors in the melanocyte stem cells. Once the melanocyte stem cells have been activated by this receptor, they deplete from the bulge, impairing the deposition of melanin in the growing hair fibre and therefore promoting hair greying[108]. Overall, these 2 different examples to illustrate how the neurons innervating the HF can release substance to affect ORS cells in the bulge.
As stated above, the interaction between cells and neurons in the bulge of the HF is vast: neurons can modulate bulge cell fate and function and LTMRs responses via secreting NTs and matrix proteins.

Up to this point, I have explained how the somatosensory system is organized, and how sensory neurons which process touch and pain are organized around mouse hairy skin.

The murine HF is highly innervated in the bulge region with different LTMRs and HTMR for specialized endings. The next section will focus how sensory neurons processing touch together with HF cells become activated after tactile stimulus as a first step of touch coding.

1.12 Mechanotransduction of touch sensation

After a tactile stimulus is delivered into our skin, how do sensory neurons process this tactile information? Is the HF and its cellular components able to facilitate this process? To explain such phenomena, I will cover how putative proteins with mechanosensitive properties convert tactile stimulus into bioelectrical signals and how they are activated by its microenvironment. Finally, I will also cover how non-neuronal cells in the HF and skin play a role in tactile perception. LTMRs are the first cell types capable to transform tactile or mechanical stimulus into electrical signals therefore can convert gentle indentation or hair deflection into action potentials[21]. The first stage of this process is the activation of mechanosensitive cationic channels in the cell surface; therefore, the activation of this mechanosensitive molecule mediates the first response in the LTMRs.

1.12.1 Mechanosensitive ion channels in touch perception

Mechanotransduction is virtually present in all cell types and there's been decades of research to find the molecules which allow cells to transform mechanical cues into physiological signals[109–111]. First, research in primitive organism like *c. elegans* has shown that degenerin channels (DEG/ENaC) were involved in touch perception: loss of the genes coding for that channels leave touch insensitive animals and also abolish mechanical currents recorded from LTMRs from the same animals[112]. However, these channels were not found in mammals suggesting that higher species might express different mechanosensitive cationic channels to transduce tactile sensation[113].

In mammals, the mechanosensation ion channels for touch perception compromises 2 families: the transient receptor potential (TRP) family and the Piezo family[114].

1.12.1.1 TRP channels in touch sensation

TRP channels form a large family of channels involved in sensory mechanotransduction. These channels are broadly present in mammals, forming 7 different families with more than 33 genes encoding TRP-forming proteins[115]. Studies in non-mammalian organisms have shown the requirement of TRP channels to transduce mechanical information. For example, research in mouse models have demonstrated a role of TRP vanilloid receptor 4 (TRPV4) and TRP cation A member 1 (TRPA1) in and mechano-nociception[116]. Recent research using mouse models has also revealed the activation of TRPV1 after low-threshold mechanical stimulation, suggesting a potential role of TRPV1 in touch sensation[88].

1.12.1.2 Piezo channels

Piezo channels are a recent type of ion channels composed by 2 subtypes: Piezo1 and Piezo2. These channels have been shown to be indispensable for normal proprioception and tactile perception and have been found widely in LTMRs, therefore suggesting that Piezo channels are the main mechanosensitive ion channels for touch perception in mammals[117–119]. The channels have a propeller-like structure formed by several protein domains; when a tension is applied on the cell surface, the blades of the channel flip up and open the channel triggering cell activation[120,121]. Piezo2 has been involved in most of the slow and rapid adapting mechanical current after tactile stimulation in LTMRs[122,123]. A recent study also show that Peizo2 channels are present in mice lanceolate endings, supporting the idea that Piezo2 could be involved in caused the typical rapid-adapting mechanical current that arises after hair movement[124].

Aberrant genetic variants in genes forming Piezo2 channels have been found in humans with impairment in discriminative touch and proprioceptive problems and ataxia suggesting this channels play an important role in tactile perception also in humans[125–127]. Overall, TRP and Piezo2 channels are important in touch perception. However, another point of interest is to understand how the ion channel gets activated after tactile stimulus are applied in the skin.

1.12.2 Ion channel activation mechanism

As explained, the first requirement for mechanotransduction is the presence of a putative mechanosensory molecule-mechanical sensitive. Normally, mechanosensory molecules tend to form or to be part of an ion channel in the cell membrane and to be mechanically gated. The ion channel would become activated with a specific gating mechanism while a mechanical force is applied, for example in the cell membrane itself. There are several gating mechanisms proposed which depend on the requirement of accessory proteins or extracellular matrix (ECM) **(Figure 1.14).** For example, Piezo channels has been shown to be gated by a plug-and-latch mechanisms, as showed in figure 1.11. When a tactile stimulus is applied into the cell membrane, the blades like structure of the channel flip up the pore, therefore opening the channels and permitting the influx of ions that depolarize the cell[128,129].

In summary, to be able to transform tactile stimulus into electrical signals cells must have in its cell membrane mechanosensitive channels such as TRP and Piezo that can be activated by several mechanisms. However, this is just the small part of the bigger picture. In the next section we will cover how in the skin the process of tactile mechanisms involved several elements more than just mechanosensitive ion channels.

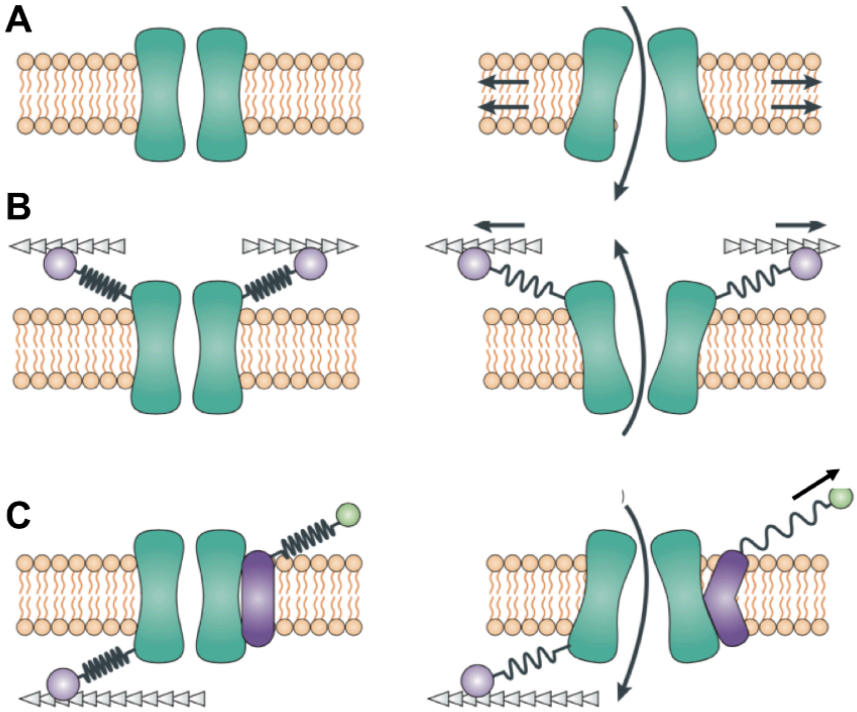


Figure 1.14. Potential gating mechanisms in the human HF. (A) Membrane model: a tension in the lipid bilayer causes channel opening. (B) Tether model: hemidesmosome or tether protein in the extracellular matrix (ECM) attaches to the channel. Tension in the ECM causes therefore channel opening. (C) Accessory tether model: hemidesmosome or tether protein are attached to accessory proteins and associated directly to the ion channel or closely located in the lipid bilayer. Tension in the tether activate the accessory protein opening the ion channel. Vertical arrows represent the movement of ion spices. Horizontal arrows represent the direction of applied force.

1.13 Mechanotransduction in HF LTMRs

LTMRs are the first sensory receptors in be activated by tactile stimulus and are involved in signalling tactile information towards the dorsal column nuclei and ultimately the brain LTMRs are the first sensory receptors to be activated after tactile stimulus. This is the first contact and the first step in touch coding. After LTMR activation, secondary mechanosensitive cell types such as Merkel cell neurite complex in the HF can become activated and therefore modulate the LTMRs responses[38,130].

1.13.1 Mechanotransduction in the Merkel cell neurite complex

As explain before, in HFs but also in non-hairy skin the Merkel cell neurite complex is the association between Merkel cells and a Aβ-SA-LTMR. In this epithelial neuronal system, the interplay between Merkel cells and LTMRs is what gives the full functional feature in signalling light touch. Once something touches our skin or moves the hair shaft of one of our follicles, Piezo2 channels located in the LTMRs, get activated by membrane distention and permit the flux of Na+ and Ca^{2+} inside the LTMR therefore depolarizing the cell membrane[124,131] (**Figure 1.15**). This first response which last for few milliseconds is called dynamic phase and is mostly mediated by the Aβ-SA-LTMR[132]. The response of the Merkel cell neurite complex is far longer than few milliseconds. Recent research has shown that a more long-lasting static phase arises after the dynamic phase and Merkel cells are the ones trigger this response in the LTMR. Therefore, now is it known that Merkel cells express the mechanosensitive ion channel Piezo2, making Merkel cells a sensitive epithelial cells capable to signal tactile information to their associated Aβ-SA-LTMR[117]. Mice lacking Merkel cells display an aberrant response to tactile stimulus and impaired texture discrimination suggesting that Merkel cells are required for the normal activation of their associated Aβ-SA-LTMR and therefore for the overall response of the Merkel cell neurite complex[133]. Although the mechanism in understanding how Merkel cells communicate with their associated Aβ-SA-LTMR has remained elusive for decades, recent research has given light about it. First, Gu and colleagues showed that in the mouse whisker Merkel cells are able to release serotonin after tactile stimulus to activate their associated Aβ-SA-LTMR via the serotoninergic receptors 2 and 3 (5HTR2 and 5HTR3)[134]. More recently, Hoffman and colleagues dissatisfy the serotoninergic signalling model in the Merkel cell neurite complex evidencing that in ex vivo skin preparations Merkel cells release adrenaline after tactile stimulation which start responses in Aβ-SA-LTMR via the beta2 adrenergic receptor (B2AR)[135].

Further experiments carried again by Gu and colleagues were not able to show adrenergic signalling between Merkel cells and their associated Aβ-SA-LTMR in murine whiskers suggest that perhaps whiskers follicles and guard follicles display different signalling mechanisms[68,136].

Although without consensus about the signalling mechanism in the Merkel cell neurite complex, is it clear that the interaction between epithelial cells and neurons mediates its tactile responses. Although Merkel cells are the clearest example of epithelial cells with tactile properties, recent research has shown that in non-hairy skin other epithelial cells are able to modulate how LTMRs response.

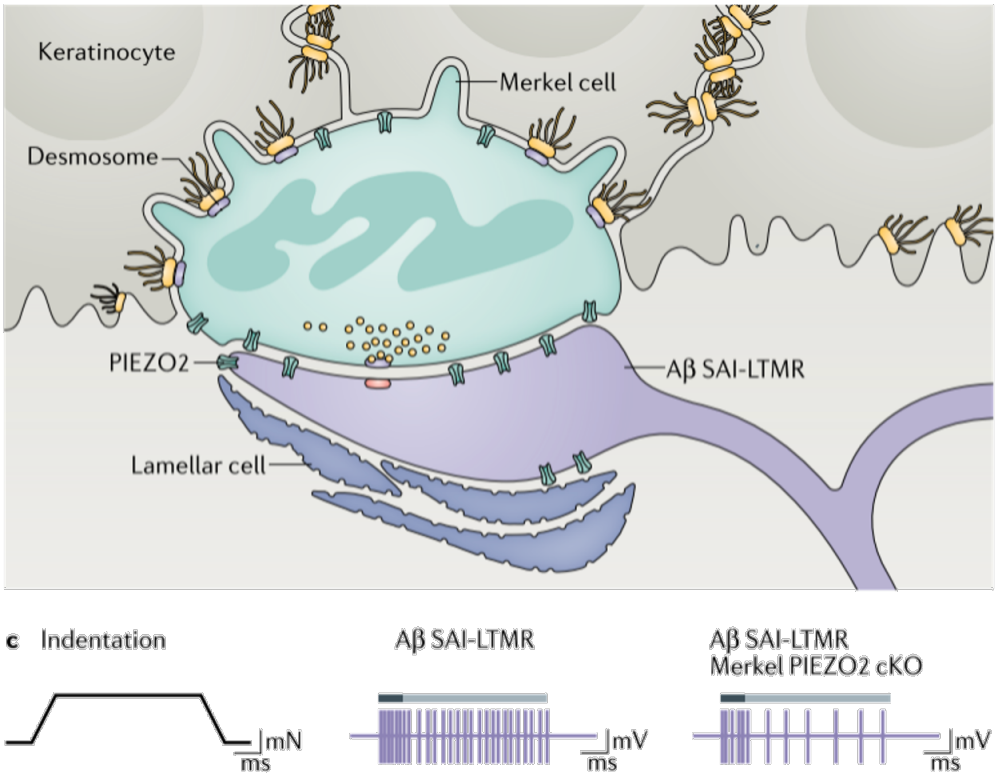


Figure 1.15. Touch signalling in the Merkel cell neurite complex
Tactile indentation applied on the skin activate Aβ SAI-LTMRs by opening Piezo2 channels and starting the static phase of the mechanical current. After Aβ SAI-LTMRs activation, indentation is transmitted to keratinocytes and Merkel cell via desmosomes. Membrane indentation open Piezo2 channels in Merkel cells activating the cells and releasing neurotransmitters which mediated a dynamic current in Aβ SAI-LTMRs. Mouse lacking Merkel cells show no dynamic current after tactile indentation[67].

1.14 Mechanotransduction in the epidermis: keratinocytes as tactile receptors

Keratinocytes (KC) are epithelial cells which form the epidermis, the most external layer of the interfollicular skin[11]. As a forefront layer in the skin, KC respond to some of the sensory stimulus reaching the skin[95]. Indeed, although in early stages, recent research in the last decade has shown that KC are mechanosensory cells which can active LTMRs. Preliminary in vitro experiment showed that tactile stimulation of keratinocytes is able to elicit calcium response in close located sensory neurons[137]. Further, in vivo optogenetics and electrophysical experiments showed that KC are able to respond to tactile and nociceptive stimulus and to initiate action potentials to a wide range of LTMRs and HTMRs[138].

ATP is famously known to be the main energetic molecule in most type of cells, however it is also an important excitatory neurotransmitter in central and peripheral nervous system. In sensory ganglia such as DRG neurons, ATP can modulate neuronal responses by the activation of 3 main post synaptic purinergic receptors: P1 and P2Y and P2X. These receptors become activated after ATP binding and their role is to promote cell activation.[139]

More recently employing the drug apyrase which blocks ATP it has been shown that KC can communicate with sensory neurons after noxious, light touch, heat and cold stimulus to activate neurons via the P2X receptor. In their model, ATP release from KC after tactile and noxious stimulus reached the P2X receptor in the neurons activating them. This data suggest that ATP is a signalling mechanism which mediate KC-sensory neurons communication[140,141]. Although ATP is famously known to be the main energetic molecule in most type of cells, it is also an important excitatory neurotransmitter in central and peripheral nervous system, aspect that helps to explain why KC can activate neurons via ATP[142,143].

Finally, it has been shown that KC form synapses between sensory neurons suggests that a quicker synaptic mechanism can arise between KC and sensory neurons. The neurotransmitter in question, however, remains to be tested[144]. Overall, this data supports the idea that epidermal KC are involved in sensory process and that is not just a structural cell forming the epidermis.

1.15 The human HF as a novel niche for touch signalling.

The innervation patterns in mouse HFs is mostly restricted in the bulge region which is the region of the follicle composed by epithelial cells with a wide range of signalling mechanism with neurons. Many examples have shown that this neuroepithelial interaction is bidirectional; neurons have an effect in the epithelial cells but the epithelial cells also an effect in the neurons. Therefore, the bulge of the HF represents a niche for many biological functions. Furthermore, several investigations have shown that the sense of touch is in part mediated by neuroepithelial interactions rather that by just sole neuronal responses. Nevertheless, this research has been carried out in murine hairy skin and no studies have looked into human skin.

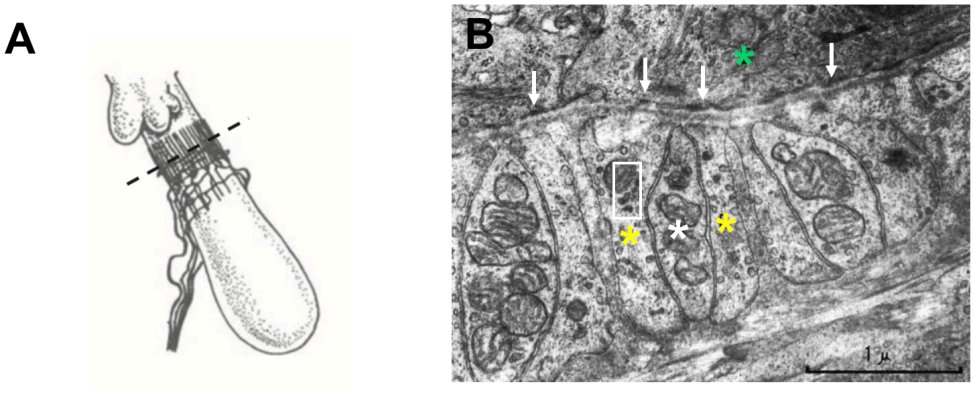


Figure 1.16. Transverse electron microphotograph of lanceolate endings in the human HF.
(A) Exemplification of the imaged region in B. Dashed line represent the point of the bulge and sectioning. **(B)** Longitudinal endings (white asterisk) wrapped by TSC (yellow asterisk) and closely located opposite HF epithelial cells (green asterisk) and basilar membrane. TSC present small pinocytotic vesicles (white box). Note the presence of hemidesmosomes-like tethers (white arrows) just opposite to the axon and/or TSC. Longitudinal oriented collagen fibres (black arrow) are located in the outer part of the lanceolate endings[142].

Regarding human HFs, the ultrastructural relationship between LTMRs and the HF suggests that a combination of different cell types, for example terminal Schwann cells (TSC) or HF ORS cells could mediate tactile signalling in the HF (**Figure 1.16**)[145].

1.16 Comparison between human and mouse hairy skin innervation

Most of the research about HF innervation and neuroepithelial interaction has been performed in murine HFs and research in human hairy skin has been relatively limited. Back in the 1950s, Montagna showed for first time that human HFs were innervated by lanceolate and circumferential endings, suggesting that humans can have similar innervation patterns as mice[146]. More recent studies using modern immunolabelling techniques have also show that human HFs have longitudinal and lanceolate endings with myelinated afferents. These studies however have not looked at specific type of neurons innervating the follicles nor the exact location of where the neurons form the endings[147–150]. Furthermore, while mice have several types of hairs, in human adults, there are only 2 main types of hairs: vellus and terminal[13,151]. Terminal hairs are larger pigmented hairs whereas vellus hair are the smallest, barely noticeable hairs. Terminal hairs are located mostly on scalp but also in other parts of the body such as beard, pubic region etc after puberty whereas vellus hair are located in most parts. There are important differences between males and females in terminal hair distribution: men have a higher amount of terminal hairs distributed along the body compared to women[152]. Another difference between mice and human HFs is how they are organized. In mice, each HF forms an independent unit with its own sebaceous glands and APM, in humans, HFs are organized in follicular units with 2-4 follicles attached to a single APM[153,154]. The HF in these units grow independently from one another but the fibres exit at the surface from a single pore (**Figure 1.17**)[155].

Therefore, having in mind these differences, is difficult to make a direct extrapolation of the findings in mice to humans. Thus, to draw a phylogenetical continuum between mouse and human HF innervation can be challenging.

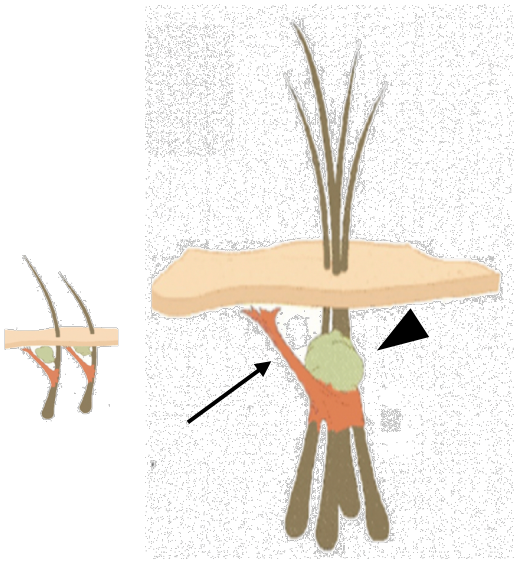


Figure 1.17 Comparison between mice and human follicular units.
Murine HFs grown independently per unit, with a single sebaceous gland and APM whereas human HFs grown in units with multiple follicles sharing the same sebaceous gland (arrowhead) and APM (arrow). Image not at scale

1.17 Aims

I hypothesise that the human HF epithelium can function as novel niche for tactile sensation. With this idea in mind, there are several objectives to consistently test this hypothesis:

- Understand how the human terminal HFs are innervated: type of sensory neurons innervating and localization
- Find cell types in the human HF epithelium with capabilities to respond to tactile stimulus
- Test in vitro the association between ORS epithelial cells and DRG neurons.
- Investigate the communication between ORS cells and neurons in vitro
- Screening the possible mechanisms of this interaction

These aims will be addressed sequentially in the results chapter of this thesis. Before the results chapter I will introduce the methodology used to investigate the beforementioned hypothesis.

2. Material and Methods

2. 1 Samples

2.1.1 Human samples

Follicular units and skin biopsies from occipital scalp skin were taken from subjects aged 23-54 undergoing hair transplant surgery at Mediteknia Clinic (Las Palmas de Gran Canaria) and Farjo Clinic (London). All experiments and extractions were approved by Imperial College London Research Ethics Committee. Individual follicular units composed by 1, 2 or 3 HFs were excised using follicular unit extraction (FUE) technique for whole mount experiments. Follicles isolated by follicular unit transplantation enables collection of tissue including dermis, epidermis and HFs.

2.1.2 Animals

Wild type C57BL/6 discarded from other research projects were used. The age of the animals fluctuates from 12 to 47 days old.

2.2 Immunolabelling

2.2.1 Immunolabelling of tissue sections

Discarded dissected human follicular units were fixed with 4% v/v paraformaldehyde (PFA) (Sigma) in phosphate buffered saline (PBS) (Sigma) for 8h, washed with PBS and cryoprotected with 15% v/v sucrose for 4h and 30% v/v sucrose in PBS another 4 hours. Samples were frozen with dry ice and cut at 50µm using a cryostat. First, samples were cleaned with PBS and permeabilized with 0.1% v/v Triton-X for 30min at room temperature (RT) and then incubated with blocking solution with 0.1% v/v Triton-X containing 5% v/v goat and donkey serum for 1h at RT. Next samples were incubated with primary antibodies in 0.1%

v/v Triton-X for 8h at 4°C. Then samples were washes with 0.1% v/v Triton-X (Sigma) 3 times for 30min and incubated with secondary antibodies for 2h at RT and washed again with 0.1% v/v Triton-X 3 times for 30min. Samples were mounted using Vectashield© (Vectorlabs) with DAPI for imaging.

2.2.2 Immunocytochemistry

Cells were fixed for 10min with 4% v/v PFA in PBS and then washed 2 times with PBS for 30 seconds. Cells were then incubated with blocking solution with 0.1% v/v Triton-X containing 5% v/v goat and donkey serum for 30min at RT. Next samples were incubated with primary antibodies in 0.1% v/v Triton-X for 1h at RT. Then samples were washed with 0.1% v/v Triton-X 3 times for 5min and incubated with secondary antibodies for 30min at RT and washed again with 0.1% v/v Triton-X 3 times for 5min. Coverslips were mounted using Vectashield© with DAPI for imaging.

2.2.3 Immunohistochemistry

Sample processing for volumetric imaging was performed using a modified version of iDISCO (immunolabeling enabled 3D imaging of solvent-cleared organs) technique[156]. Samples were fixed overnight at 4C in 4% v/v PFA in PBS and washed with PBS twice during 1h. Fixed samples where dehydrated with methanol/H2O series 20% v/v, 40% v/v, 60% v/v, 80% v/v, 100% v/v; 1h each. Dehydrated samples were chilled at 4C and incubated overnight at RT with 66% v/v dichloromethane (Sigma) / 33% v/v methanol (Sigma). The following day, samples were washed twice with methanol and bleached with 5% v/v H_2O_2 in methanol overnight at 4°C. After bleaching, samples were rehydrated with H_2O/methanol series 20% v/v, 40% v/v, 60% v/v, 80% v/v and 100% v/v PBS; 1h each. Samples were finally washed in PBS with 0.2% v/v Triton X-100 (Sigma) twice for 1h.

Pre-treated samples were incubated in permeabilization solutions consisting of PBS with 0.2% v/v Triton X-100, 20% v/v DMSO (Sigma) and 0.3M glycine at 37C for 12h. Samples were then incubated in blocking solution consisting of PBS with 0.2% v/v Triton X-100, 6% donkey serum (Sigma), 6% v/v goat serum and 10% v/v DMSO for 24h at 37°C. Finally, samples were incubated with primary antibodies diluted in PBS with 0.2% v/v of Tween-20, 0.1% v/v of 10mg/mL Heparin (Sigma) solution, 5% v/v DMSO, 3% v/v donkey serum and 3% goat serum for 24h at 37°C. Samples were then washed 4 times 4h each in PBS with 0.2% v/v of Tween-20 (Sigma), 0.1% v/v of 10mg/mL Heparin solution and incubated with secondary antibodies in PBS with 0.2% v/v of Tween-20, 0.1% v/v of 10mg/mL Heparin solution, 3% v/v donkey s1erum and 3% v/v goat serum for 24h at RT and washed again 4 times 4h each in PBS with 0.2% v/v of Tween-20, 0.1% v/v of 10mg/mL Heparin solution.

Immunolabelled samples were dehydrated again with methanol/H2O series 20% v/v, 40% v/v, 60% v/v, 80% v/v, 100% v/v; 1h each for clearing. Samples were then incubated in a rocking platform in 66% v/v dichloromethane / 33% v/v methanol at RT for 3h for the incubate twice with 100% v/v dichloromethane for 10min. Finally, clearing was performed incubating the samples with DiBenzyl ether (Sigma) for 1h. Overall, the protocol takes 9 days to complete with our timeline optimized for whole human follicles. Samples were imaged with Leica SP8 confocal

microscope to a depth of 500-700mm.

Antibody	Company	Concentration used
Anti NFH (Chicken)	Merck Millipore	1/1000
Anti PGP9.5 (Rabbit)	Abcam	1/200
Anti PGP9.5 (Guinea Pig)	Abcam	1/200

Anti S100 (Rabbit)	Abcam	1/100
Anti K20 (Rabbit)	Abcam	1/75
Anti RET (Rabbit)	Abcam	1/500
Anti CGRP (Rabbit)	Abcam	1/500
Anti K15 (Rabbit)	Proteintech	1/700
Anti K15 (Mouse)	Abcam	1/1000
Anti K14 (Mouse	Abcam	1/500
Anti TrkB (Rabbit)	Santa Cruz	1/200
Anti Gli1 (Mouse)	Santa Cruz	1/200
Anti TH (Rabbit)	Abcam	1/100
Anti α6 Integrin (Mouse)	Santa Cruz	1/50

Table 2.1 List of the primary antibodies in this thesis

2.3 Culture of primary cells

2.3.1 Keratinocytes

Human skin KC were isolated from discarded skin pieces. Briefly, hairs were removed, and the sample was trimmed down with scalpel. Tissue was then incubated with Dispase© overnight at 4°C and the following day forceps were used to separate the dermis and epidermis. Dermis was discarded and epidermis was incubated at 37°C for 30 min in 0.5% v/v trypsin. After 30 min the epidermis was dissociated by pipetting in FAD containing a mixture of Dulbecco's Modified Eagle Medium (DMEM) (ThermoFisher) and Ham's F-12 medium (1:1) containing 10% v/v foetal bovine serum (FBS), L-glutamine (2 mM), penicillin-streptomycin (P/S) (50 IU/mL), epidermal growth factor (10 ng/mL), insulin (5 µg/mL), adenine (0.18 mM), hydrocortisone (0.4 µg/mL), cholera toxin (0.1 nM), and triiodothyronine (2 nM). Cells were

seeded to a dish coated with a NIH3T3 feeder layer previously treated with mitomycin C (Sigma). Cells were cultured for 7 days with FAD then used for experiment**s**

2.3.2 HF epithelial cells

Human ORS cells were cultured from excised and plucked hairs. For plucked hairs, hairs were plucked with a fast tweezer pull and incubated with P/S for 10min. Hairs were plated into petri dishes containing a confluent layer of murine NIH3T3 fibroblast feeders at a rate of 3 follicles per dish. Cells were kept up to 10 days or until the day of the experiment with FAD at 37°C. For excised HFs, single HFs were dissected from tissue after FUE or FUT surgery (**Figure 2.1**).

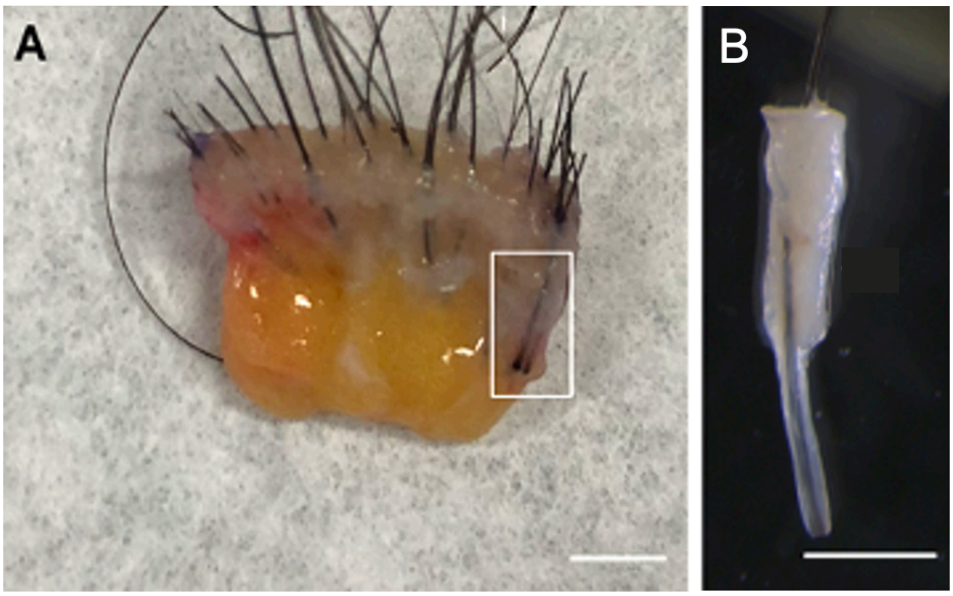


Figure 2.1 Example of sample taken after follicular unit strip surgery
Piece of tissue from a strip from a patient undergoing hair transplant surgery (A) and example of dissected single follicle from the white box in A. Scale bars 500μm A and 200μm in B

After obtaining single follicles, the sample was incubated with DMEM with antibiotics (1% v/v P/S) for 10 min at RT. Then, the follicle was incubated with Dispase® (Thermo) for 15min at RT to separate the ORS from the follicle mesenchyme. After Dispase® incubation, follicles

were plated into petri dishes containing a confluent layer of murine NIH3T3 fibroblast feeder at a rate of 3 follicles per dish. Cells were kept up to 10 days or until the day of the experiment with FAD at 37°C in CO_2 air.

2.3.3 DRG and TG neurons extraction and culture

DRG and TG neurons were isolated from C57BL/6J carcasses, sacrificed for other research purposes. For DRGs, the spine was removed and opened transversally and the dorsal root ganglions from C2-L5 removed using 0.5mm forceps (**Figure 2.2**). For TG, the brain was removed exposing both TG which were removed carefully with 0.5 forceps. DRGs and TGs were incubated with Hans Balanced Salt Solution (HBSS) solution containing 2mg/ml collagenase II (Gibco) at 37°C for 1h. The DRGs and TGs were next dissociated with a fire polished Pasteur pipettes with small tip diameters and plated onto petri dishes coated with the attachment agent 0.1% v/v poly-L-lysine solution (Sigma). DRGs and TGs were seeded into NIH3T3 feeder layers with FAD and kept growing for several days until axons develop (**Figure 2.3**).

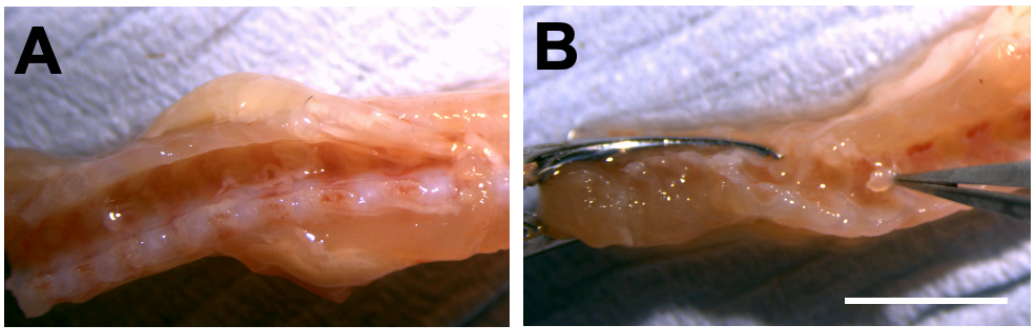


Figure 2.2 Extraction of DRG from adult mice.
Transversal cut from murine spine showing cervical and thoracis vertebra (A) and DRG exposed (B). Scale bar 1cm

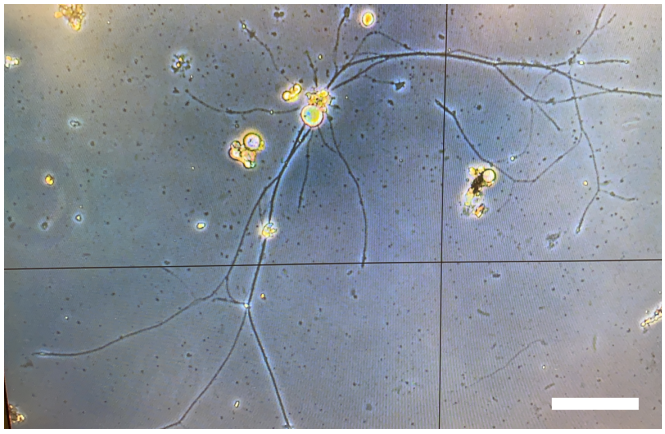


Figure 2.3 Example of DRG/TG culture
Sensory neuron extracted from the trigeminal and dorsal root ganglion growing axons in vitro after 3 days. Scale bar 50µm

2.3.4 Co-culture between human ORS cells and murine DRGs/TGs

For the co-culture system we used mouse DRG neurons and human ORS cells. Briefly, mouse DRGs and TGs were extracted as described previously and then seeded onto a mature ORS cells culture on NIH3T3 feeder layers and kept with FAD at 37°C. Experiments were performed after observing an axonal network developing towards the ORS cell culture, which usually occurred after approximately 10 days (**Figure 2.4**).

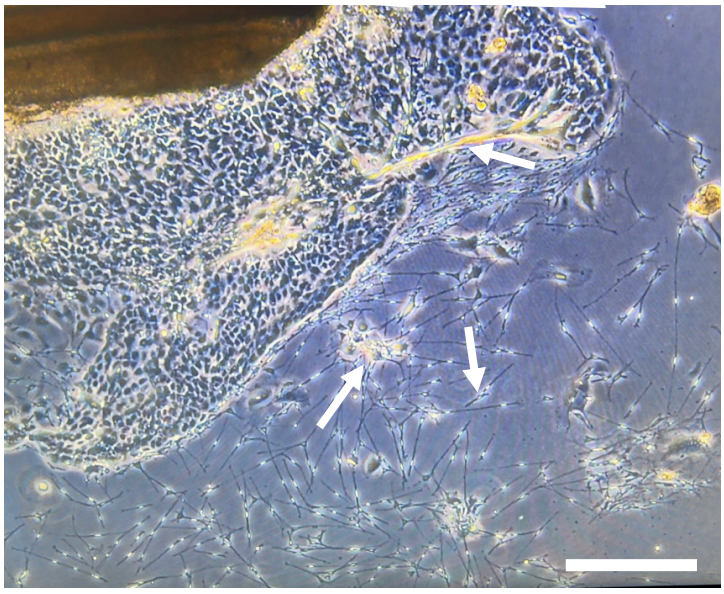


Figure 2.4 Example of a c-culture between ORSc and DRG/TG
After 7 days after plating DRG/TG neurons (arrows) develop axons towards the ORS cell cluster whereas other neurons rest on top (arrowheads). Scale bars 100µm

2.4 Calcium dynamics experiments

2.4.1 Calcium transients after tactile-like stimulus with ORS cultures

Calcium imaging was performed on ORS cells cultures using the fluorescent calcium indicator Cal-520 (AAT Bioquest). Cells were incubated with the dye working solution (10µM Cal-520 in HHBS with 0.04% v/v Pluronic F-127) for 90 minutes at 37°C and 30 minutes at RT. Cells were washed one time for 1 min with PBS and incubated in HBSS for experimentation. Experiment was performed in an inverted microscope (Leica) with the temperature maintained constant at 30°C. Cells located close to the hair shaft were selected for experimentation. Before stimulation, a 60 second baseline was recorded to ensure there were no fluctuations in the calcium-fluorescence ratio within cells. For the recordings, we capture one frame per second. To deliver a stimulus that mimics touch, we approximate the cell of interest with the micropipette with a 2-3 µm round tip until we contact the cell. Then from the point of contact we deliver a 5µm indentation into the cell membrane. To calculate the change in intracellular calcium concentration increase, we use the formula:

$$\Delta F/F = (F - F_i)/F_i$$

F is the fluorescence of the intracellular calcium concentration in each frame and F_i is the fluorescence of the intracellular calcium concentration at the frame prior to stimulation. Because we want to record the intracellular calcium concentration after stimulating the cells one by one, we leave 2 min between stimuli to avoid cell-to-cell activation. After poking the cell, we can record an increase in intracellular calcium concentration suggesting that the cell respond to tactile-like stimulus. Responsive cells were those with a noticeable increase of fluorescence from the baseline.

For the experiments with GsMTx-4, dishes were incubated for 20min with 8μM GsMTx-4 and experiments were performed as previously described selecting the same cells previously used. For experiments with Thapsigargin, dishes were incubated for 8 hours with 3μM thapsigargin. During the experiment, the dishes in a no calcium condition were loaded with HBSS and HEPES but substituting the calcium for magnesium.

2.4.2 Calcium dynamics experiments with ORS-DRG co-cultures

As before, calcium imaging was performed on ORS-DRG/TG co-cultures using the fluorescent calcium indicator Cal-520. Cells were incubated with the dye working solution (10μM Cal-520 in HBSS with 0.04% Pluronic F-127) for 90 minutes at 37C and 30 minutes at RT. Cells then were washed with PBS for 1 min and loaded with HBSS for experimentation. Experiments were performed with the cells in HBSS and using an inverted microscope with constant temperature at 30°C. Cells located close to the hair shaft were selected for experimentation. Before stimulation, a 60s baseline prior to stimulation was recorded to ensure there were no fluctuations in calcium-fluorescence ratio within the cells. Tactile stimulation was delivered with a glass pipette with a diameter of 2-3μm. The pipette was located near the cell surface and a displacement of 5μm was applied to obtain a response. Responsive cells were those with an 20% increase of fluorescence from baseline. LTMRs were selected by soma size and shape, rounded ones and with axonal processes growing. and shape with an average distance of 140μm from the ORS cells stimulation site. To further validate the neuronal origin and the LTMRs signature of the cells selected post-hoc staining using neuronal markers was used. To prevent activating LTMRs themselves by delivering direct stimulation, we consider experiments with a delay no less than 2 seconds were considered

For experiments with apyrase, dishes were incubated for 200 units with apyrase before repeating the same experiment again. For bafilomycin A1 experiments, for each experiment, 2 dishes from the same patient were used: one dish was incubated with 200µM bafilomycin A1 for 24h before the experiments. For mirtazapine experiments, control experiments were performed and then dishes were incubated with 200µM mirtazapine for 30min at 37°C. Then experiment was perform again using the same dish but with different cells.

2.5 Fast-scan cyclic voltammetry with tactile stimulus in ORS cultures

2.5.1 Experimental set-up and tactile stimulation

We built a set-up containing the FSCV system attached to a patch clamp rig with an Olympus microscope with x20 magnifications and with 2 micromanipulators (Sutter Instruments MP-200-ROE). One micromanipulator containing the carbon fibre recoding electrode from the FSCV system and the other micromanipulator containing a patch micropipette with 2-3 diameter tip for tactile-like stimulation. On the day of the experiment, we load the cells with HBSS at pH 7.4 and osmolality 300mol/kg and we approach the cells on interest with both micromanipulators (**Figure 2.5**). For the tactile stimulation, the same protocol as in the calcium experiments was used but with some modifications. Cells were approached until contact was made because the pipette created a small distention in the cell membrane. The position of the micromanipulator was read in the manipulator computer and recorded. Then a 5µm poke-indentation from the recorded point of contact was applied onto the cells after 5 second of starting the FSCV recording. For 3 and 5 poke stimuli, there was a second between each stimulus. For the 1 long sustained poke a 10um poke-indentation was applied but sustained for 15 seconds.

2.5.2 Data acquisition

FSCV signals were recording using a Dagan Potentiostat, (Dagan Corporation, Minneapolis, NM, United States), National Instruments multifunction device USB-6341 (National Instruments, Austin, TX), WCCV 4.0 software (Knowmad Technologies LLC, Tucson, AZ, United States), a Pine Research headstage (Pine Research Instrumentation, Durham, NC, United States) and a precision analog switch (ADG419, Analog Devices, Norwood, MA, United States). Data filtering (zero phase, Butterworth, 2 kHz low-pass). Low pass filtering to remove high frequency noise was performed using a 2D 3rd order Butterworth filter [CITE 1] with cut-off frequencies of 25 kHz (y-axis) and 0.5 Hz (x-axis). At each voltage point time the current of the signal was recorded 10 times per second. 60s recordings were obtained with 600 current points.

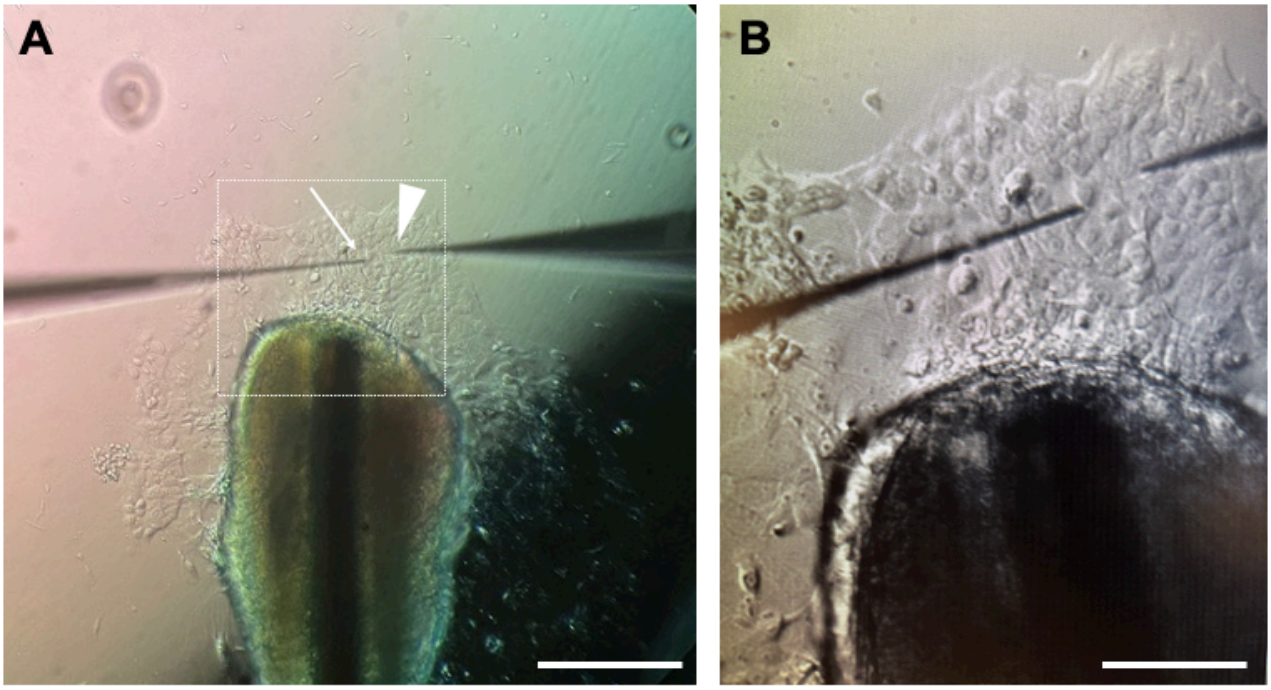


Figure 2.5 Example of the FSCV preparation with ORSc cultures
ORSc preparation with for FSCV with the carbon fiber electrode (arrow) and the stimulating pipette (arrowhead) (A). Magnification of the white dashed line square of A. Scale bars 100µm in A and 50µm in B

2.6.3 Current-concentration transformation

Our collaborators developed the following method to convert the current from the FSCV into concentration. They developed and trained computational models using Python 3.10 and the scikit-learn library [CITE]. A Partial least square regression (PLSR) model for each electrode is used to convert the Faradaic current into concentration of serotonin and histamine. The calibration model was designed to reduce the dimensionality of the cyclic voltammogram from 3000 samples (inputs) to 15 features and to simultaneously predict the concentration of serotonin and histamine (2 outputs). The number of components of the regression were chosen to reduce the predictive error of in vitro flow injections used to train the model and avoid overfitting. Cyclic voltammograms were normalised by removing the mean and scaling to unit variance (standardisation). Models were trained using k-fold cross validation with 5 different train-test sets, a limit of 1000 iterations and 1e-6 tolerance.

Flow injection signals of serotonin and histamine mixtures in HBSS buffer were used to train the model to predict these two analytes.

2.7 qPCR

RNA was collected from ORS cells and keratinocyte cultures using Qiagen microkit. cDNA was generated with SSIV and Oligo dT primers. Primers were designed in house, for the tryptophan hydroxylase gene: TPH forward: TCCCTTCTATACCCCAGAGC and TPH reverse: GAAGAAAGTAAGCCAGCACC whereas for the Keratin 14 gene: K14 forward: TGCCGAGGAATGGTTCTTCACC and K14 reverse: GCAGCTCAATCTCCAGGTTCTG. RT-PCR was performed using Sybr Green PCR mix on a Applied Biosystems QuantStudio 3 real-time PCR thermocycler. Relative expression was calculated based on ΔΔCt.

2.8 Image analyses and data processing

Whole mount images were stitched with Leica LAS-X software. For the calcium experiments, cells were selected by drawing the regions of interest (ROIs) by hand and using the multi-ROI intensity time plot macro created by the FILM facility at Imperial College London. Calcium raw data was converted to ΔF/F using Matlab 2020b and the formula from 2.5.1. Graphs were made with GraphPad Prism

2.9 Statistical analyses

Statistical significance is defined as $p < 0.05$. All statistical tests are performed using Graph Pad Prism. Distribution of samples are shown as mean ± standard error of the mean (SEM), and standard deviation (SD) for RT-PCR if not stated otherwise, with n on the graphs representing the number of cells in total across experiments. While our collaborators are developing an analysis tool to analyse the FSCV traces, for now, we analyse serotonin and histamine differences across the dataset using an analysis of variance (ANOVA) of the peak of release and with Turkey's or Bonferroni's post-hoc test. For the calcium experiments comparison, a student t-test or ANOVA with a post-hoc test was used depending on the number of experimental conditions. In relation to the t-test, this was either paired or unpaired depending on whether the same or different cells were stimulated after drug treatments. Detailed statistical parameters are described in the figure legends. For statistical analysis, the total number of different cells stimulated was compared across experimental conditions, as appose to the total number of experiments or patient samples used. This is consistent with how this type of data is presented within the literature[140,141]. All three values (total number of cells, total number of experiments and patients) are described on each figure legend. For each whisker plot figure, data points represent single cells in calcium experiments and stimulus in FSCV.

3. RESULTS

3.1 Humans have morphologically and molecularly distinct mechanoreceptors innervating terminal HFs.

LTMRs and HTMRs are the only cell types in the skin capable of sending tactile information towards the brain. Consequently, to understand if human HFs can act as a sensory receptor, first we aim to unravel the morphology and molecular identity of the sensory neurons innervating human HFs.

3.1.1 Revealing the morphology of LTMRs and HTMRs innervating human HFs

First, frozen human follicular units from hair transplant surgery were used to test the presence of nerve endings innervating human HFs. Thus, samples were cut at 50µm using a cryostat and used in a common frozen-tissue immunostaining protocol (see methods) with the primary antibody PGP9.5 which targets all types of neurons. Images were taken with a Leica SP8 confocal microscope. (**Figure 3.1**). From the image, it is noticeable the APM axons (asterisk) which form the sympathetic follicular network and some longitudinal endings following the direction of the follicle (dashed lines). This data suggest that humans have axons located close to the follicle.

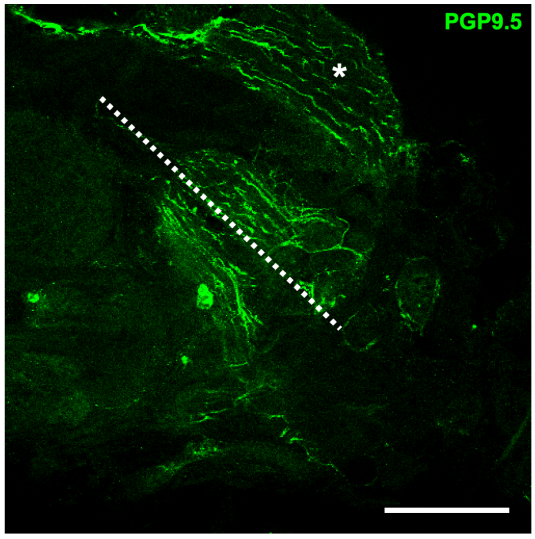


Figure 3.1 Human HFs are innervated by longitudinal axons.
PGP9.5 antibody reveals the presence of APM (asterisk) nerves but also longitudinal nerves around the HF (dashed line). Scale bars 50um. Representative example of 15 samples from 7 patients.

A close look to the picture at figure 3.1, does not provide a clear pictures about the morphology of the nerves. Also, is it difficult to depict which nerves come from the APM and which from the follicle. Furthermore, with 50µm sections is difficult to verify the presence of circumferential endings. Therefore, to better appreciate the follicular morphology and try to identify both circumferential and longitudinal endings, we increased the thickness of the sections to 100µm. In addition, to better identify the identity of the longitudinal and circumferential axons, I used the NFH antibody which target specific LTMRs with medium and fast conductance velocities together with the S100 antibody, which target myelinating and non-myelinating Schwann cells. Thus, the use of these 2 antibodies combined can give information about the morphology of LTMRs and their conductance velocities (**Figure 3.2**). Increasing the thickness of the section helped to reveal in more detail the morphology of the nerves around the follicles and, used in combination with the NFH and S100 antibodies is it certain to confirm that these longitudinal and circumferential endings are from LTMRs with medium-high conductance velocities. To further confirm the presence of this LTMRs making longitudinal and circumferential endings in humans, we used HFs samples from 2 more patients to confirm that all follicles from all individuals are innervated by LTMRs **(Figure 3.3)**

A closer look at the pictures suggests that these longitudinal axons could form lanceolate complexes however with the resolution of the pictures is it not possible to determine this type of structure. Therefore, immunostaining of frozen tissue sections of 100µm fails to reveal the lanceolate morphology of the LTMRs longitudinal endings around human HFs.

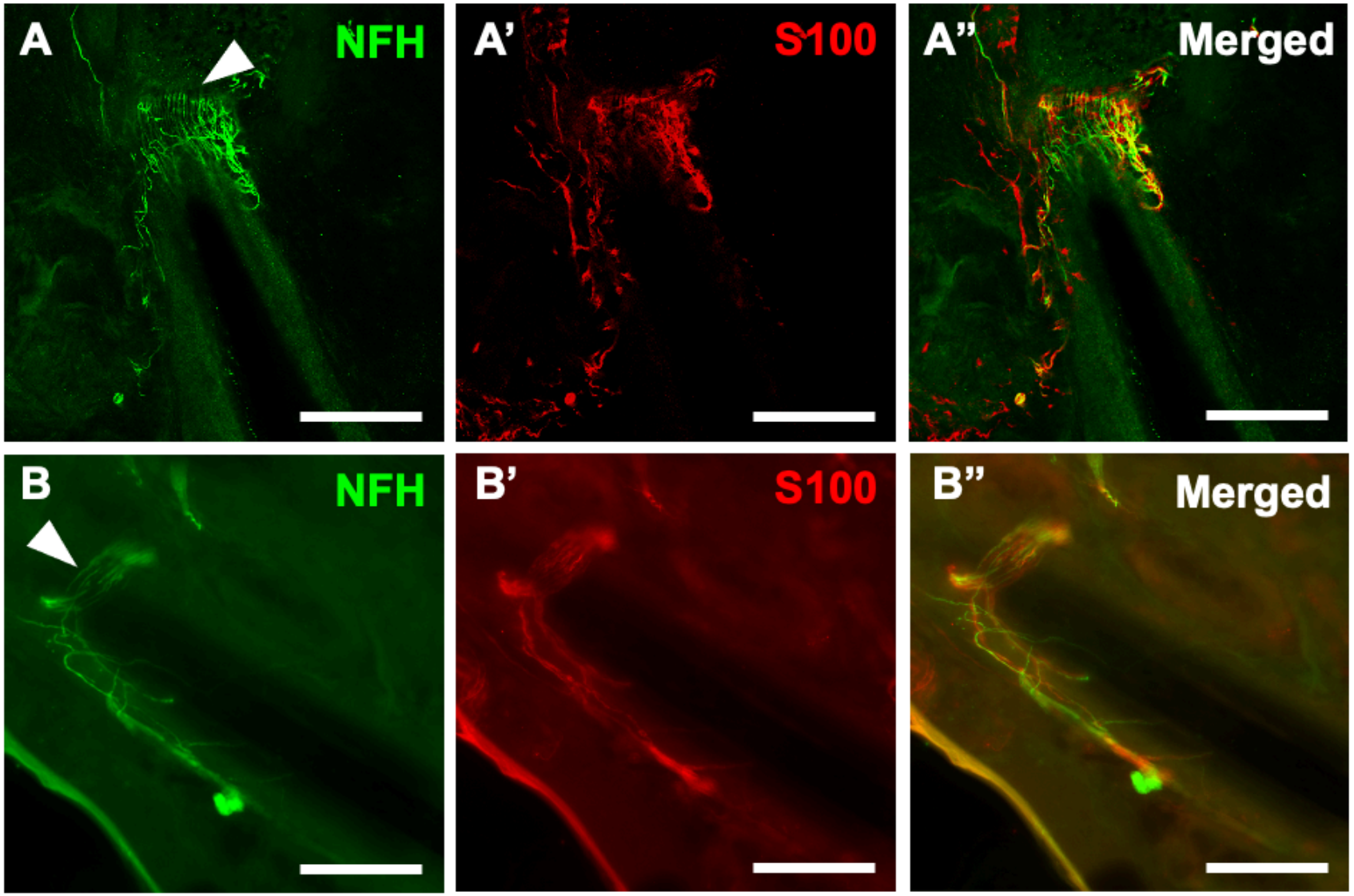


Figure 3.2 Human HFs are innervated by LTMRs forming circumferential and longitudinal endings.
Immunostaining of tissue sections reveals the presence of longitudinal (A, arrowhead) and circumferential (B, arrowhead) endings NFH+ around human HFs (dashed lines). Immunostaining with S100 (A' & B') reveals high level of colocalization between myelinating Schwann cells and LTMRs (A'' & B''). Scale bars 100μm. Representative example of 11 samples from 5 patients.

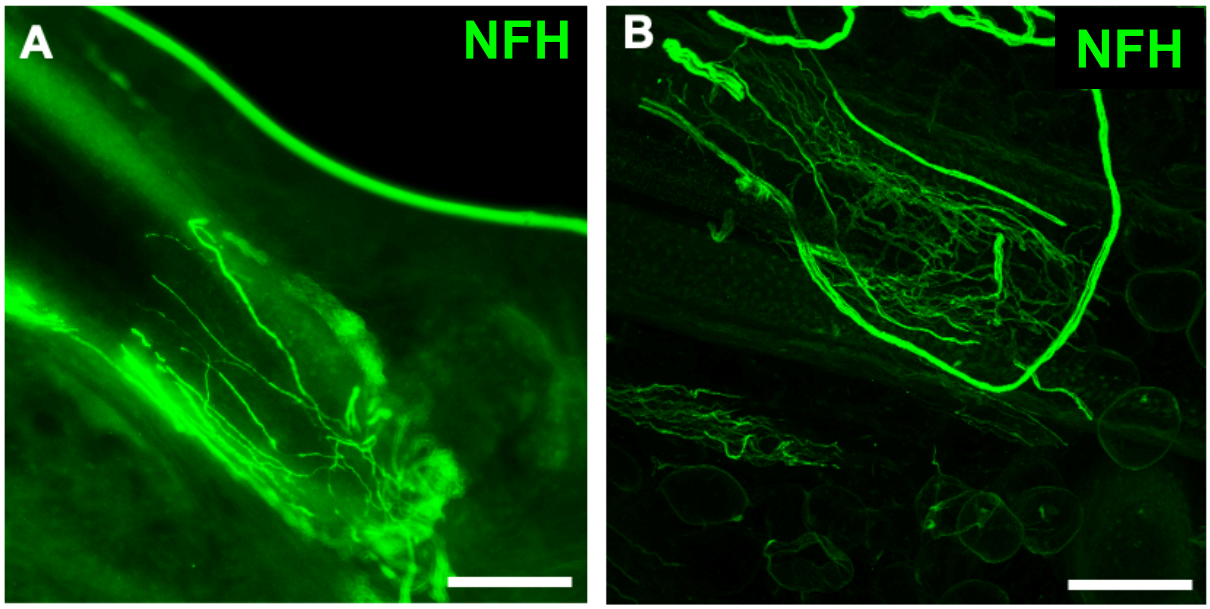


Figure 3.3 Human HFs from different patients are innervated by LTMRs forming circumferential and longitudinal endings.
NFH Immunostaining of tissue sections reveals the presence of longitudinal and circumferential endings NFH+ around human HFs (dashed lines) from a 47 years old patient (A) and 37 years old patient (B). Scale bars 100µm. Representative example of 28 samples from 8 patients.

Since the freezing process can damage tissue even though the application of cryoprotective steps, such as sucrose incubation[157], I decided to try a w hole-mount protocol based on clearing steps with BABB[67]. With this approach, we aim to avoid freezing therefore preserving tissue integrity but also increase with the capabilities to increase the penetration of the microscope to about 600µm. Thus, we collected human follicular units composed with 2-3 HFs each unit from hair transplant surgery and fixed them with 4% PFA overnight to perform the whole mount immunostaining protocol with BABB clearing.

The whole mount protocol was tested using the PGP9.5 and NFH antibodies. I imaged sections of 250µm and plot the z-stack **(Figure 3.4)** Using this whole mount protocol is easily appreciated the cylindrical shape of the follicles and the axons wrapping around it. However, the pictures show a high level of autofluorescence that is consistent between primary antibodies and between antibody concentrations and incubation times. Thus, as with the tissue section, this whole mount stating with BABB failed to reveal the integrity of the lanceolate and circumferential endings around human HFs.

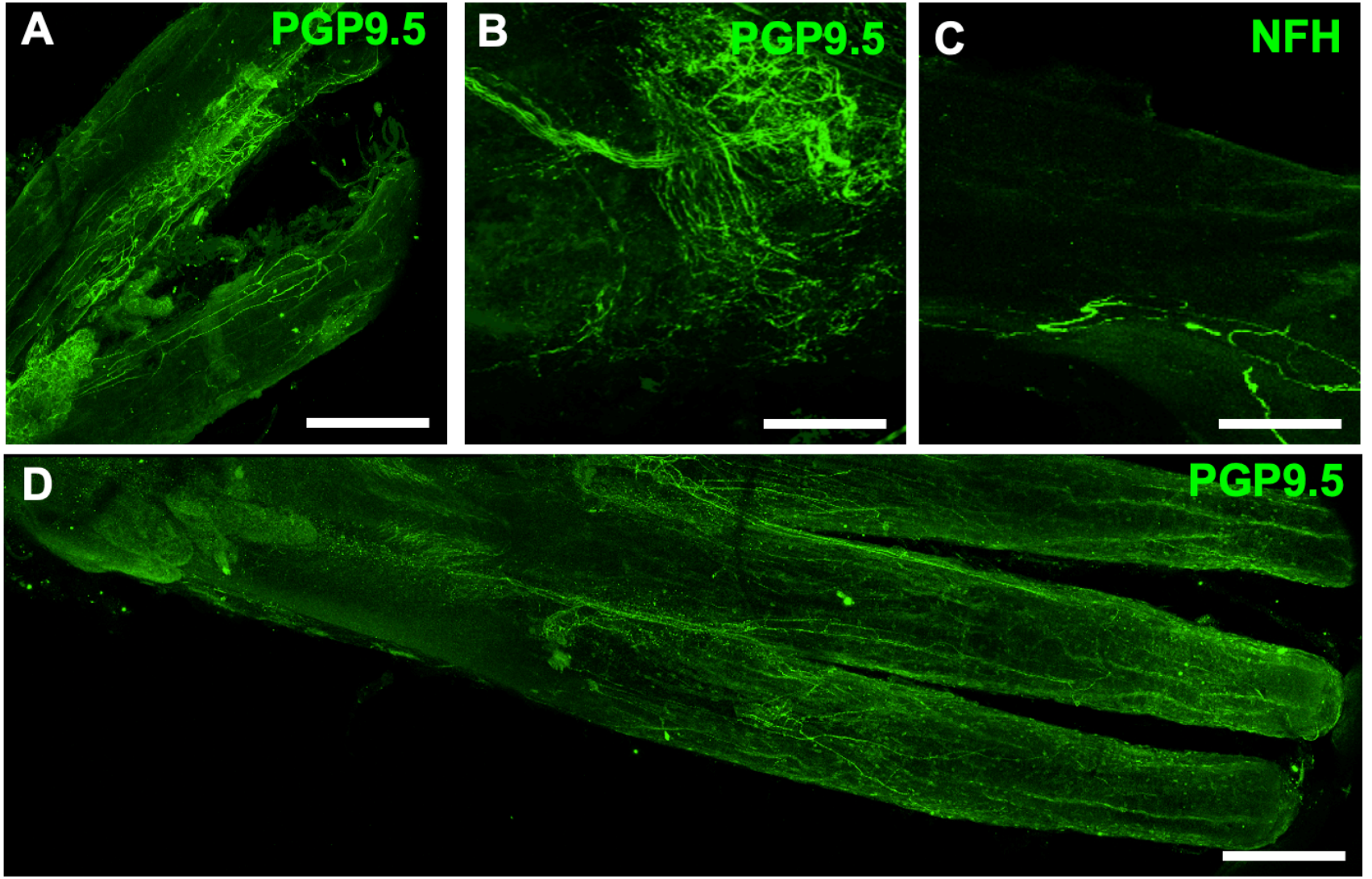


Figure 2.4 Human HFs are innervated by LTMRs forming circumferential and longitudinal endings.
Whole-mount immunostaining with BABB clearing shows PGP9.5 and NFH+ nerve endings from LTMRs around human HF from different patients (A-D). Scale bars 100µm. Representative example of 15 samples from 7 patients

Even with cleared tissue, the BABB staining protocol could lead to high autofluorescence in skin tissue due to the high level of extracellular proteins which are difficult to clear with organic solvents. Therefore, instead of trying to optimize the BABB protocol, I decided to try iDisco protocol which uses different organic solvents and has been used with large skin samples without apparent autofluorescence[158,159]. With iDisco, instead of BABB, DBE is used as a clearing agent. The protocol also uses a pre-treatment with methanol and an alternative pre-treatment without methanol which uses non-ionic surfactants instead. Both pre-treatments were evaluated with our neuronal antibodies PGP9.5 and NFH. The pre-treatment without methanol was selected because of less autofluorescence and better tissue morphology preservation (**Figure 3.5)**

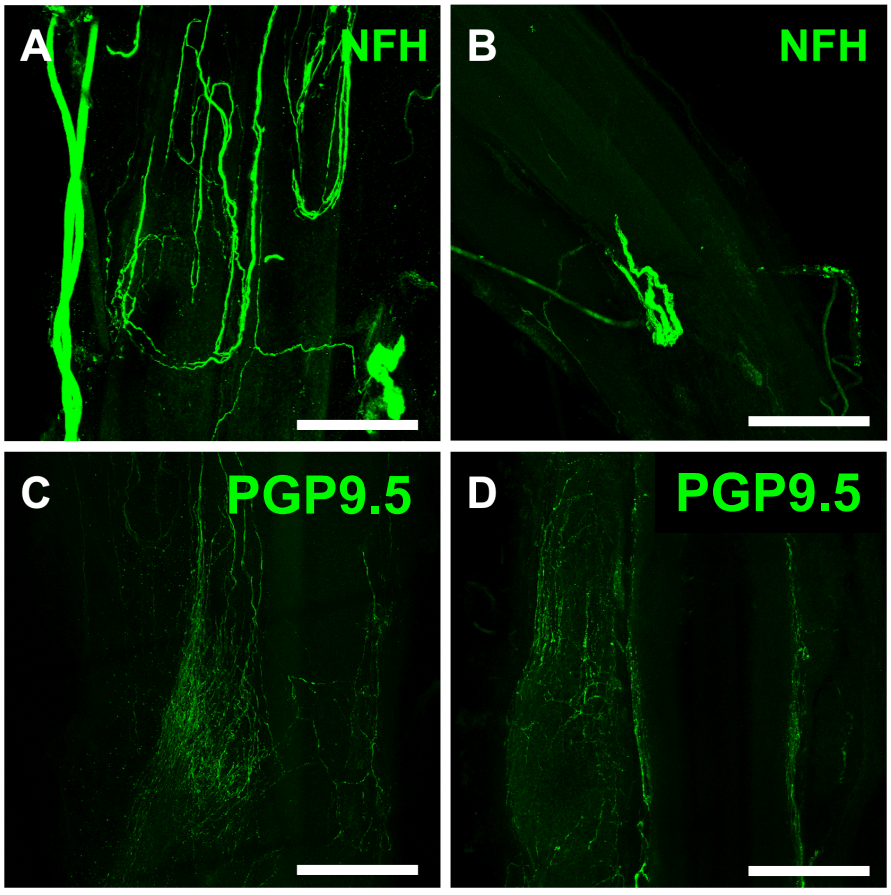


Figure 3.5 iDisco whole-mount protocol optimization for whole human follicular units using methanol and alternative pre-treatment.
(A-B) Immunostaining of 200µm follicular unit using NFH antibodies with pre-treatment (A) or methanol pre-treatment (B).
(C-D) Immunostaining of 200µm follicular unit using PGP9.5 antibodies with alternative pre-treatment (C) or methanol pre-treatment (D).
Scale bars 200µm. Representative example of 28 samples from 8patients (A-B) and 15 samples from 7 patients (C-D).

The antibodies PGP9.5 and NFH were used again this time with the iDisco protocol with non-methanol pre-treatment to try to reveal the lanceolate structure of the longitudinal endings and the complete innervation patterns of the whole follicular unit. To visualize the data, a whole tile scan together with z-stack was used to image the sample in a 3D fashion **(Figure 3.6)**. As shown by our previous data and protocols used, all HFs per follicular unit are innervated by LTMRs. Although both antibodies, PGP9.5 and NFH marked positive axons and the quality and that the morphological information of the LTMRs endings has increased using iDisco protocol compared with BABB, the protocol still failing to reveal the lanceolate shape structure of the longitudinal ending around human HFs.

I realize that most of the whole mount protocols to image mouse and human skin use a quick, fast and sometimes double fixation protocol. In mice, animals were immediately transcardially perfused with 4%PFA in PBS at 4C. Afterwards, skin was removed and post-fixed again in 4%PFA in PBS at 4C overnight[67]. In humans, sections were used from skin that has been fixed immediately after extraction using Zamboni solution, a variation of PFA with added picric acid[148].

The HFs I used were extracted and kept in DMEM and or William's Medium E for extended periods of time and were fixed 5-6h after surgery. In the peripheral nervous system, because axonal regeneration occurs, axons start to degrade as earlier as 1h after nerve injury, a process known as Wallerian degeneration[160]. This process involves immune cells and Schwann cells which use different catalytic processes to clean the old, excised axons giving space for new axons[161]. Because the lanceolate endings are highly covered with terminal Schwann cells processes, I postulate that the process of nerve clearing could be extremely quick after HF excision.

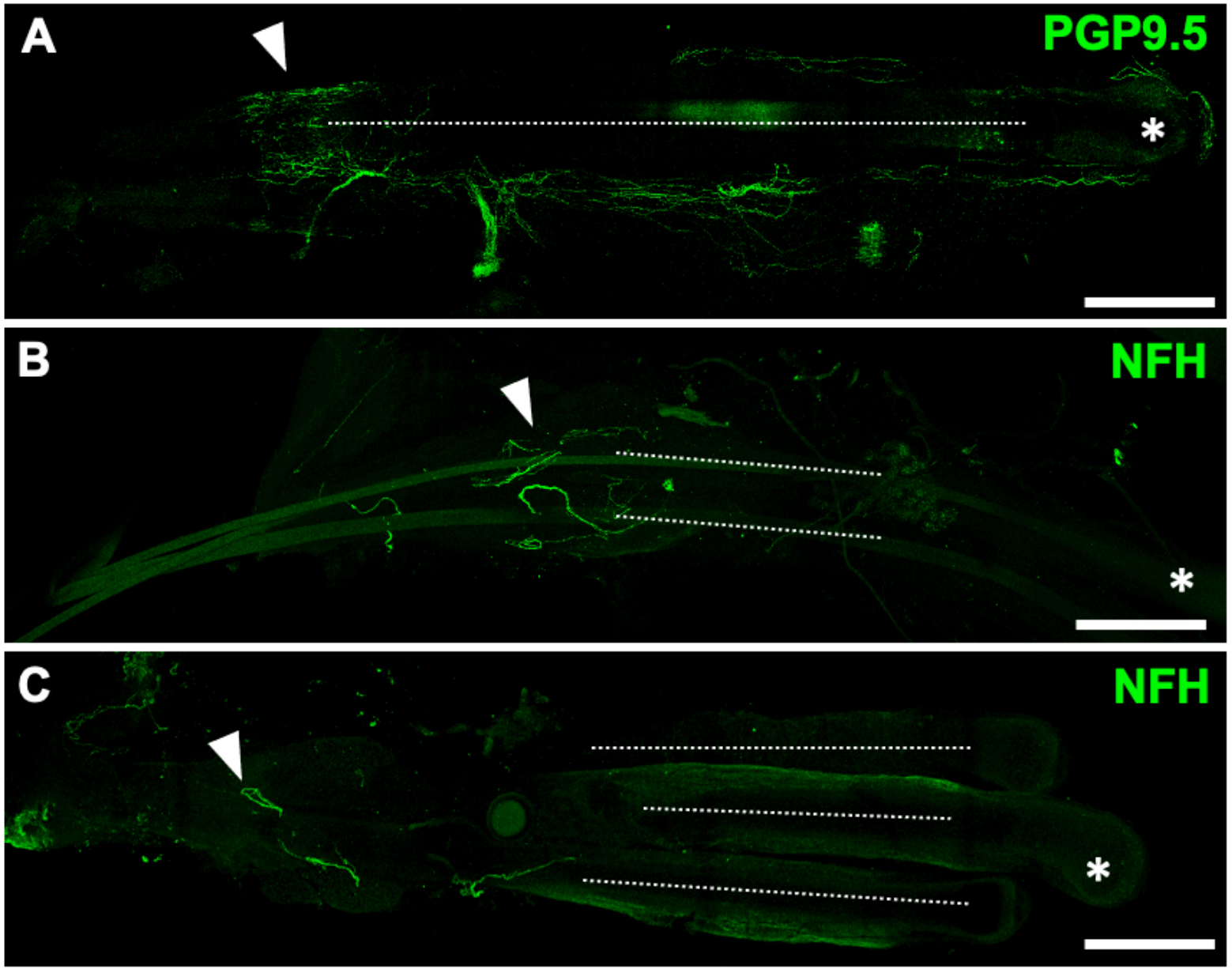


Figure 3.6 iDisco whole-mount protocol with whole follicular units reveals LTMRs axons
(A) Follicular unit staining using PGP9.5 antibody showing a follicular unit innervated in the upper region of the follicle (arrowhead). Dermal papilla (asterisk).
(B-C) Immunostaining of 500µm follicular unit using NFH antibodies showing LTMR axons in the upper region of the follicle. (arrowhead) and dermal papilla (asterisk) (B-C). Scale bars 500µm. Representative example of 15 samples from 7 patients (A) and 28 samples from 8 patients (B-C).

Therefore, the lack of lanceolate shape axons in the imaging was because of a late fixation step rather than a problem in the immunostaining protocol could be the problem. Consequently, we start a new collaboration with a hair transplant surgeon who allow me to go to the clinic on the day of the surgery and to collect the sample and put them into 4%PFA in PBS straightaway after excision. I collected a total of 70 follicular units from 7 different patients which were undergoing hair transplant surgery which accounted for more than 70 human HFs (Some examples of raw follicular units can be seen in Figure A1 in appendix). A combination NFH and S100 antibodies was used, to target longitudinal axons from LTMRs and S100 to target myelinating terminal Schwan cell processes respectively with the iDisco whole-mount protocol without methanol pre-treatment in whole follicular unit fixed immediately after excision **(Figure 3.7A & B**). In the first follicular unit, there are 3 different hairs: one vellus hair innervated by myelinated S100+ LTMRs NFH+ making longitudinal-lanceolate endings (asterisk) and 2 terminal hairs, which both display myelinated S100+ LTMRs NFH+ making longitudinal-lanceolate and circumferential endings (double and triple asterisk). A closer look to the longitudinal endings **(Figure 3.8)** reveals a collar of lanceolate endings suggesting that the quick fixation step is critical to preserve the morphology of the LTMRs end organs. To investigate further the lanceolate structure of different follicular units, we employ the whole mount protocol with NFH immunostaining with follicular units from different patients **(Figure 3.9).** Interestingly, in figure 3.8 A' there are 2 different NFH afferent branches leaving the follicle suggesting that 2 different types of LTMRs are innervating the same HF. Overall, this data suggest that humans have LTMRs innervating HFs which form circumferential and longitudinal lanceolate complexes. Furthermore, for immunostaining of large skin samples where the aim is to target axons, to understand its morphology is it required to use immunostaining protocols with clearing steps and to fix the tissue a soon as possible to prevent axonal

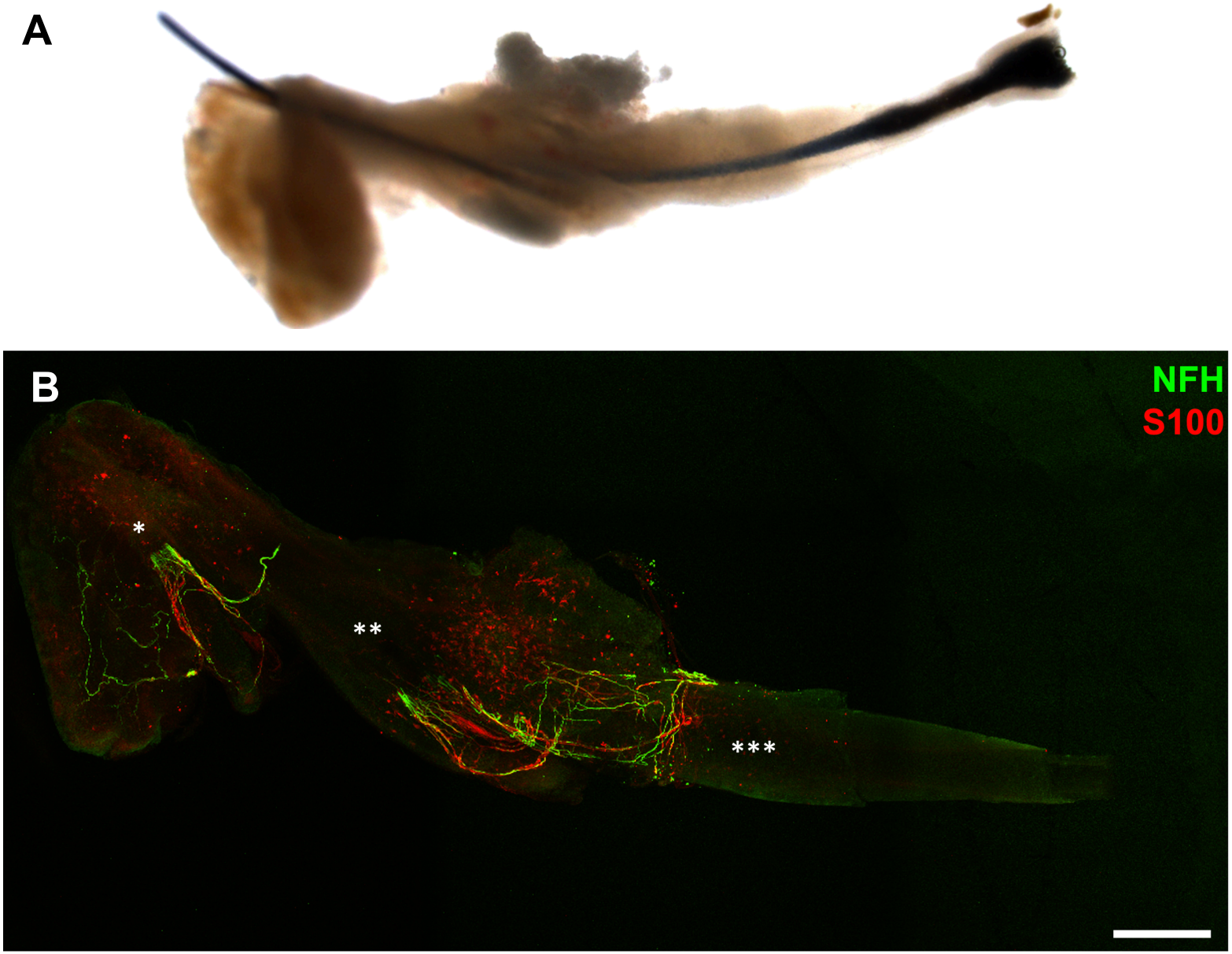


Figure 3.7 iDisco whole-mount immunostaining of whole follicular units reveals highly myelinated longitudinal-lanceolate complexes and circumferential endings.
(A) Example of excised follicular unit from human scalp skin fixed immediately after excision
(B) Human follicular unit (from A) composed by a vellus hair (asterisk) showing myelinated longitudinal-lanceolate complexes, circumferential endings (left arrowhead) and NFH+ afferents. Terminal hair (double asterisk) showing myelinated (S100+) longitudinal-lanceolate complexes NFH+ (right arrowhead). Dominant terminal hair (triple asterisk) with few longitudinal endings and a complex network of myelinated S100+ circumferential endings NFH+ (arrow). Scale bar 500µm. Representative example of 11 sampled from 5 patients.

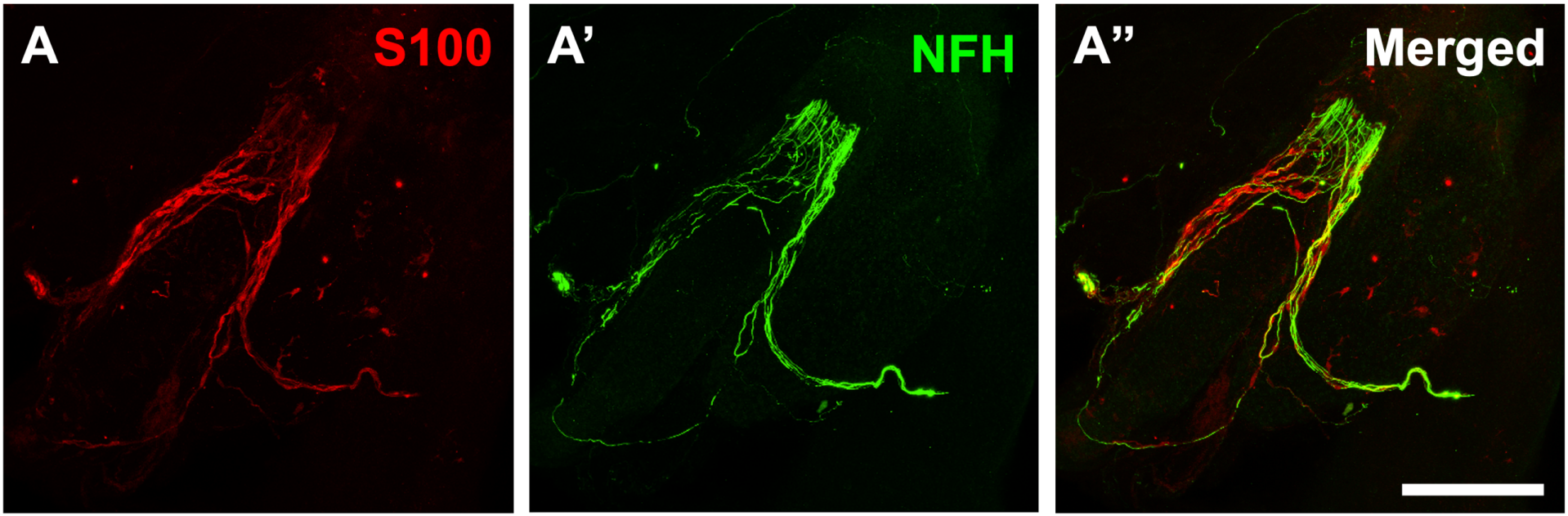


Figure 3.8 20x magnification of the vellus hair longitudinal endings (asterisk) on Figure 3.6.
S100 (A), NFH (A') and merged (A'') signal showing the highly myelinated collar of longitudinal lanceolate complexes in a vellus HF. 2 different NFH+ afferent processes leave the follicle. Scale bars 500µm. Representative example of 11 samples from 5 patients.

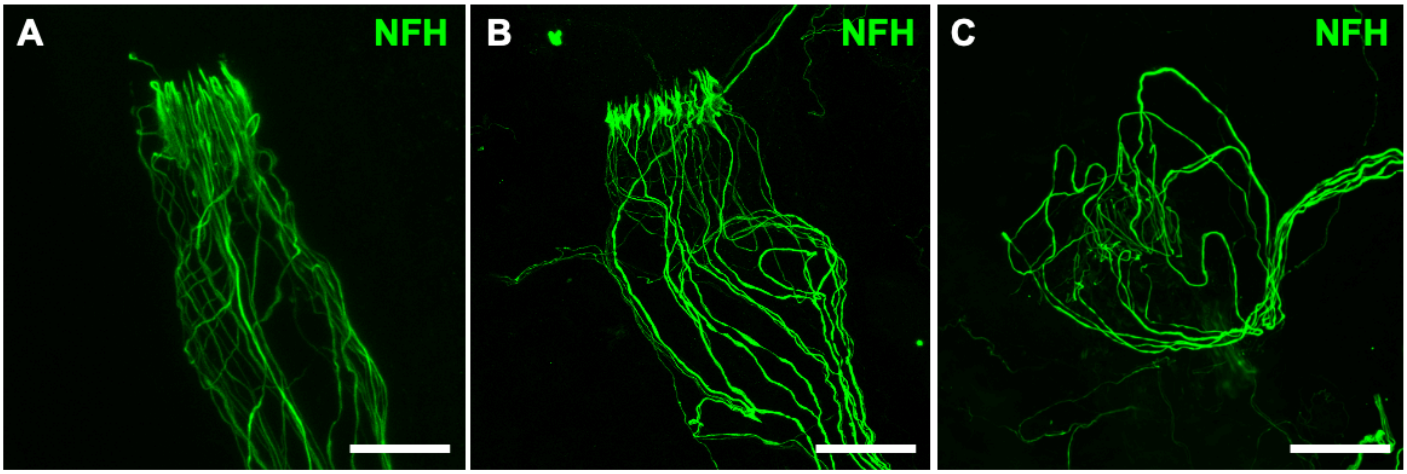


Figure 3.9 Terminal hairs from 3 different patients innervated by longitudinal-lanceolate and circumferential endings
Longitudinal-lanceolate and circumferential endings around human scalp terminal HFs from 3 different patients (A-C). Longitudinal endings forming the typical lanceolate structure-shape structure signature of HF innervating LTMRs (B, arrowhead). Scale bars 200µm. Representative example of 28 samples from 8 patients.

3.2 Human HFs are innervated by different types of mechanoreceptors.

After optimizing the iDisco whole mount immunolabelling method for human follicular units to show that human HFs are innervated by LTMRs making circumferential and lanceolate longitudinal edgings, we want to investigate if, as mice do, humans have different types of LTMRs innervating HFs. As said previously in the introduction, mice have 5 different types of LTMRs and a type of HTMR innervating different HF types. Each of these mechanoreceptors has been targeted in genetic reporter mouse using specific markers which are stated in table 1. Therefore, to try to target these specific sensory neurons in human HF, we decide to use antibodies against these markers and use our optimized whole-mount protocol to unravel its presence and morphology. Apart from these specific molecular markers, we will use again NFH and PGP9.5 as pan neuronal markers which will give validity about the neuronal origin of the targeted axons.

Before moving to specific markers, NFH is quasi pan neuronal marker because although it targets 4 different types of LTMRs innervating HFs, these LTMRs show different morphology

which allows specific identification. For example, there is just one type of NFH+ LTMRs which is associated with Merkel cells, Aβ-SA-LTMRs and in combination with a K20 antibody which is specific for Merkel cells it is possible target Aβ-SA-LTMRs.

3.2.1 Circumferential Aβ-Field-LTMRs

Aβ-field LTMR is the only NFH+ LTMRs which form circumferential endings around HFs to Figure 3.10 is it possible to see circumferential endings which are positive for NFH+ suggesting that this circumferential nerve endings comes from a Aβ-Field-LTMRs. Furthermore, this circumferential ending is highly myelinated with S100+ myelin suggesting high conductance velocities in the Aβ range therefore supporting the idea that indeed this axon comes from an Aβ-Field-LTMR. In figure 3.10 staining with NFH with follicular units shows the presence of a model circumferential ending.

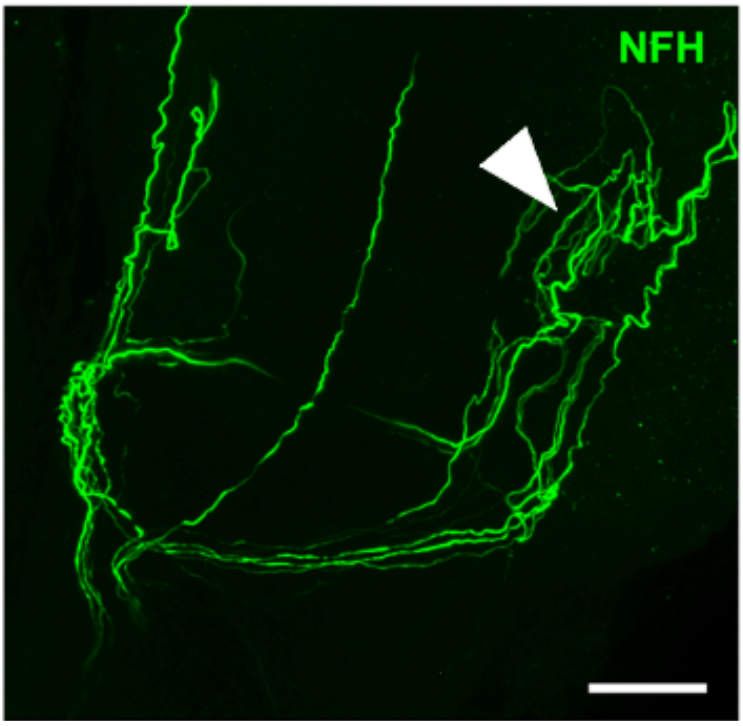


Figure 3.10 Terminal hair innervated by Aβ-Field-LTMR circumferential endings
Circumferential endings around human scalp terminal HFs Longitudinal endings can also be seen in the top part (arrowheads). Scale bar 50μm. Representative example of 28 samples from 8 patients.

3.2.2 Merkel cell neurite complex

Next, we wanted to assess the presence of the Merkel cells neurite complex in the human HF which is composed of Merkel cells and a Aβ-SA-LTMR. Therefore, we use a combination of NFH antibodies together with K20 which is a specific marker of human Merkel cells. Using whole-mount imaging is it possible to reveal the Merkel cell neurite complex around human HFs and its NFH+ afferent (**Figure 3.11**). Several investigations using K20 and K18 antibodies in human skin and human HFs have shown the presence of Merkel cells, however, these investigations have failed to show the afferent fibre and the complete organization of the Merkel cell neurite complex around the follicle[69,162,163]. From our knowledge, out data is the first one to show clearly the collar of Merkel cells and its afferent fibre. Therefore, human HFs have Merkel cell neurite complexes to process light touch.

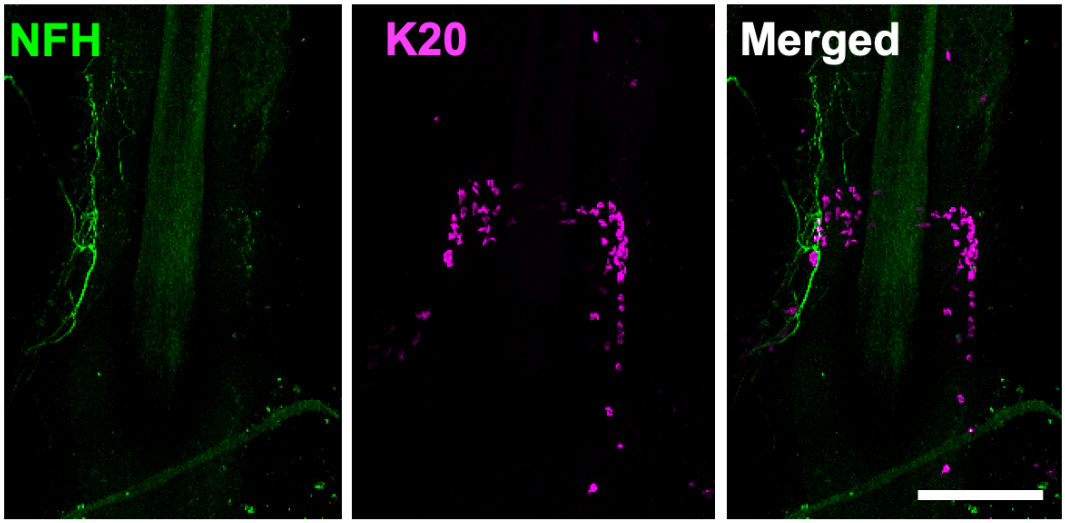


Figure 3.11 Whole-mount staining of human terminal HF showing Merkel cells neurite complex.
Aβ-SA-LTMRs NFH+ (A) are grouped in the region where Merkel cells K20+ are (C) forming the Merkel cell neurite complex. Scale bars 50μm. Representative example of 2 samples from 1 patient.

3.2.3 Longitudinal Aβ-RA-LTMR

To investigate the presence of Aβ-RA-LTMR, we use a combination of NFH and Ret antibodies. Ret is expressed in 3 different LTMRs innervating HFs (table 2), of which just one has longitudinal endings: Aβ-RA-LTMR. Therefore, Ret+ longitudinal ending will be from Aβ-RA-LTMR. Consequently, we use the whole-mount protocol together with NFH+ and Ret+ antibodies (**Figure 3.13**). We found that some NFH+ longitudinal endings, are also positive for Ret + suggesting that human HFs are innervated by from Aβ-RA-LMTRs. Interestingly, some LTMR longitudinal endings in figure 2.11 are NFH+ but Ret negative suggesting that this LTMRs could be Aδ-RA-LTMR.

3.2.4 Longitudinal Aδ-RA-LTMR

To investigate if some of the longitudinal endings innervated human HFs originate from Aδ-RA-LTMRs, we use a combination of NFH+ and TrkB antibodies. TrkB is a transmembrane protein expressed specifically in Aδ-RA-LTMRs. Hence, it's a unique signature of this LTMR since there is no other LTMR expressing TrkB. Using this approach, with two separated TrkB antibodies we failed to map any longitudinal ending therefore it was not possible to reveal the presence of Ad-RA-LTMRs innervating human HFs **(Figure 3.14).**

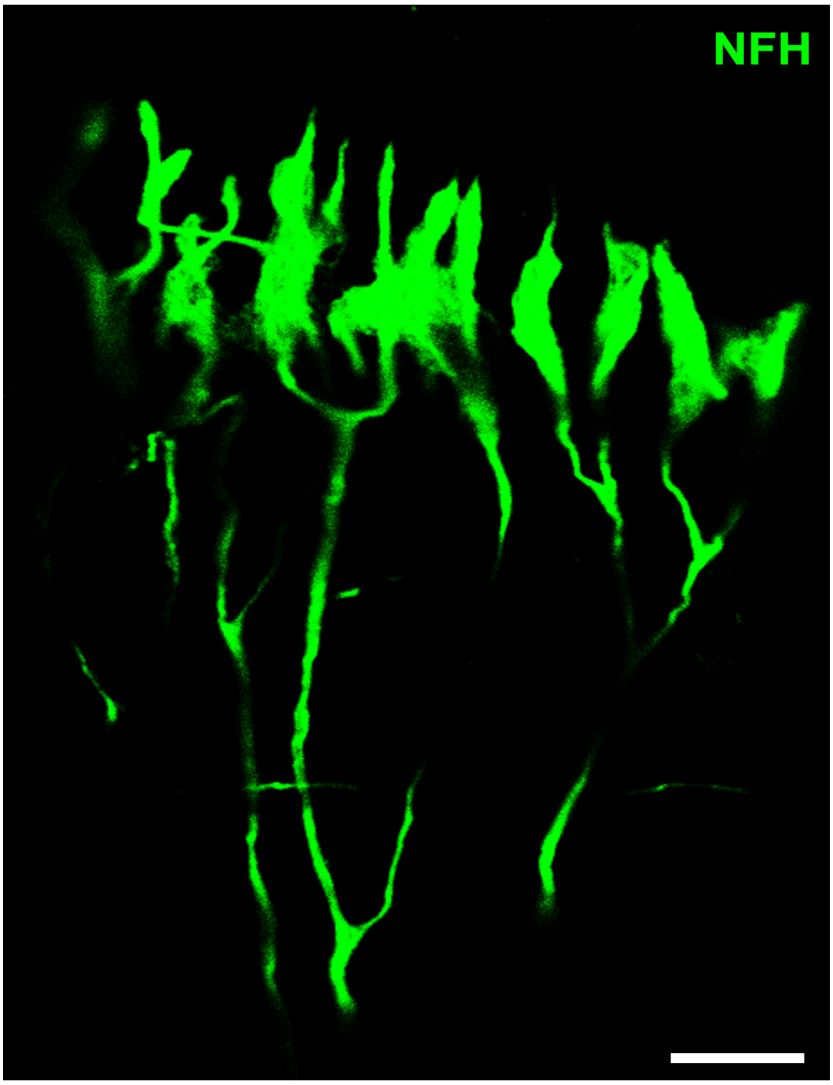


Figure 3.12 Terminal hair from human scalp skin innervated by LTMRs forming longitudinal-lanceolate endings
LTMRs forming longitudinal-lanceolate endings NFH+ reveals the specialized lanceolate-like structure (arrow) on the collar of the extreme axon end. Scale bars 20μm. Representative example of 28 samples from 8 patients.

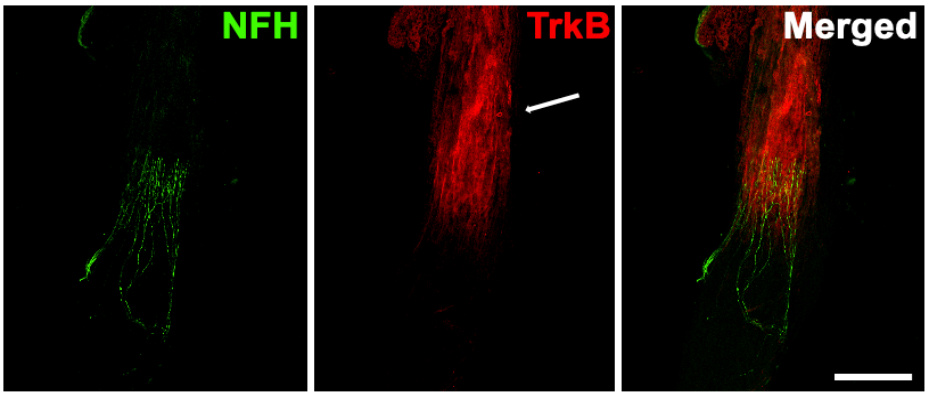


Figure 3.14 TrkB antibody fails to label Aδ-RA-LTMR on terminal hairs from human scalp innervated by longitudinal endings NFH+
LTMRs forming longitudinal-lanceolate endings NFH+ are TrkB- failing to reveal Aδ-RA-LTMR. The upper region of the follicle is TrkB+ (arrowhead). Scale bar 200μm. Representative example of 2 samples from 1 patient.

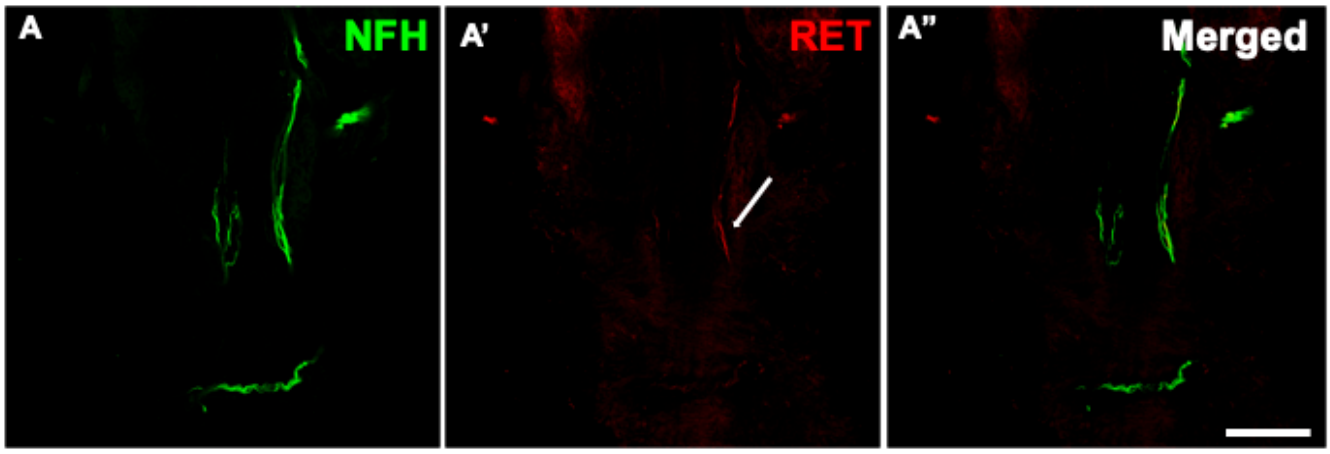


Figure 3.13 Terminal hair from human scalp skin innervated by Aβ-RA-LMTR Ret+ forming longitudinal endings
LTMRs forming longitudinal-lanceolate endings NFH+ (A) are also Ret+ revealing by Aβ-RA-LMTR (B). Some Ret- longitudinal endings suggest the presence Aδ-RA-LTMR (A, arrowhead) of Scale bar 200μm. Representative example of 4 samples from 2 patients.

To assess the validity of our antibody, we use DRG section from mice a positive control. Section stain show TrkB positive cells suggest that this antibody works in mice **(Figure 3.15).** Although with caution that data suggest that human HF might not be innervated by Ad-RA-LTMRs so this LTMRs can be specific for mice or rodents. Again, is also possible the antibodies work with mice but not in humans so further research should be done to validate our results.

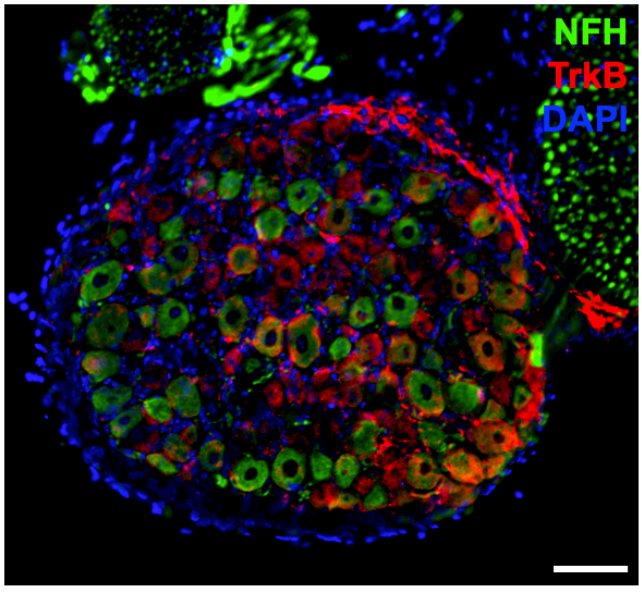


Figure 3.15 TrkB antibody labels medium and some large soma size murine DRGs
Large soma size DRG neurons NFH+ Aβ-RA-LMTR (B). Some Ret- longitudinal endings suggest the presence Aδ-RA-LTMR (A, arrowhead) of Scale bars 200μm. Representative example of 1 sample from 1 mouse.

3.2.5 Longitudinal C-LTMR

Finally, to test the presence of slow conduction velocity C-LTMRs, we used an antibody against the enzyme TH+, a precursor of the neurotransmitter dopamine which is specific for C-LTMRs and for the sympathetic nerves associated with the APM[164–166]. Therefore, the only longitudinal end organ that is TH+ antibody will be from a C-LTMR. Thus, we use a combination of TH and PGP9.5 antibodies to test the presence of C-LTMRs and their longitudinal endings around human HFs. Using our whole-mount protocol, with the combination of these antibodies, it is possible to depict some Th+ longitudinal endings around the HF from 2 different patients **(Figure 3.16).**

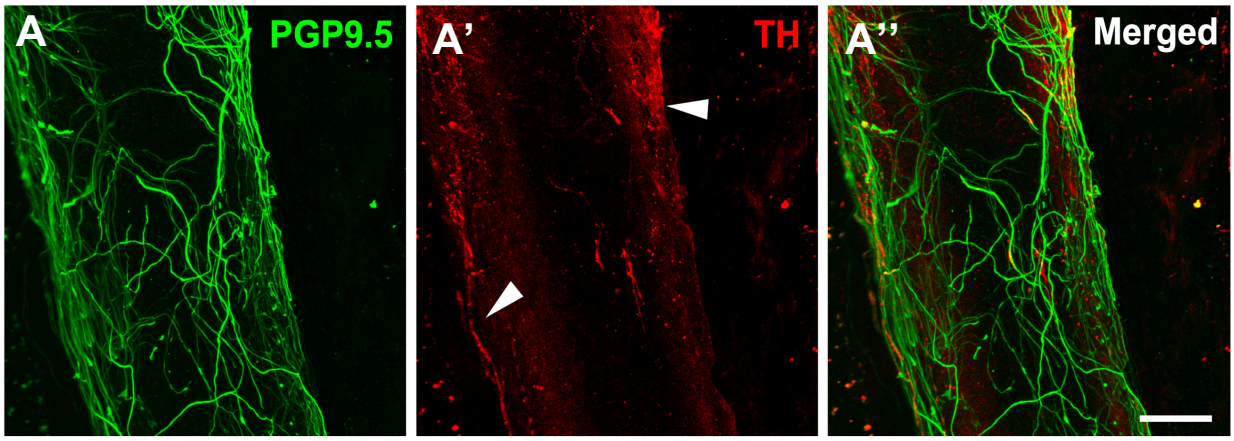


Figure 3.16 Terminal human HFs are innervated by C-LTMRs
Human terminal HF innervated by longitudinal and circumferential endings PGP9.5. Th antibody targets few longitudinal endings which are also positive for PGP9.5 suggesting C-LTMRs innervate human HFs. Scale bar 50μm. Representative example of 7 samples from 3 patients.

Next this TH antibody was tested with different patients to try to see the whole collar of longitudinal endings around the HF. Other patients also show longitudinal axons which are TH+ but NFH- suggesting that this are longitudinal endings originating from C-LTMRs.

As said before, C-LTMRs are NFH- so this data suggests this TH+ and NFH- longitudinal axons are from C-LTMRs **(Figure 3.17).** Furthermore, is possible to see the TH+ sympathetic nerve from the APM suggesting the antibody works well. Again, although is it not possible to

see the whole lanceolate structure or collar of nerves around follicles, these longitudinal-like endings are in the region where other longitudinal endings are located as show by the antibody NFH, therefore we suggest that this longitudinal-like endings are from C-LTMRs. A possible explanation of this impossibility to find the whole collar of C-LTMR longitudinal nerves could be due that C-LTMRs are the smallest LTMRs with no myelin. Therefore, although the fixation step is done straight away after follicular unit extraction, C-LTMRs might start degrading first leading to less longitudinal ending preservation.

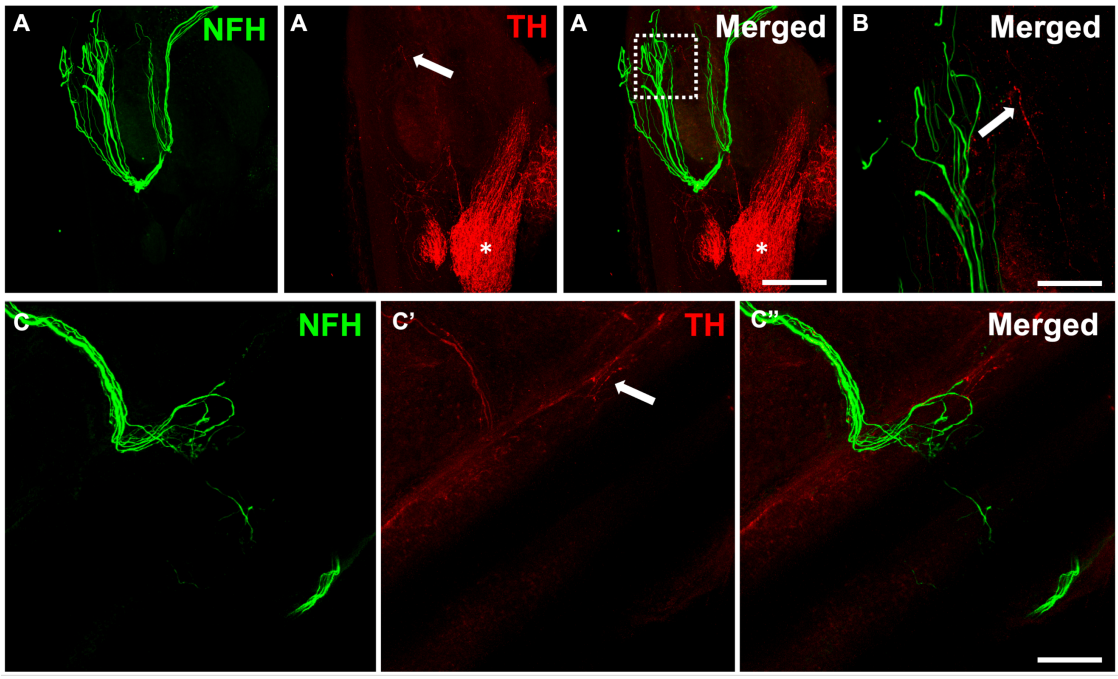


Figure 3.17 TH antibody shows C-LTMRs longitudinal endings around human terminal HFs from 2 different patients.
(A) LTMRs longitudinal endings form a collar of nerves around HFs NFH+. Sympathetic nerves from the APM (asterisk) and longitudinal endings TH+ (arrow) suggesting C-LTMR innervation. Scale bars 200µm
(B) Magnification from the white box in A'' showing longitudinal endings TH+ but NFH-. Scale bar 50µm
(C) LTMRs longitudinal and circumferential endings form a collar of nerves around HFs NFH+. Longitudinal endings TH+ (arrow) are NFH- suggesting C-LTMRs innervation Scale bars 50µm. Representative example of 4 samples from 4 patients.

Up to now, using a combination of immunolabelling with our optimized whole-mount protocol we were able to show that human HFs are innervated by 4 different types of LTMRs: Merkel cell neurite complexes K20+ with their Aβ-SA-LTMR afferent, longitudinal Aβ-RA-LTMR NFH+ and RET+, circumferential Aβ-RA-LTMR NFH+ and longitudinal C-LTMRs TH+.

3.3 Human HFs are innervated by a type of HTMRs

3.3.1 Circumferential Aδ-HTMRs

Finally, as explained before, recent research has shown that murine HFs are also innervated by a type of HTMR which make circumferential endings. This ending is CGPR+ and is involved in processing nociceptive stimulus like hair shaft pulling[84]. To investigate the presence of this HTMR in human HFs, we employed our whole-mount protocol together with an antibody against CGRP. This molecular marker is specific for this HTMR, therefore a circumferential ending CGRP+ should be from this Aδ-HTMR.

After using the beforementioned experiment, we were able to see circumferential ending CGRP+ suggesting that human HFs are innervated by Aδ-HTMRs **(Figure 3.18)**.

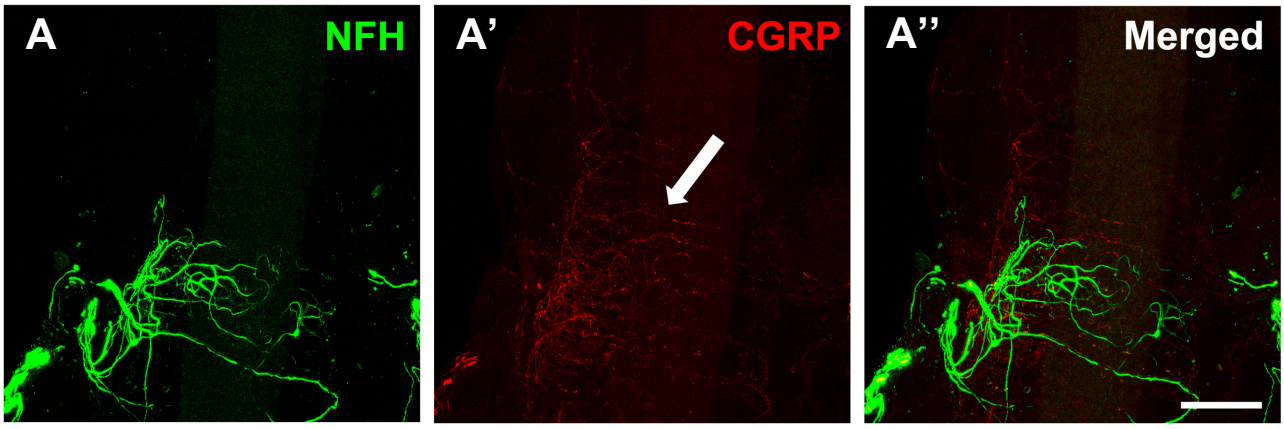


Figure 3.18 Human terminal HFs are innervated by Aδ-HTMRs forming circumferential endings
Longitudinal and circumferential endings NFH+ around human HFs and CGRP+ circumferential endings (arrow) but NFH- suggest the presence of circumferential Aδ-HTMRs. Scale bars 100µm. Representative example of 2 samples from 2 patients.

Thus, humans have an HTMR innervating HFs which we suggest is involved in processing hair pulling. That will help explain the pain and uncomfortable sensation we feel when our hairs are plucked or pulled.

Apart from the 4 different types of LTMRs innervating human HFs, it has been showed that a HTMR making circumferential endings also innervate human HFs. Thus, a total of 5 different types of sensory neurons innervates human HFs: 4 of them processing light touch and one processing pain. Our results help to explain the excitability of our HFs to hair deflection and to justify the sensitivity of our hairy skin.

3.4 Localization of LTMRs within the human HF

Looking collectively at the whole-mount immunostaining with whole follicular units, it is noticeable that longitudinal and circumferential endings are attached to a specific follicular region. In mice, it has been shown that the bulge and upper bulge region of the HF where Gli1, K15 and CD34 positive cells have their niche is the zone where LTMRs attach[98,167]. In human HFs, there is no investigation about the follicular region and cells which LTMRs innervate. Unraveling the cell types which are located close to the longitudinal endings can give valuable insight in understanding if other cell types located in the LTMR vicinity are capable of responding to tactile stimulus (i.e hair shaft movements) and to modulate how LTMRs send information towards higher centres such as the spinal cord and the brain. Thus, we sought to investigate the compartment of the human HF where LTMRs form circumferential and longitudinal endings. Since seems that LTMRs innervate the follicle in the bulge region, we will use ORS markers specific for the bulge region.

To unravel the zone where LTMRs reside in the follicle, we use our whole mount protocol with whole follicular units with the LTMR marker NFH together with several HF bulge markers. Thus, we use the whole-mount protocol in combination with our NFH and K15 antibody on whole follicular units (**Figure 3.19**). In this picture is possible to see a human follicular unit composed by 3 terminal hairs in anagen phase and a single hair in telogen phase.

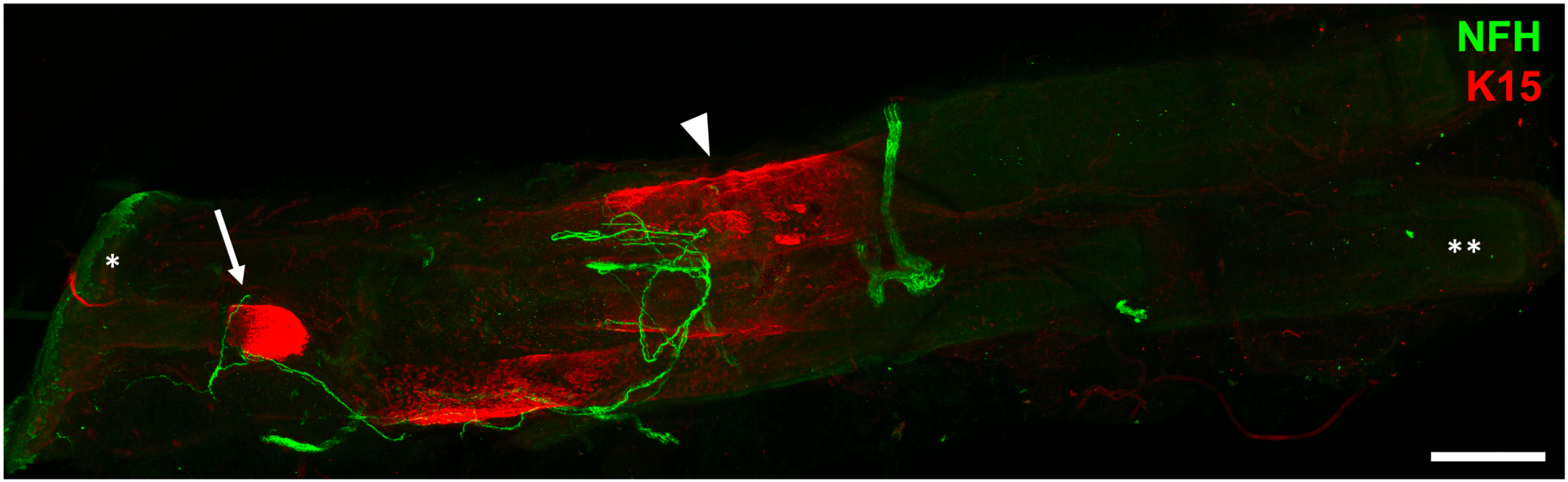


Figure 3.19 Whole mount from entire follicular unit shows NFH+ LTMRs are localized in the upper and bulge follicular region where K15+ cells have their niche.
Whole follicular unit composed by one telogen hair (arrow) and 3 terminal hairs. NFH+ longitudinal and circumferential endings are localizer in the upper region where K15+ HF stem cells have their niche (arrowhead). Epidermis is localized in the left (asterisk) while dermal papilla is localized on the right (double asterisk). Scale bar 500µm. Representative example of 20 samples from 7 patients

The mid-region of anagen hairs are K15+ suggesting that these cells are HFSC and that this region of the follicle could be considered as the bulge. Having a look at NFH+ nerve endings, is it possible to see that both longitudinal and circumferential endings are in the upper K15+ region suggesting a co-localization of LTMRs and the upper bulge. To validate the localization of NFH+ positive LTMRs within the follicle, we used the same staining as per figure 3.19 in different patients. As with 3.19, longitudinal and circumferential endings are in the K15+ upper region **(Figure 3.20).**

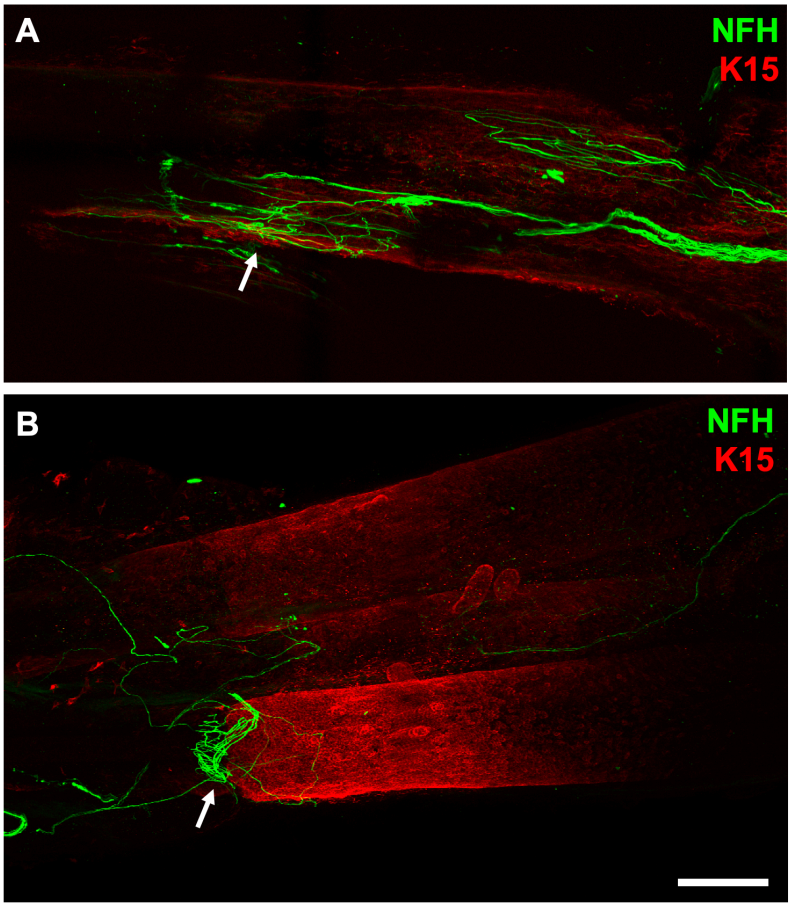


Figure 3.20 Follicular unit whole-mount staining from 2 different patients shows NFH+ LTMRs are localized in the upper and bulge follicular region where K15+ cells have their niche.
Follicular units composed by different anagen hairs. NFH+ longitudinal and circumferential endings are localizer in the upper region where K15+ HF stem cells have their niche (arrows). Scale bar 500µm. Representative example of 20 samples from 7 patients.

Although in figures 3.19 and 3.20 is it possible to see a close localization between NFH+ LTMRs in the bulge region where K15+ HFSC are, some pictures are not clear. For example, in figure 3.20A longitudinal LTMRs NFH+ and the K15+ HFSC co-localize but in figure 3.20B, the longitudinal endings are located clearly in the upper K15+ HFSC region. (**Figure 3.20A**). Therefore, to better understand the localization between LTMRs NFH+ in the bulge region of the follicle with the K15+ HFSC, we use a use higher magnification at the regions between the K15+ and NFH+ signals (**Figure 3.21**). NFH+ LTMRs are localized close to bulge region where K15+ HFSC reside. Whereas circumferential endings are on the K15+ region, longitudinal endings are more located in the upper part suggesting that the most innervated regions are the bulge and the upper bulge region of the HF. Again, a close look to pictures 3.21 suggests that longitudinal and circumferential LTMRs NFH+ are located in the K15+ region of the follicle. Still, after using samples from 7 different patients we still do not understand the exact follicular region where LTMRs innervate the follicle.

Therefore, to try to unravel this specific region, we have used different antibodies as bulge markers to reveal the cell types in the same plane of the longitudinal endings. We decided to use antibodies against the bulge markers CD200, a6 integrin, Nestin and Gli1.

The bulge region of the human HF is composed by different cell types composed of different molecular markers[168]. A close look at figures 3.20B, 3.21D and 3.21 E shows that the NFH+ longitudinal endings from LTMRs are wrapped more toward the upper bulge region.

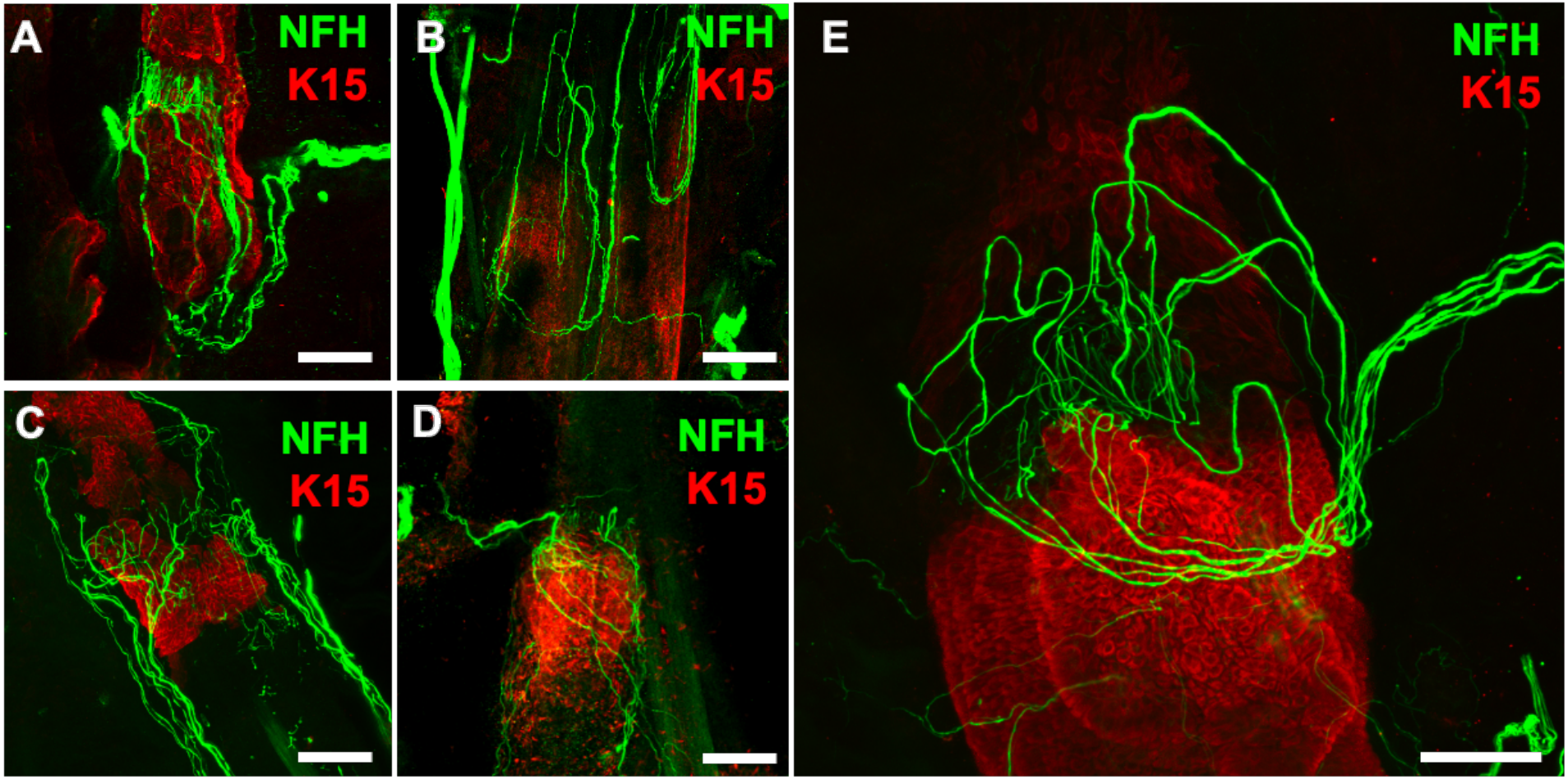


Figure 3.21 Whole-mount staining from several patients shows NFH+ LTMRs localized in the upper and bulge follicular region close where K15+ cells have their niche.
(A) longitudinal and circumferential LTMRs are located in the upper part of the K15+ region where HFSC reside.
(B) Longitudinal endings located in the K15 region but on the part where the K15 signal diminishes.
(C) Longitudinal endings located in the upper region
(D) Longitudinal endings locate in the k15 region
(E) Longitudinal endings located in the upper regions. in the Scale bar 500µm
Representative example of 20 samples from 7 patients.

The K15 antibody signal diminishes suggesting that the cell types which are in the same region where longitudinal endings are do not express K15. For example, in mice has been shown that this upper region is composed by HFSC which express Gli1 but not K15[98]. Therefore, to try to unravel this specific region with HFSC, we have used different bulge markers. We decided to use antibodies against the bulge markers CD200, a6 integrin, Nestin and Gli1 which are the ones have been found previously some in mice some in humans to be located in the bulge or upper bulge[98,169].

First, we use the general bulge marker CD200 which targets CD200+ HFSC (**Figure 3.22**). With this marker we obtained the same results as the K15 antibody, both markers target HFSC which are locate in the bulge region but not the ones located in the upper bulge region where longitudinal endings innervate the follicle.

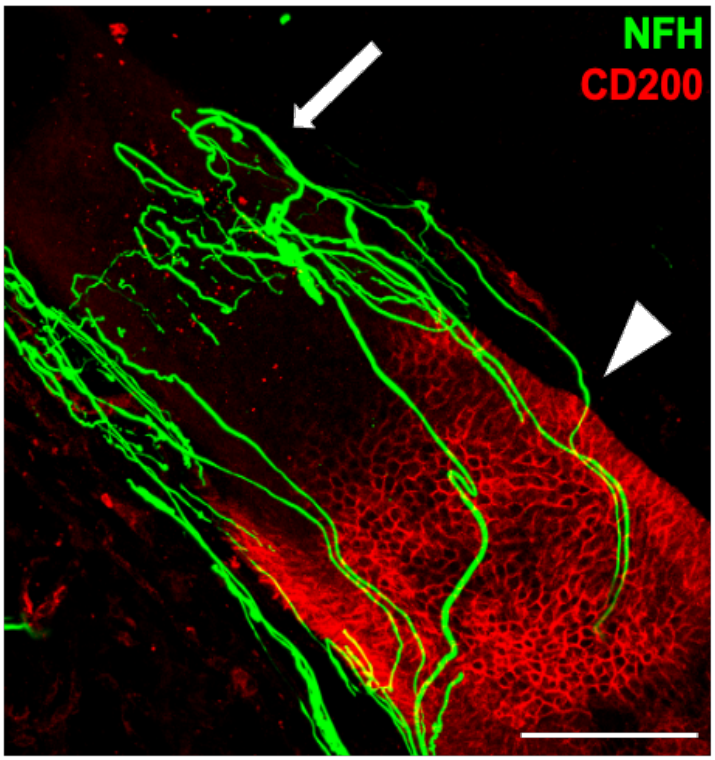


Figure 3.22 Whole-mount staining of human HF showing LTMRs NFH+ innervating the upper CD200+ region.
Human HF showing CD200+ HFSC in the bulge region (arrowhead) and longitudinal LTMRs NFH+ in the upper region of the bulge (arrow). Scale bar 50 100µm. Representative example of 6 samples from 2 patients.

After failing to find this specific region with CD200 antibodies, we continue by using other bulge markers such as α6 integrin, Nestin and Gli1 antibodies (**Figure 3.23**).

Gli1 and Nestin antibodies do not seem to target any follicular structure in the human HF (Figure 3.23). Although some research has shown the presence of these markers in the bulge cells located close to the longitudinal endings[98,170,171], these 2 antibodies have never been tested in human HFs therefore, it could be either that the proteins are not expressed or that the antibodies do not work. For limitations and time, we did not continue to try to see HFSC expressing Gli1 or Nestin. However, α6 integrin seems to mark the same region of the follicle similar to our CD200 and K15 antibodies.

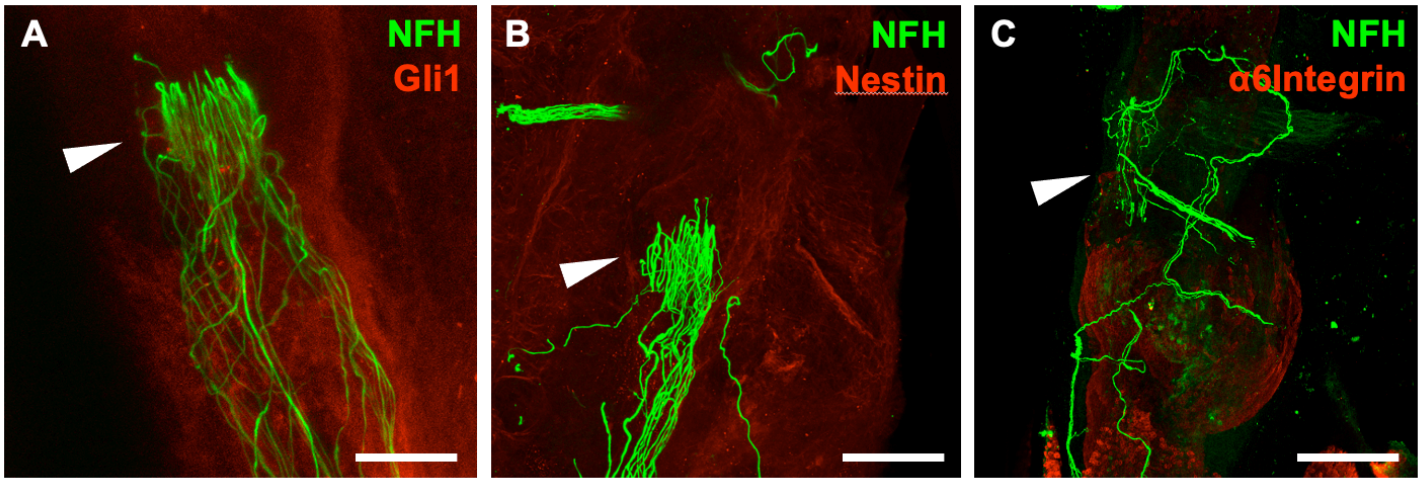


Figure 3.23 Whole-mount staining of human HFs showing LTMRs NFH+ together with antibodies against Gli1, Nestin and α6integrin.
(A) LTMR NFH+ forming longitudinal endings and Gli1 antibody which do not target any follicular structure. Scale bar 50
(B) Longitudinal LTMR NFH+ and Nestin antibody with no specific target. Scale bar 50
(C) α6integrin antibody targets HFSC in the bulge region but fails to target the cells on the upper bulge region where longitudinal LTMRs NFH+ are. Scale bar 100
Representative example of 2 samples from 2 patients.

After failing to find the specific cell marker for the bulge cells located close to LTMRs, we decided to take a different approach to try to target the cell types within the closest range of the LTMR.

We have found that different types of LTMRs form longitudinal and circumferential endings around human HFs. We also suggest that the region of the follicle that these LTMRs innervate is composed of K15 epithelial cells.

Therefore, we hypothesise that the ORS region of the follicle composed by epithelial cell types could be involved in processing tactile information.

3.4 LTMRS innervate multiple HFs

We next performed the whole mount protocol to investigate the receptive field of LTMRs innervating HFs (**Figure 3.24**) In human hair skin LTMRs innervate multiple follicles between and within follicular units, suggest that the receptive fields expand to many follicles. These findings help to understand the high sensitivity to the neurons innervating HFs

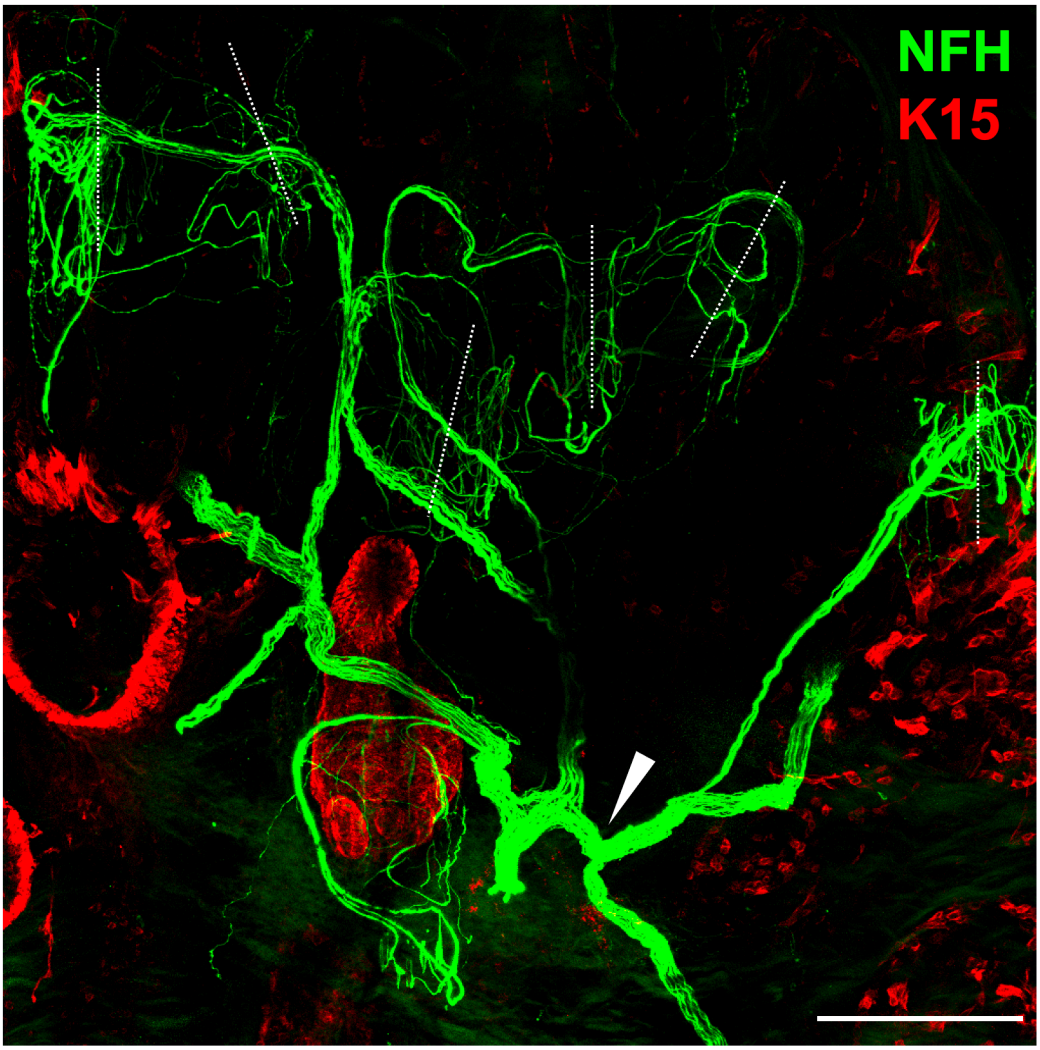


Figure 3.24 Whole-mount staining of scalp skin strip showing a single LTMR NFH+ (arrowhead) innervating up to 6 different HFs (dashed lines) in the upper part of ther bulge region K15+. Scale bar 150µm. Representative example of 1 sample from 1 patient.

3.5 ORS cells are mechanosensory cells

After identifying that LTMR endings are located close to the ORS, I wanted to ask if the ORS cells have any role in responding to tactile stimulus. Deflection of the hairs result in direct mechanical stimulation of LTMRS, however do the ORS cells have a supplementary role? To try to understand if ORS cells can respond to tactile stimulus, I first established a hair fibre explant using HFs from patients undergoing hair transplant surgery, to obtain ORS cells cultures. Briefly, I adapted a method developed by Nowak & Fuchs to grow ORS cells from explanted hair fibres[97]. Hair fibres within the ORS attached when plated in petri dishes on top of feeder cells treated with mitomycin C on FAD media. After 4 days of plating the ORS across the dish in an explant. With this method a high confluency of cells was achieved **(Figure 3.25).** Full details can be found in in methods section 2.4.2.

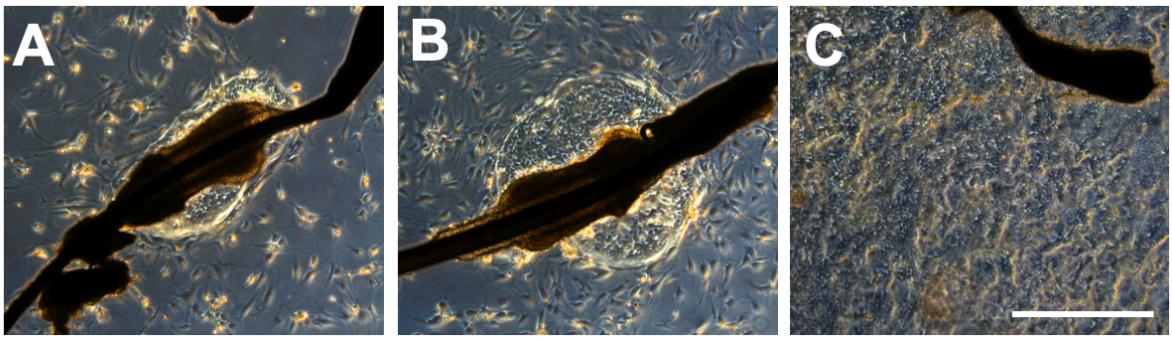


Figure 3.25 ORS cultures from human HFs growing on a petri dish on top of feeder layers.
After 5 days of planting a cluster of ORS cells start to expand from the fibre (A). On the 7th day, a colony of ORS cells can be seen surrounding the fibre (B). After 2 weeks, the dish achieves total confluence of ORS cells. Scale bar 100um

First, we characterized these explant cultures using immunostaining with K14 and K15 antibodies. We found that the culture expresses a mix of the bulge cell marker K15 and the ORS marker K14, indicating a similar composition to what I found in the ex vivo whole-mount immunostaining experiments (**Figure 3.26**). This in vitro model of the HF ORS was next used to test if ORS cells can respond to tactile stimulus.

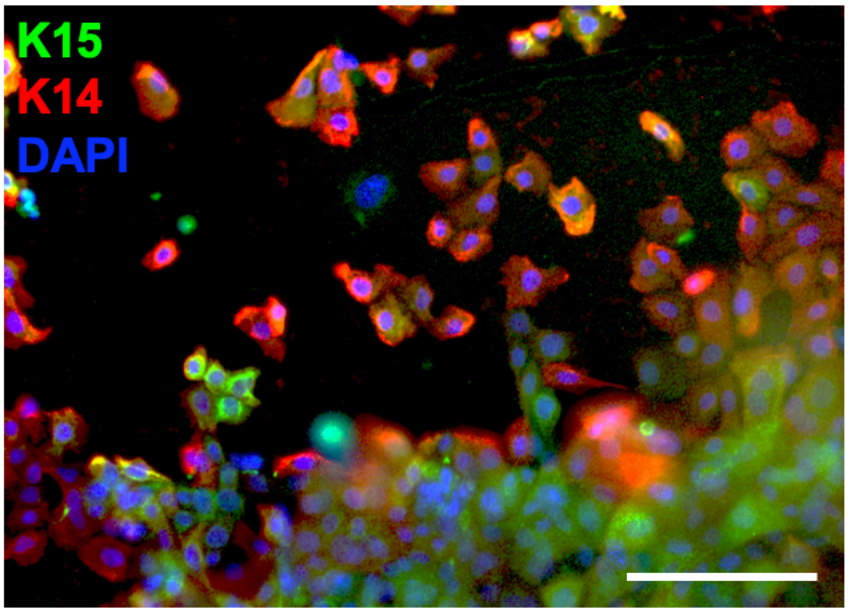


Figure 3.26 Immunostaining of ORS cultures from human HF show the presence of K14 and K15 ORS cells. Scale bar 100µm. Representative example of 6 different samples from 3 patients.

To test the capabilities of ORS cells in responding to tactile stimulus, we decided to measure changes in intracellular calcium concentration as a read out of cell activation after tactile-like stimulus. The fluctuation of the calcium ion inside the cell have been using a direct read out of cell activation and is the method have been using to test if epithelial cells responds to tactile stimulus[138,139]. When the cell response to external stimulus, increases its intracellular calcium concentratio which in turn start signalling process in the cell to communicate sensory information to surrounding cells. This process is triggered by the opening of transmembrane cationic channels which permit the influx of calcium from the extracellular space toward the cytoplasm. Thus, we employed the calcium dye Cal520 to measure if after tactile-like stimulus, the ORS cells increase their intracellular calcium concentration to show signs of cell activation. Briefly, we incubate the cells with 10µM Cal520 for 1h at 37°C and for 30min at RT. We use a fast camera system build into a confocal microscope recording at one frame per second at 8000Hz and a micromanipulator with a micropipette with a tip diameter of 2-3µm.

We recorded between 20-30 cells per dish, and we use a total of 7 dishes from 4 different patients **(Figure 3.27).** To measure the increase in intracellular concentration, we use the formula ΔF/F where F is the amount of fluorescence before the stimulus and ΔF the fluorescence after stimulus. Thus, ΔF/F gives a relative measure to quantify the increase in calcium concentration after stimulation. On average, cells increase 1.7-fold their ΔF/F after tactile-like stimulus, therefore, this data suggests that ORS cells culture from human HFs are capable to respond to tactile-like stimulus.

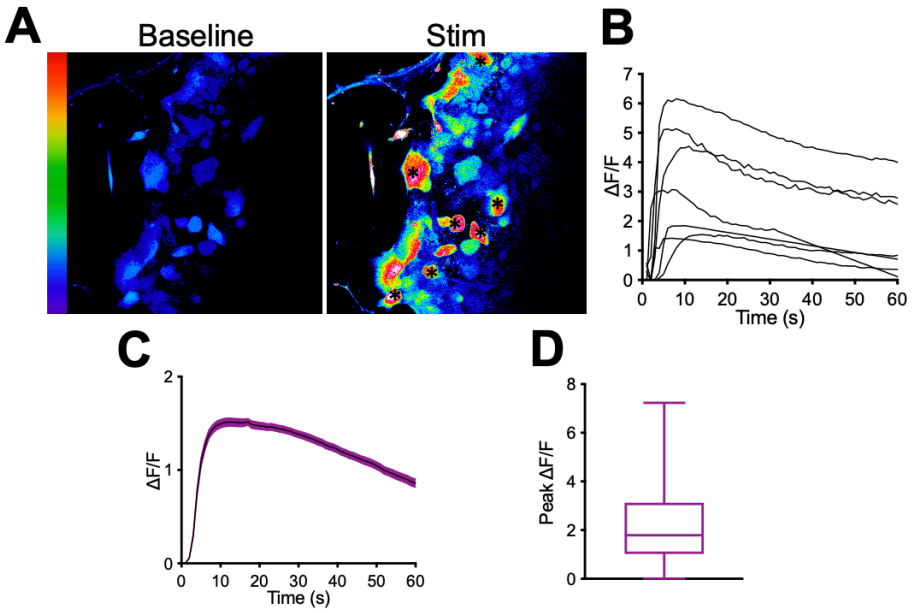


Figure 3.27 ORSc cultures from human HFs show mechanosensitive properties after tactile-like stimulus. Increase of fluorescence after tactile stimulation (STIM) in a group of ORS cells compared to baseline (A). Example of ΔF/F traces of mechanically activated calcium transients of ORSc from A and average (left panel) and average of ΔF/F traces (C) and peak (D) from G. Data in C and D represents the mean +/- SEM for 7 experiments carried out in 173 (25 cells per experiment) from 4 patients.

However, mimic tactile-like stimulus in vitro can be challenging. Tactile activation of the skin is a complex process which involves the activation of several components, such as skin matrix distention, neuronal and cellular activation, and active feedback. Mechanosensitive cells are extremely sensitive and a tactile stimulus into the cell membrane can rupture the membrane and produce cellular death[114].

Therefore, to mimic a tactile-like stimuli in vitro we aim to deliver a gentle but firm stimulus into the cell membrane of about 5µm. Since calcium is a widely used cellular signalling molecule we aimed to apply 5µm indentation to see if there is an increase of intracellular calcium concentration. For example, the calcium source which mediates this increase in fluorescence gives information regarding if ORS cells can response to a tactile like stimulus. Calcium can be released intracellularly from the endoplasmic reticulum (ER) or can influx into the cell from the extracellular space. To investigate the calcium source which mediate the increase in ΔF/F, we use the same experimental set up using Cal520 as an indicator in the ORS cell cultures but modified the levels of calcium from inside and outside the cell to verify where the calcium originates. Therefore, 3 different conditions were created. The first dish was a control dish with just HBSS. The second dish contained the cells with HBSS but substituting the calcium for magnesium. In the third dish, we incubate the cells with thapsigargin, which is a non-competitive inhibitor of ER Ca2+ ATPase (SERCA)[172]. Whit thapsigargin, the cells are prevented from using the intracellular calcium stored in the ER. I next stimulated the cells with a tactile-like stimulus of 5µm indentation using 2 dishes per group from 2 patients with a total of 27-30 cells per group (**Figure 3.28**).

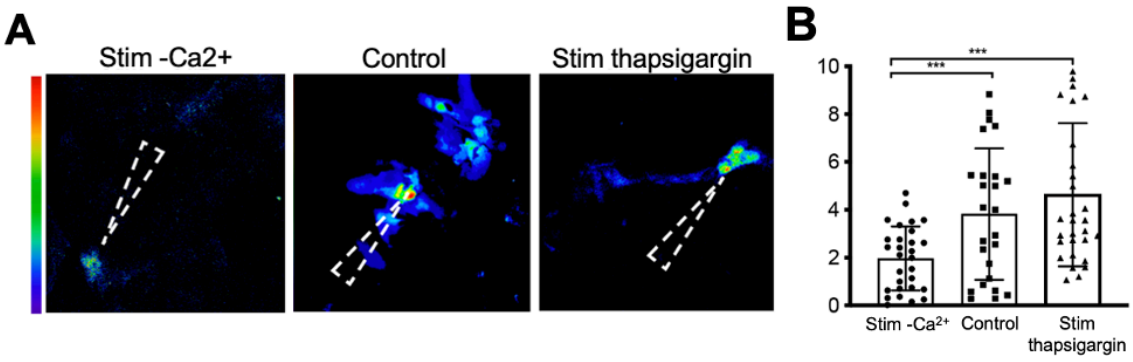


Figure 3.28 ORSc stimulated with tactile-like stimulus use mostly extracellular calcium to mediate ΔF/F increase.
ORS respond to tactile-like stimulus after incubation with 3µM of thapsigargin and loaded with media with and without calcium shows an example point of stimulus (A). Comparison of each ΔF/F cell peak per condition showing a significantly lower ΔF/F p extracellular calcium free media compared to the Ca+ media. Data represents the mean +/- SEM for 27 individually stimulated ce experiments with cells from 2 patients. An ANOVA with a Bonferroni post hoc test was used to compare ΔF/F values from the 27 inc cells. ***p < .0001.

In the control condition cells respond ΔF/F is on average 4-fold higher that the non-stimulated baseline whereas in the stim thapsigargin condition cells responds 4.7-fold higher suggesting a minor, non-significant difference. This data suggests that the ORS cells do not use intracellular calcium as a major source of calcium to mediate the increase of ΔF/F after tactile like stimulus. However, ORS cells which have been incubated with the calcium free media (Stim -Ca^{2+}) show a 2-fold ($p<0.0001$) significant reduction in ΔF/F compared to the control condition after stimulation. This data suggests that ORS cells use extracellular calcium to mediate the increase in intracellular calcium concentration after tactile like stimulus.

In other mechanosensitive cells, for example, Merkel cells or sensory neurons, a tactile stimulus produces a distention in the cell membrane which opens mechanosensitive ion channels such as Piezo or TRP channels, which leads to the influx of extracellular calcium triggering cell activation. First, to see if ORS cells in vitro express mechanosensitive ion channels, I use Piezo2 antibodies to stain the ORS cultures. We found that the cells are indeed Piezo2+ suggesting they harbour mechanosensitive ion channels (**Figure 3.29**).

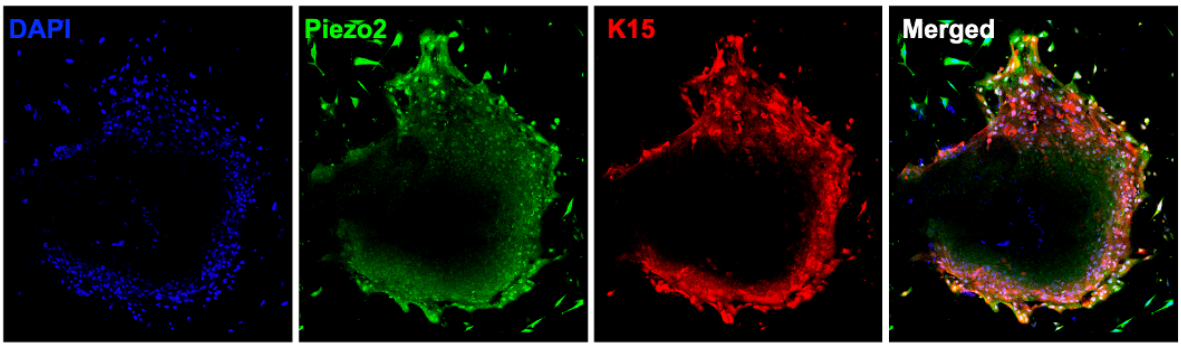


Figure 3.29 Immunostaining of ORS cells cultures from human HFs show expression of K15 and Piezo2. Representative example of 4 samples from 4 different patients.

Although immunostaining is a powerful technique to have a first insight to check the presence of proteins, sometimes it is not adequate to fully demonstrate the presence of small proteins such as Piezo channels. Thus, another experimental approach was tested to unravel the presence of Piezo2 channels in our ORS cultures.

Pharmacological ablation permits the blockage of responses mediated by specific molecules and receptors; therefore, I used pharmacology to detect Piezo2 channels and to understand if this mechanosensitive ion channel is involved in mediating the increase in intracellular calcium concentration. Piezo channels are a newly discovered ion channel, and their pharmacology is not well understood. For Piezo1 channels yoda1 is a specific drug which blocks just Piezo1 channels[173]. For Piezo2, there is not an endogenous antagonist. Nevertheless, GsMTx4 is a newly discovered drug present in the venoms of the Chilean rose tarantula - *Grammostola spatulates,* which has shown ability to block ionic currents mediated by both Piezo1 and Piezo2[174]. Hence, GsMTx4 was used to test the responses of ORS cells after tactile-like. The same cells from figure 3.27 were incubated with 8µm GsMTx4 for 30min to consequently perform the same experiment: 5µm tactile-like stimulus to the cells and record one frame per second to measure intracellular calcium fluorescence increase. Between 20-30 cells per dish were recorded of total of 7 dishes from 4 different patients (**Figure 3.30**).

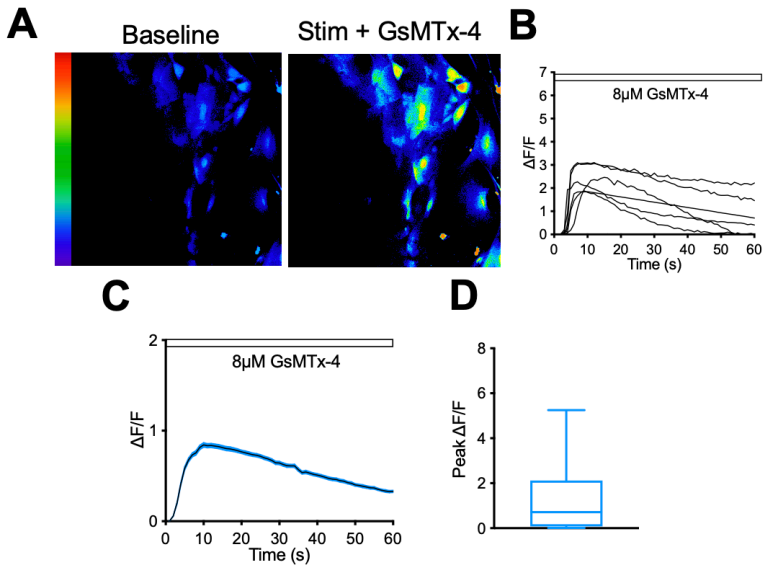


Figure 3.30 ORSc cultures from human HFs are show mechanosensitive properties after tactile-like stimulus which are partially blocked by GSMTMS.
Increase of fluorescence after tactile stimulation (STIM) in ORS cells compared to baseline and after incubation. Example of ΔF/F traces of mechanically activated calcium transients in ORS cells from A (B) and average ΔF/F traces (C) and ΔF/F peak (D). Data represents the mean +/- SEM for 7 experiments carried out in 110 cells (14-15 cells per experiment) from 4 patients.

After GsMTx4 incubation and tactile-like stimulus, cells increase their intracellular calcium concentration by 0.8-fold compared to unstimulated baseline. ΔF/F comparison between the control and GsMTx-4 show a significantly lower calcium transient in the GsMTx-4 treated condition (**Figure 3.31A**). Furthermore, if we consider the peaks, there is a significant decrease in intracellular calcium concentration in the GsMTx-4 treated cells ($p<0.05$) (**Figure 3.31B**).

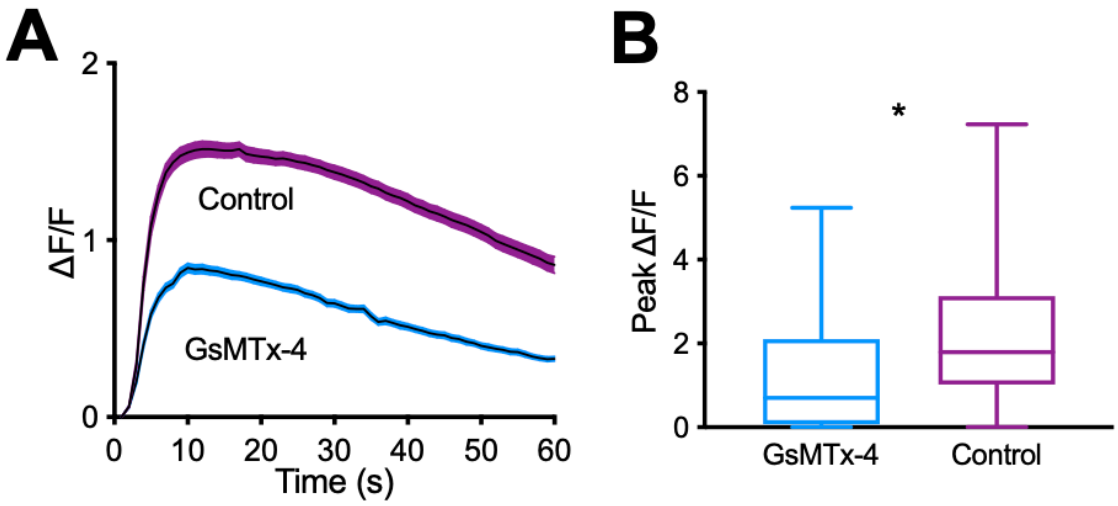


Figure 3.31 Comparison between ORSc stimulated with tactile-like stimulus before and after GsMTx-4 incubation
Average ΔF/F traces from ORS cells before and after GsMTx-4 show less ΔF/F after GsMTx-4 incubation (A). Average ΔF/F peaks comparison show significantly lower ΔF/F after GsMTx-4 incubation. Data represents the mean +/- SEM for 110 cells stimulated in 7 separate experiments (14-15 cells per experiment), established from 4 patients. A paired t-test was performed to compare the data (n=110) between the two experimental conditions.

This data suggest that ORS cells in vitro are mechanosensitive cells capable of responding to touch using Piezo channels. With this data, however, is it not possible to conclude if the channels involved in mediate this signalling are Piezo1, Piezo2 or both.

Taking all this results together, they suggest that ORS cells are mechanosensitive cells with mechanosensitive ion channels that get activated after a tactile like stimulus that triggers extracellular calcium influx. Thus, ORS cells fulfil the requirements to be considered touch receptors. The only cell type capable of sending encoded tactile information towards the brain is the Aβ-LTMRs. Therefore, there should be an association between LTMRs and ORS cells which enables the information processed by ORS cells to be sent towards the brain. In the next section we will try to answer if LTMRs in the HF can respond to tactile-activated ORS cells.

3.6 Activated ORS cells transmit stimulus to LTMRs

To investigate if ORS cultures can transmit tactile-like stimulus to associated LTMRs, a co-culture system was designed between ORS cultures and sensory neurons from DRG and TG. Due of the impossibility to obtain human DRG sensory neurons because of obvious ethical concerns, I aimed to find an adequate in vitro model to work with using murine DRG and TG. As showed previously, we found that human HFs are innervated by LTMRs expressing the same molecular markers found in mouse LTMRs. Therefore, I suggest that using murine DRG and TG is a valid model to understand if ORS cells can activate sensory neurons such as LTMRs. As both TG and DRG show overwhelmingly similar gene expression and the same LTMRs molecular markers expression, sensory neurons with both ganglions were extracted[175].

As described in the introduction (figure 1.1), the DRG is a highly heterogenous ganglion. Apart from LTMRs, there are also proprioceptors and nociceptors, therefore, before starting the co-culture with the ORS we characterized the DRG we obtained from mice (**Figure 3.32**) As expected, DRG/TG cultures show heterogenous neurons, with all neurons expressing the pan neuronal marker PGP9.5. Is it possible to see that there are other neurons which are

PGOP9.5+ and NFH+ suggesting these LTMRs could be Aβ-LTMRs. After characterizing the murine DRG/TG cultures, these were seeded into human ORS cultures on FAD media for a week. After a week of co-culture, neurons start to branch out and associate with the ORS cells (**Figure 3.33**).

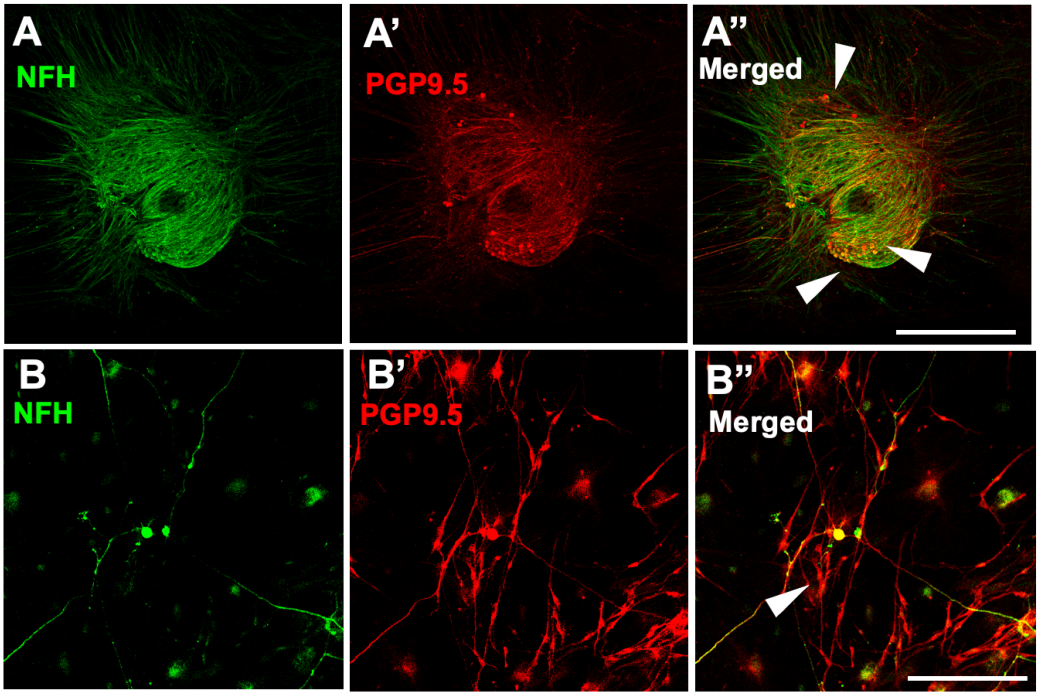


Figure 3.32 Characterization of murine DRG/TG
Primary culture of murine DRG/TG expressing and heterogenous culture with LTMRs NFH+ and sensory neurons PGP9.5 (arrows) (A). Mature culture with LTMRs NFH+ growing axons (B). Scale bars 100µm in A and 50µm in B. Representative example of 2 samples from 2 mice.

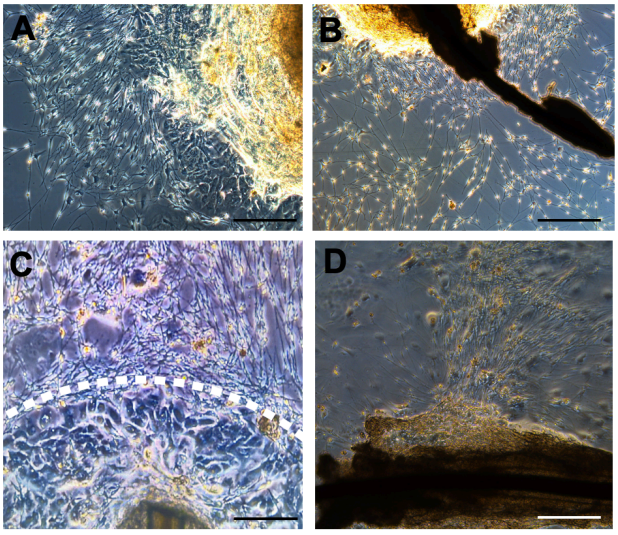


Figure 3.33 Examples of petri dishes with co-cultures between murine DRG-TG and human ORS cells.
Association between murine DRG/TG and human ORS after 10 days of plating (A-B) and after 15 days (C-D). Scale bars 80µm in A, B and D and 50µm in C. **Representative example of 10 samples from 7 different patients.**

After achieving a mature co-culture between DRG/TG neurons and ORS cells, we characterized the co-cultures and found that NFH+ LTMRs are closely located to the K15+ ORS cells. Cells are located about 5-10µm from each other suggesting that these cells are located close enough to communicate between them after tactile-like stimulus. Interestingly, there are also TH+ and PGP.9.5+ neurons which could be classified as C-LTMRs (**Figure 3.34**).

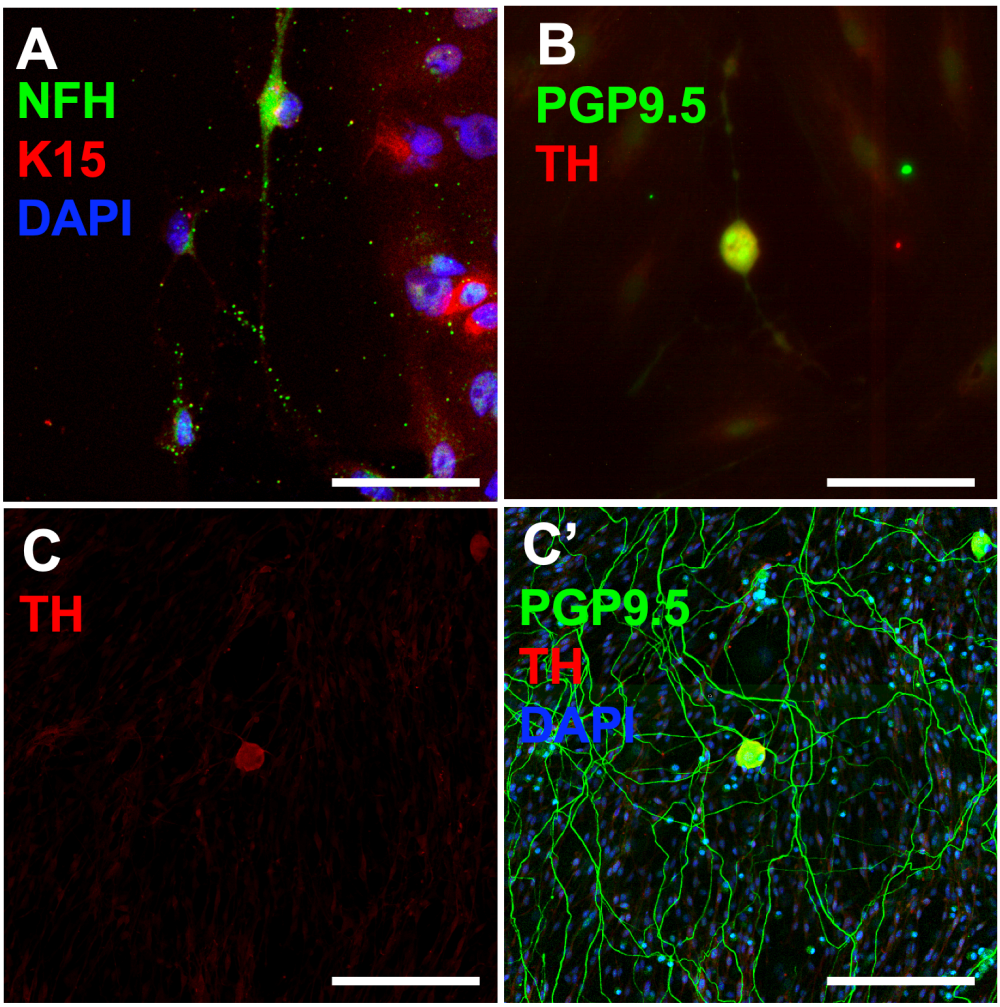


Figure 3.34 Characterization between co-cultures between human ORSc and murine DRG/TG Close localization between LTMRs NFH+ and K15 ORSc (A). C-LTMRs TH+ were also observed in the co-culture system with ORSc (C' DAPI). Scale bars 15µm in A & B and 50µm in C. **Representative example of 4 samples from 3 mice.**

After establishing the ORS-LTMR co-cultures system, I used the calcium dynamics experiments previously used with the ORS to test if ORS cells can transmit tactile information to surrounding LTMRs. The same calcium dye, Cal520, was employed and incubated the co-culture system for 1.5h and a half to then performed the experiments.

Baseline was recorded and then ORS cells were stimulated with a 5um tactile-like stimulus indentation. As before, ORS cells show an increase of intracellular calcium concertation almost immediately following the tactile like stimulus (**Figure 3.35**).

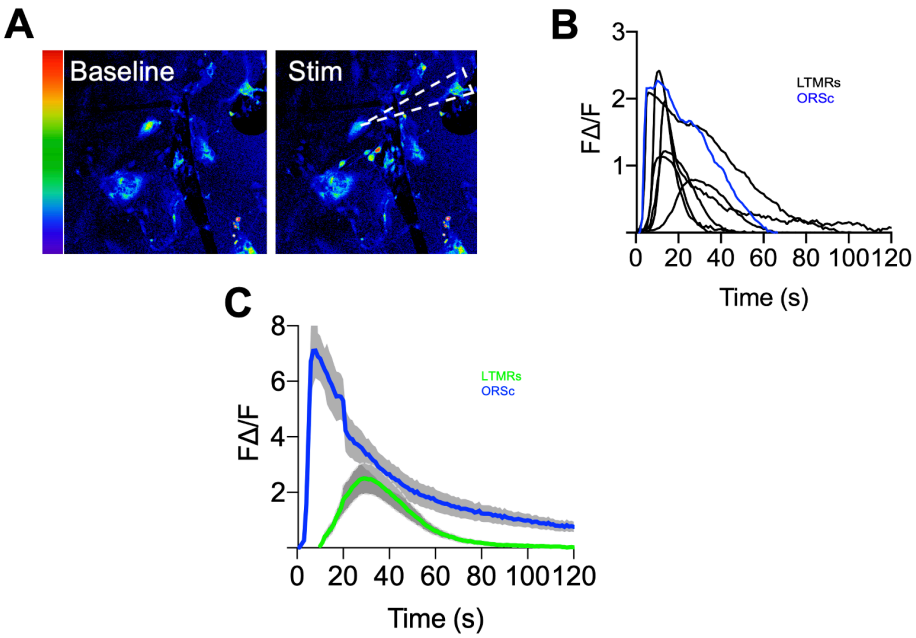


Figure 3.35 Tactile activated ORS cells transmit calcium transient to associated LTMRs.
ORSc transmit tactile-like stimulus (arrow) to LTMRs (A). Example of ΔF/F traces from stimulated ORS cells (blue) and LTMRs (black, 5 cells) in A (B). Average ΔF/F traces from ORSc (blue, 3 cells) and LTMRs (green, 21 cells) from data in C. Data represents the mean +/- SEM for 3 experiments from 3 patients.

In parallel the ΔF/F in LTMRs was recorded after ORS cells indentation. LTMRS are activated on average 10 seconds after stimulation reaching its peak at 30 seconds after the ORS cells triggering a 2.2-fold increase in ΔF/F compared to baseline. From this data we can conclude that tactile activated ORS cells are capable of activating associate LTMRs in a co-culture

model. Since in the co-culture model the only activated cell is an ORS, they must employ a signalling mechanism to activate LTMRs.

We next design a series of experiments to understand this type of inter cellular communication between ORS cells and LTMRs. First, we design an experiment to confirm that indeed the activation of LTMRs is due to the release of a molecule from the ORS cells after tactile like stimulus and second an experiment to try to unravel the nature of this molecule.

3.6.1 Tactile activated ORS cells release an unknown molecule which activates LTMRs.

To understand if a substance released from tactile-activated ORS cells can start calcium responses in LTMRs, I incubated the cells with the drug bafilomycin A1, which inhibits the V-ATPase enzyme and disrupts exosomes formation by pH increase which inhibits the trafficking between multivesicular bodies and lysosomes[176,177]. Several studies have shown that bafilomycin A1 also prevents exosome formation to release substances such as neurotransmitters and ATP[142,178]. Therefore, using this drug will prevent ORS cells from releasing substances into the media and can help to understand if the activation of LTMRs is due to a substance released by tactile activated ORS cells. As before, for each experiment we incubated the dishes with the ORS-LTMRs co-cultures for 1.5h with Cal520 in HBSS. In this experiment we also previously incubated a dish with cell medium with 200µM of bafilomycin A1 in the incubator at 37C for 24h prior to the addition of Cal520. We use a total of 2 dishes per condition and repeated the experiment 2 times. In both treatment and control dishes, healthy ORS cells were stimulated with a tactile-like stimulus of 5µm. The increase in intracellular calcium concentration in both ORS cells and surrounding LTMRs was reduced (**Figure 3.36**). After quantifying the increase in intracellular calcium concentration, ORS cells show a 12.2-fold increase of ΔF/F which produces an increase of 7-fold in associated LTMRs.

On the other hand, the treatment dishes which has been incubated 24h with bafilomycin show a different result: tactile activated ORS cells show ΔF/F increase of 12-fold, like the increase obtained in the control dish, however, associated LTMRs remain completely unresponsive.

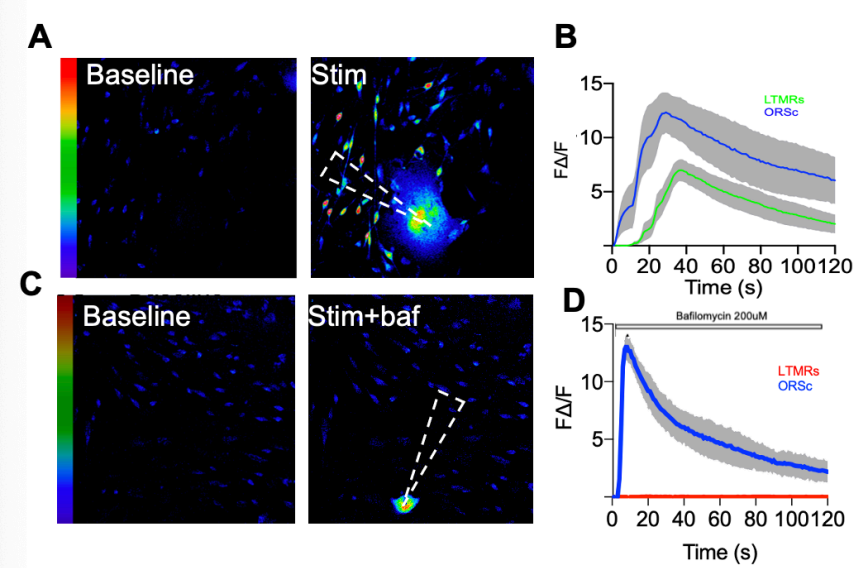


Figure 3.36 ORSc-LTMRs cultures incubated with bafilomycin A1
ORS cells transmit tactile-like stimulus to surrounding LTMRs in control condition (A). Average of ΔF/F traces from ORSc (blue) and LTMRs (green). ORS cells stimulated with tactile-like stimuli (dashed arrowhead) do not transmit intracellular calcium increase to surrounding LTMRs (C). Average ΔF/F traces from ORSc (blue) and LTMRs (red) (D). Data represents the mean +/- SEM for 2 experiments from 1 patient.

This data suggests that the LTMRs increase of intracellular calcium concentration is due to the release of an unknown molecule by tactile-activated ORS cells

3.6.2 Tactile activated ORS cells employ ATP to activate LTMRs.

To unravel the molecule which ORS cells employ to activate LTMRs, we decided to investigate ATP, a molecule that has been already shown to be involved in mediating tactile signalling between epithelial tissue and neurons. As the previous experiment we performed with bafilomycin A1 prevented ORS cells from releasing any substance, now apyrase was used, a chemical that degrades ATP in a fast manner. Apyrase is a ATP-diphosphohydrolase which catalized the hydrolysis of ATP into ADP[179]. Therefore, in this experiment we manipulate the

levels of ATP in the media rather that preventing ORS cells from in releasing ATP[180]. Thus, ORS-LTMRs co-cultures were incubated for 1.5h with Cal520 in HBSS and then we stimulated ORS cells with a tactile-like stimulus to measure the increase of intracellular calcium concentration (**Figure 3.37**).

As shown in other control experiments, ORS cells show an average increase of 9.8-fold of ΔF/F after tactile-like stimulus which is transmitted to all associated LTMRs triggering a 2.2-fold increase in ΔF/F. Since apyrase is a fast-acting enzyme, dishes with the ORS cells and LTMRs co-cultures were loaded with 200U of apyrase at the end of the control experiments. Thus, I incubate cells with apyrase for 10min and then ORS cells were stimulated in the same dish but in different locations. After adding apyrase to the dish, ORS cells show an increase of intracellular calcium concentration of 6.9 ΔF/F which corresponds to a 1.1 ΔF/F increase in LTMRs. Therefore under apyrase incubation ORS cells activate less LTMRs compared to control.

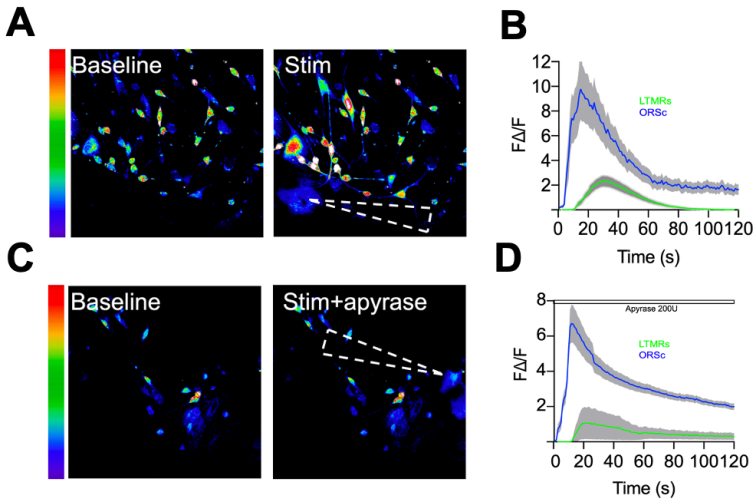


Figure 3.37 Tactile activated ORSc transmit calcium transient to associated LTMRs using partially ATP
ORSc transmit tactile-like stimulus (arrow) to LTMRs (A). Example of ΔF/F trances from ORSc (blue) and LTMRs (black) in A (B). After incubation with apyrase, few LTMRs respond with less ΔF/F (C). Average ΔF/F traces from ORSc (blue) and both responding and non-responding LTMRs (green) (D). Data represents the mean +/- SEM for 4 experiments from 3 patients.

Considering this data, is it possible to deduct that LTMRs respond less in the presence of apyrase because ORS cells also show less increase in ΔF/F. Consider the peaks of each stimulated ORS cells in each dish, there is a decrease in ΔF/F between control ORS cells and apyrase ORS cells therefore it can be concluded that the decrease in LTMRs ΔF/F on apyrase condition is due to the ΔF/F decrease in ORS cells and not due to the addition of apyrase. However, considering LTMRs, after apyrase incubation there are fewer activated LTMRs after ORS stimulation compared to control (**Figure 3.38**). One possible explanation is that with time the calcium dye starts to fade, since these dishes have been previously stimulated, it has been more time difference since the dye is taken out of the media and the recording started. Thus, in the 4 dishes we used in the experiment 28 out of 28 identified LTMRs become activated in the control compared to 7 out of 34 after apyrase incubation. Considering the average peak ΔF/F, there is a 2-fold decrees after apyrase incubation of ΔF/F in LTMRs. This dramatic change in LTMRs responses cannot be explained by the small reduction in ORS cells ΔF/F. Therefore, these results support the idea that at this change is because of apyrase and not because ORS cells decreased response.

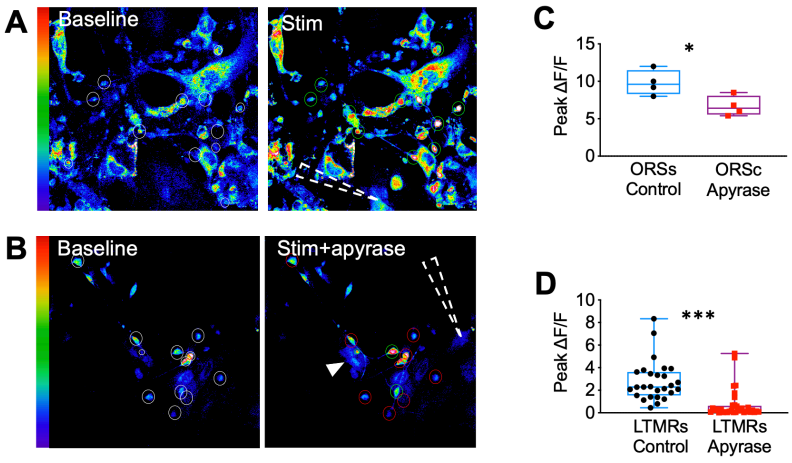


Figure 3.38 Comparison between activate LTMRs after ORSc tactile-like stimulus before and after apyrase incubation
In control conditions, virtually all LTMRs associated (white circles, left) to the stimulated ORSc (arrow) become activated (green circles, right) (A). After apyrase incubation, most of the associated LTMRs (white circles, left) to the stimulated ORSc (arrow) become silent (B). Peak ΔF/F comparison between both conditions show a significant less ΔF/F in ORS cell between control under apyrase condition, paired t-test $p<0.005$ (C). Peak ΔF/F comparison between both conditions show a significant lower number of LTMRs activated under apyrase condition (D), paired t-test $p<0.001$. Data represents the mean +/- SEM for 4 experiments carried out in 34 cells from 2 patients.

From this data it is understood that ORS cells partially use ATP to activate surrounding LTMRs after tactile-like stimulus. However, caution should be taken in interpreting this data. Apyrase was used to test the potential involvement of ATP release from ORS cells to activate neurons but does not directly measure that ATP is released by ORS cells after tactile stimulus. Therefore, this data should be considered as an indirect read out of ATP used by ORS cells to activate LTMRs. Interestingly, the experiments with show that 7 out of 34 (20%) of LTMRs still responded after ORS cells tactile-like stimulus. This suggest another signalling molecule different to ATP might be released by ORS cells to LTMRs.

3.7 FSCV reveals that Tactile activated ORS cells release serotonin and histamine after tactile like stimulus

As explained before, although the experiment to detect the involvement of ATP on ORS-LTMRs signalling was straightforward using apyrase, ATP could not be directly attributed of being released from ORS cells. However, in the case of neurotransmitters such as serotonin, glutamate, noradrenaline etc, is difficult to see if ORS cells could release these substances after tactile-like stimulus. These substances degrade pretty quickly and we lack of the technical set up to detect in real time if ORS cells can release neurotransmitters. Different approaches could be taken but none of those could give precise result identifying the molecule in question. For example, performing RNA screening of ORS cells could be an option, however, this approach has been done in human HFs and in murine skin keratinocytes previously and the data suggested that these cells have the machinery to release many of the aforementioned substances, such as glutamate, acetylcholine, noradrenaline between others[95,141]. Therefore, this approach was discarded. Using siRNA to block specific genes involved in the release of these substances could be another option, however, the release of each of these neurotransmitters requires several genes and involved in different steps of

vesicle trafficking, endogenous synthesis, reuptake inhibition which will be arduous and difficult to do using siRNAs[181]. Finally, another possibility was to take this technical difficulty from the other extreme: instead in try to target ORS cells to detect which substance release, we thought of blocking specific receptors of these substances in the LTMRs. For example, having the hypothesis that ORS cells release glutamate, the approach would be to block each of the 4 different glutamate receptors: AMPA, NMDA, Kainate, and the metabotropic GluR1-6 in LTMRs using pharmacology. However, even with glutamate seems a long list, there are other NTs such as a serotonin which have more that 15 different types of receptors which gives a lengthy list of receptors and therefore drugs to try mostly in a blind manner[175,182,183]. This approach was also discarded.

After consulting with neuroscientist, we end up learning that some electrochemical techniques could give a real time read out of specific substances. Therefore, we started a collaboration with Dr. Parry Hashemi, principal investigator in the electrochemical lab at the Department of Bioengineering at Imperial College London to perform fast-scan cycling voltammetry (FSCV) with our ORS cultures to understand which substances these epithelial cells might release after tactile-like stimulus.

From a basic point of view and briefly, FSCV is a technique which uses a carbon fibre electrode to detect electroactive substances. Since most neurotransmitters such as dopamine, serotonin, glutamate, adrenaline and histamine are electroactive, the carbon fibre electrode applies 2 consecutive steps in voltage and if one of these molecules is in close range, the molecule suffers an oxidation-reduction reaction which gives a current signature which can be recorded (**Figure 3.39**).

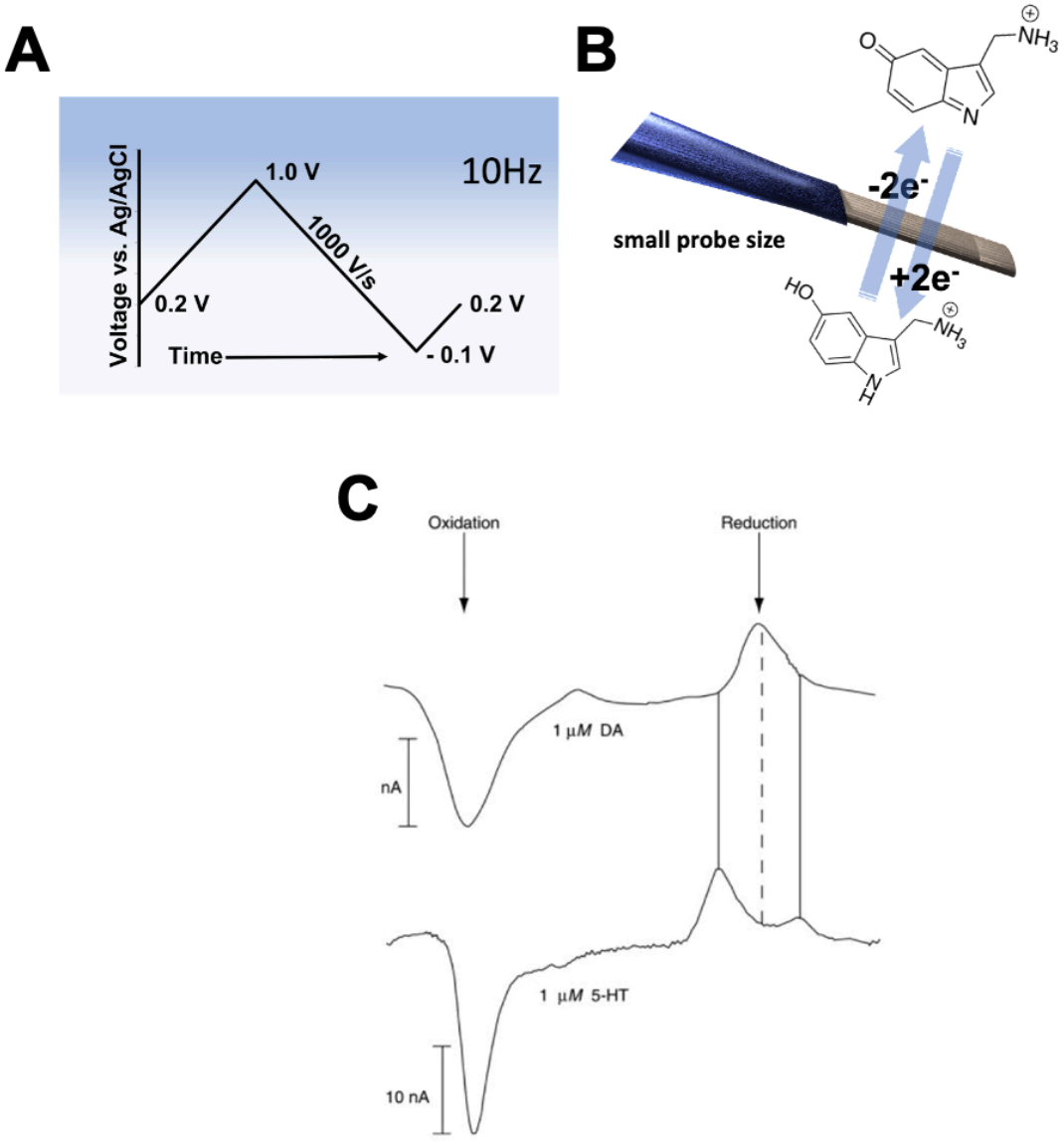


Figure 3.39 Fast scan cyclic voltammetry (FSCV) basics.
FSCV employs 2 steps in voltage along a certain time frame (A) with a carbon fiber electrode to produce a redox reaction on a electroactive molecules which interchange electrodes with the carbon from the electrode (B). The oxidation-reduction peak difference times are unique for each molecule, for example, serotonin (5HT has a shorter peak compared to dopamine (DA) (C).

The main feature of this technique is that each of the molecules in question has a unique current signature which can be derived from the time difference from the reduction and oxidation peak. Therefore, looking at this current signature is it possible to identify substances which are in the vicinity to the carbon fibre electrode.

keeping in mind the capabilities of FSCV and together with our collaborators, we designed an experiment to identify which molecules ORS cells release after tactile-like stimulus (see methods 2.6). We use our in vitro model containing just ORS cells to detect which different molecules are being released. We select the ORS cells of interest and then the two micro manipulators were lowered to the cells, one carbon fibre electrode to record the FSCV signal and another glass micropipette to stimulate the cells. Next, we start the FSCV recording and after 5 seconds we stimulate the ORS cells with a 5µm tactile-like stimulus. After 60 seconds recording, is it possible to see that ORS cells release 2 difference substances which have the signature voltammograms of serotonin and histamine when compared with control experiments using flow injection analysis performed with control median without cells and artificially loading serotonin and histamine (**Figure 3.40).**

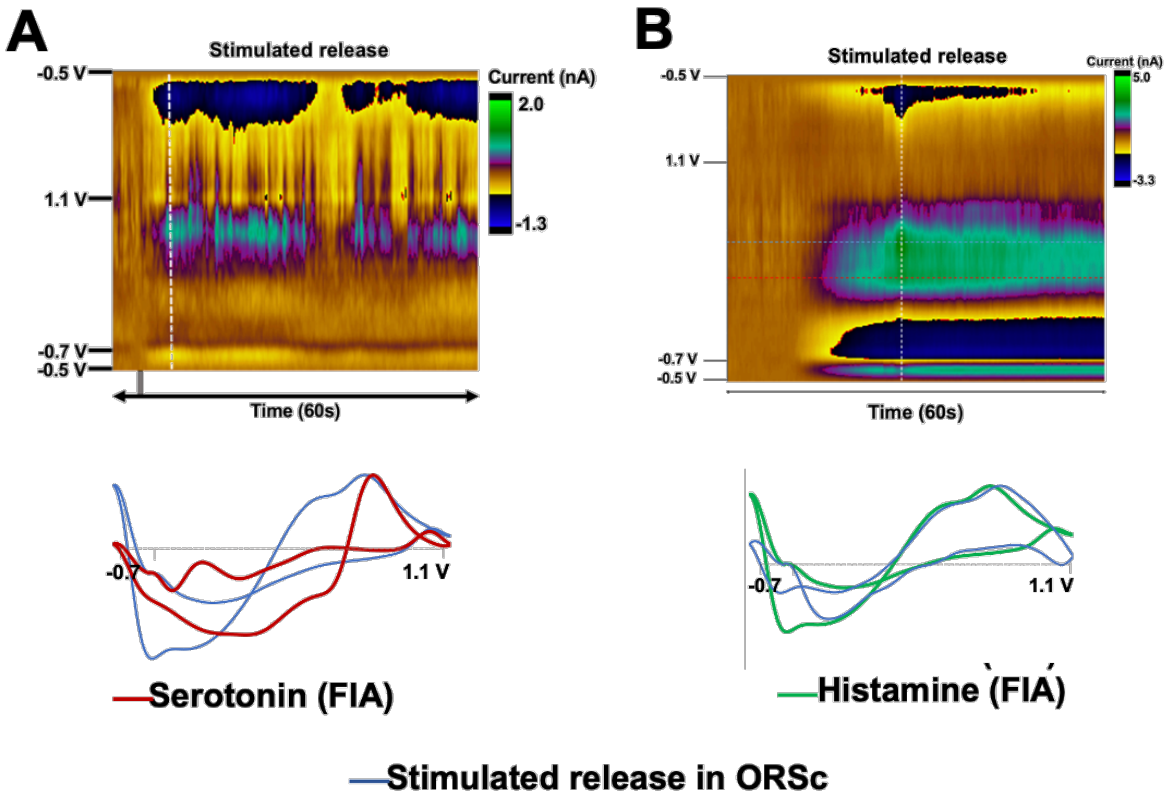


Figure 3.40 Example of raw data obtained from the FSCV set up
3D graphs showing voltage, time and current. At each voltage step there are increase of current produced by the substance is being oxidated, for example in A, serotonin at 0.7V (A). After plotting the results, the voltammogram have the same oxidation peak as the flow injection analysis suggesting the substance is serotonin. In B, same as A but with histamine, the current happens at 0.5V suggesting the voltammogram is from histamine, which is confirmed when compared with the flow injection analysis (FIA) (B).

Once we obtained the data, our collaborators use a partial least square regression (PLSR) model for each carbon fibre electrode to convert the Faradaic current into concentration of serotonin and histamine. Therefore, at the end of each experiment our collaborators from the Hashemi lab processed the raw data and gave to us the molarity data.

I then analysed the concentration data and found that histamine is release more that serotonin (**figure 3.41**). Sixty seconds after a single tactile-like stimulus, ORS cells release 9.8nM serotonin whereas they release 1554nM histamine. Therefore, tactile stimulated ORS cells release far more histamine than serotonin.

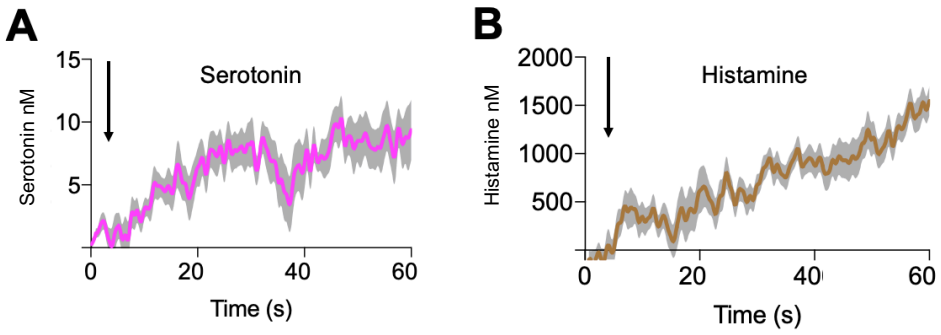


Figure 3.41 FSCV reveals ORSc release serotonin and histamine after tactile stimulus
After a single tactile like stimulus ORSc release an average of 9.8nM of serotonin (A) and an average of 1554nM of histamine. Data represents the mean +/- SEM for 21 stimulations in 7 experiments from 4 patients.

Next, we decided to stimulate ORS cells with different stimulus protocols to investigate if the release of serotonin and histamine after tactile-like stimulus can be dependent on the stimulus frequency. Thus, we modify out protocol to also deliver:

- 1 poke protocol: 1 tactile-like stimulus with 5µm indentation.
- 3 poke protocol: 3 tactile-like stimulus with 5µm indentation 1 second apart.
- 5 poke protocol: 5 tactile-like stimulus with 5µm indentation 1 second apart.

With these protocols, we found that ORS cells increase their release of both serotonin and histamine after increasing the frequency (**Figure 3.42**). This data suggests that ORS cells are mechanosensitive cells capable of releasing serotonin and histamine after tactile like stimulus.

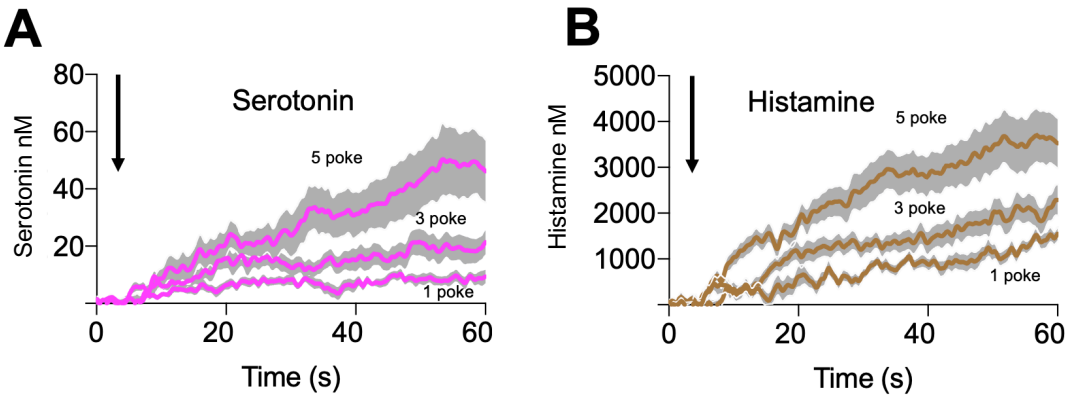


Figure 3.42 ORSc release serotonin and histamine after tactile stimulus in a frequency dependent manner
ORSc release more serotonin (A) and histamine (B) when the frequency of the stimulus is increased from 1 to 3 to 5 pokes (arrow indicate time of stimulus). Data represents the mean +/- SEM from 12 stimulations in 4 experiments from 4 patients.

Therefore, our data suggest that serotonin and histamine from ORS cells could be candidate molecules to test in ORS cells-LTMRs tactile signalling. Since increasing the frequency of the stimulus also increases the amount of serotonin and histamine being release by ORS cells, we next ask if increasing the intensity of the stimulus could have an effect on how ORS cells behave after tactile-like stimulus. Therefore, we design a protocol where we stimulate ORS cells with a long poke protocol: 1 tactile like stimulus with 10µm indentation and sustained for 15 seconds. Because this stimulus is stronger, we designate this stimulus as a pain-like stimulus with the idea to mimic a pain stimulus on the cells. Peak release was assessed for serotonin release and the average was 20nM for a 1 sustained poke whereas 19nM for a 1 short poke which was not significant ($p>0.05$).

For histamine release the average was 3146nM for a 1 sustained poke and 2257 nM for a 1 short poke which was not significant (p>0.05) (**Figure 3.43**).

Therefore, this data might suggest that even though not being significant, ORS cells release more histamine but the same serotonin after a stronger and more sustained stimulus in vitro which could mimic the psychological behind a pain stimulus in vivo. Therefore ORS cells could be pain receptors which release histamine after pain stimulus. However, further research should be carried to confirm this hypothesis.

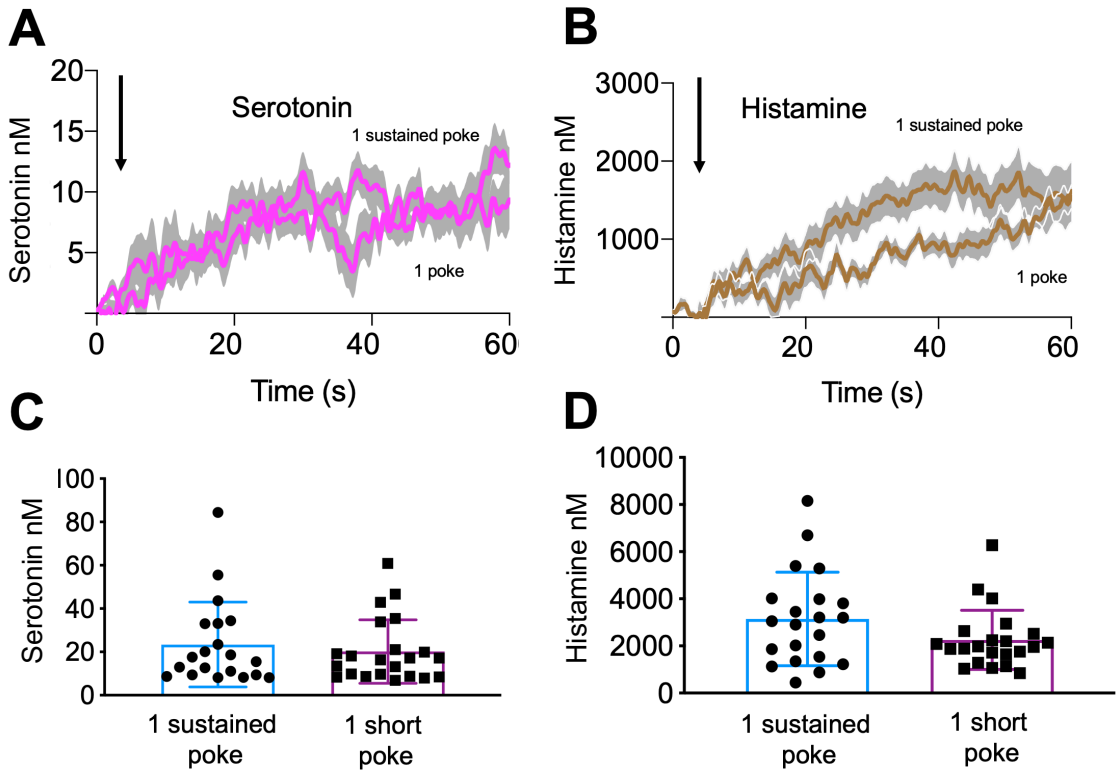


Figure 3.43 ORSc serotonin and histamine released after 1 short poke and 1 sustained poke.
ORSc release similar amounts of serotonin after 1 poke or 1 sustained poke (arrows) (A). Histamine release is higher after 1 sustained poke compared to 1 poke (B). Peak comparison between serotonin (C) and histamine (D) release after tactile-like stimulus show no significant differences between 1 sustained and short poke. Unpaired t-test p>.05. Data represents the mean +/- SEM for 21 stimulations in 7 experiments from 4 patients.

Overall, this data suggests that ORS cells release significant different amount of serotonin and histamine released after mechanical stimulus depending on the frequency of stimulation.

Since the discovery that ORS cells release these substances was unexpected, we wanted to know if other epithelial cells in the skin, such as interfollicular keratinocytes (KC), can also release histamine and serotonin after tactile like stimulus. Therefore, we performed the same experiment as before but using skin KC in comparison of ORS cells.

3.8 FSCV reveals skin keratinocytes show a different releasing profile after mechanical stimulus compared to ORS cells

Using the same experimental protocol that we used with ORS cells cultures, we load KC in HBSS at pH 7.4 and 300mol/kg and delivered the same poke protocol: 1, 3, 5 pokes. First, we characterised the KC cultures to show that the cells express K14 but not K15 suggesting KC cells are from interfollicular skin origin (Figure 3.44 A). As ORS cells, KC from interfollicular skin release of 3427nM ,3911nM and 5999nM of histamine after 1 poke, 3 pokes and 5 pokes respectively. In contrast to ORS cells, they appear not to release any serotonin because of the negative current in the FSCV recording (**Figure 3.44**).

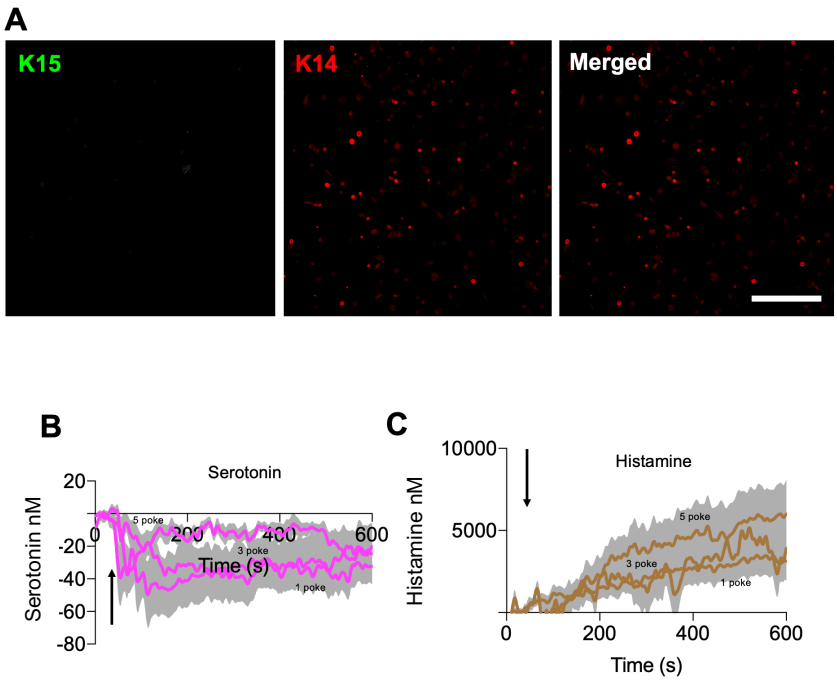


Figure 3.44 KC release histamine but not serotonin after different types of tactile-like stimulus
KC cultures from interfollicular skin express K14 but not K15 (A). Representative example of 5 samples from 3 patients. After stimulating the cells with 1, 3 and 5 pokes (arrows), KC do not release serotonin but histamine (B-C). Scale bar 100µm. Data represents the mean +/- SEM from 9 stimulation in 3 experiments from 1 patient.

We next compared the peaks of the concentrations after the different types of tactile-like stimulus between ORS cells and KC and found that KC release more histamine compared to ORS cells. After 1 poke KC release 1.75-fold more histamine compared to ORS cells ($p<0.05$), 2-fold after 3 pokes ($p<0.05$) and 1.25-fold after 5 pokes (no significant, $p>0.05$).

On the other hand, ORS cells release more serotonin compared to KC, 1.17-fold more after 1 poke, ($p>0.05$), 2.30-fold more after 3 pokes ($p<0.001$) and 3.5-fold more after 5 pokes ($p>0.05$). (**Figure 3.45**). Therefore, these results suggest that ORS cells are a different type of cell compared to KC in their responses after tactile-like stimulus.

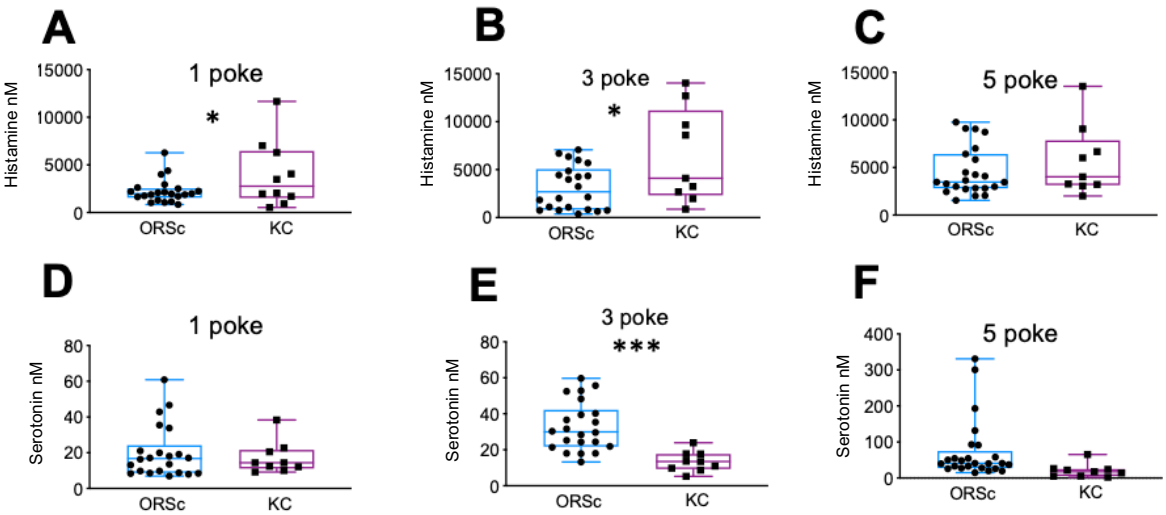


Figure 3.45 Comparison between KC and ORSc serotonin and histamine released after different types of tactile like stimulus.
KC release more histamine than ORSc in all types of tactile-like stimulus while 1 and 3 pokes being the significant ones (A, B, D). Unpaired t-test $p<0.05$. ORSc release more serotonin than KC in all types of tactile-like stimulus while 3 pokes being the only significant stimulus (D, E, F). Unpaired t-test, $p<0.001$. Data represents the mean +/- SEM from 21 (ORS cells) or 9 (KC) stimulation in 7 (ORS cells) or 3 (KC) experiments from 3 patients.

To validate this result, we performed PCR using primers against the gene tryptophan hydroxylase (TPH1), a gene involved in the catalysis tryptophan into hydroxytryptophan which the is decarboxylated into serotonin. This gene is the rate-limiting enzyme for the biosynthesis

of serotonin therefore its expression is required for any cell type capable to synthetise and release serotonin[184]. The results of the RT-PCR performed with ORS cells cDNA and KC cDNA show that TPH1 is expressed a 2.2-fold more in ORS cells compared to KC. These results are in line with what has been shown with the previous FSCV results suggesting that ORS cells express the genes requiered in synthetise serotonin. Although this is a preliminary result with just N=1, it helps to support the idea that ORS cells are capable of releasing serotonin compared to KC after tactile-like stimulus (**Figure 3.46**). K14 expression was used as the housekeeping gene for comparison to TPH.

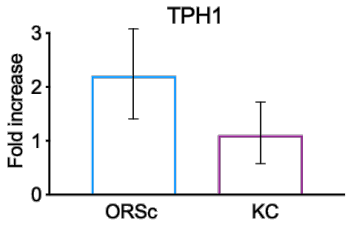


Figure 3.46 Fold change of TPH1 expression between KC and ORSc
ORS cells express 2.2-fold more expression of TPH1 gene compared to KC. N=1

Overall, FSCV revealed that ORS cells release serotonin and histamine after tactile like stimulus in a frequency dependent manner. Thus, release of serotonin is more pronounced after increasing the frequency of stimulus. Finally, KC only release histamine after tactile-like stimulus but not serotonin suggesting ORS cells are unique epithelial cells in the way they respond to tactile-like stimulus. Although these findings are important to understand how ORS cells behave after tactile-like stimulus, it remains unclear if serotonin and histamine released from ORS cells can modulate LTMRs response.

3.9 Mirtazapine incubation changes LTMRs responses after ORS cells activation

To investigate if ORS cells can activate LTMRs using serotonin and histamine, we decided to take a pharmacological approach using mirtazapine, a potent atypical antidepressant drug

which blocks serotonin 5-HT2, 5-HT3 receptors and histamine H1 receptors. With all 15 serotonin receptors known 5-HT3 is the receptors expressed in the Aβ afferent which Merkel cells activate while releasing serotonin. Therefore, we hypothesize that ORS cells employ these receptors to activate the LTMRs. To assess if serotonin and histamine released from ORS cells can modulate LTMR response, we used our previously described ORS-LTMRs co-culture system between ORS cells and LTMRs incubated with Cal520 to enable us to record calcium transients in both LTMRs and ORS cells after tactile like stimulation. As before, we incubated the cells with Cal520 for 1.5h. We next stimulate ORS cells and recorded the increase in intracellular calcium concentration in both ORS cells and LTMRs **(Figure 3.47).** After tactile-like stimulus, ORS cells showed a 4.3-fold increase in ΔF/F that is transmitted to associated LTMRs with an increase of 3.9-fold. To understand if mirtazapine affects the ability of ORS cells to communicated with LTMRs, we incubate the co-cultures with 200μM mirtazapine for 30min and perform the experiments again using the same dish but different location. ORS cells show a 3.6-fold increase in ΔF/F that is transmitted to associated LTMRs with a 1.7-fold increase in ΔF/F. This data suggests that after mirtazapine incubation ORS cells respond in a similar manner while the LTMRS response is halved.

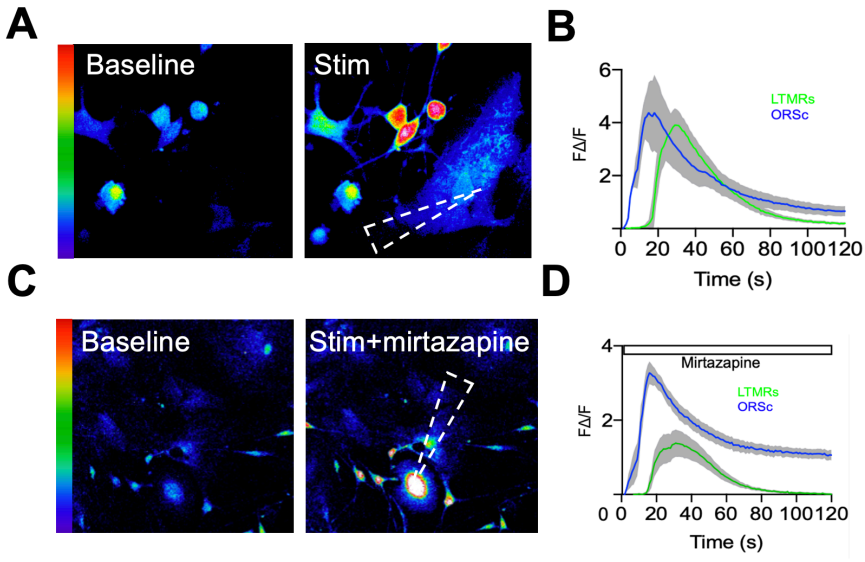


Figure 3.47 Mirtazapine blocks partially LTMRs responses after ORS cells tactile-like stimulation. ORS cells activated by tactile-like stimulus (arrowhead) triggers calcium response in associated LTMRs in a co-culture system (A). Average ΔF/F traces from ORS cells and LTMRs (B) and ORS cells activated by tactile-like stimulus triggers calcium response in associated LTMRs after 200uM mirtazapine incubation (C). Average ΔF/F traces from ORSc and LTMRs (D). Data represents the mean +/- SEM for 8 experiments from 3 patients.

Considering the peaks of each cell, there is no significant differences between ORS cells ΔF/F pre and post mirtazapine incubation whereas there is a significant reduction in LTMRs ΔF/F by half (**Figure 3.48**). This data confirms that blocking serotoninergic and histaminergic receptors impacts the ability of ORS to transmit tactile information to LTMRs.

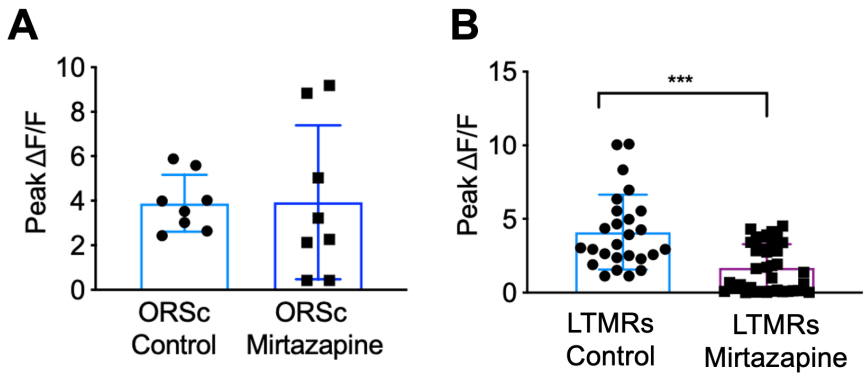


Figure 3.48 Comparison of the ΔF/F peaks for ORSc and LTMRs
After mirtazapine incubation, ORS cells show non-significant difference in ΔF/F peak. Paired t-test $p>0.05$, (A). LTMRs ΔF/F peaks after ORSc stimulation are significant smaller compared to control. Unpaired t-test ***$p<0.001$. In A, Data represents the mean +/- SEM from 8 stimulations in 8 experiments from 3 patient. In B, data represents the mean +/- SEM from 36 cells in 8 experiments from 3 patients.

Lastly, to confirm that the reduced LTMR response is due to the antagonistic effect of mirtazapine on serotonin and histamine receptors, and not just a consequence of impaired serotonin and histamine release from ORS cells treated with mirtazapine (an off-target effect), we performed FSCV with ORS cells after mirtazapine incubation. We stimulated the cells with the single tactile-like stimulus (1 poke), same stimulus we deliver previously and found no reduction in serotonin or histamine from ORS cells. In contrast, we actually but interestingly found that mirtazapine incubation triggers a 2-fold increase in serotonin and histamine release from ORS cells **(Figure 3.49).**

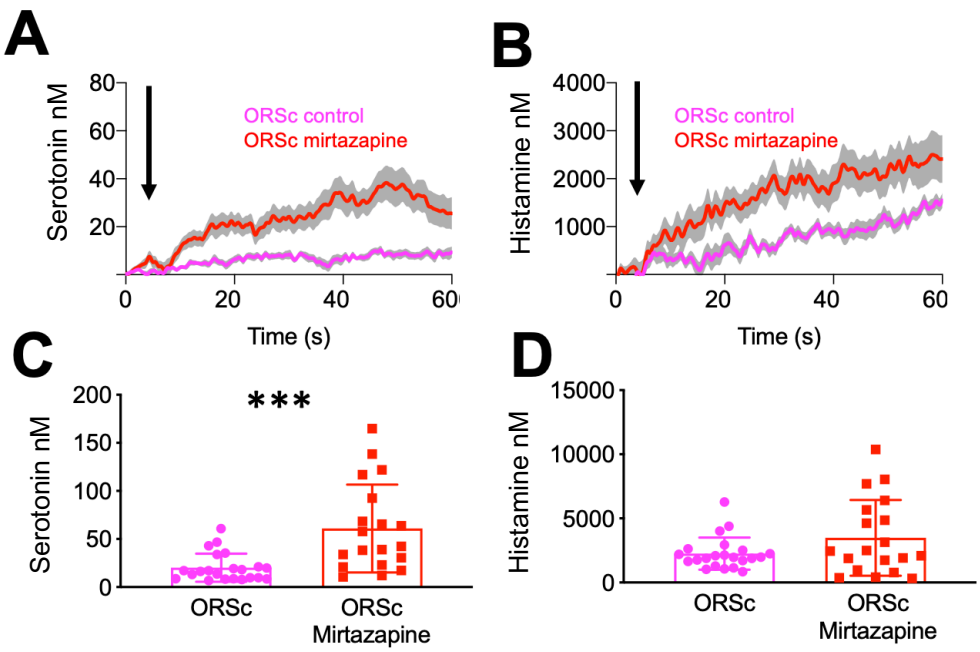


Figure 3.49 ORSc release more serotonin and histamine after tactile-like stimulus after mirtazapine incubation.
ORSc increase the release of serotonin and histamine after tactile like stimulus (A-B). Concentration peak comparison show a significant more release of both serotonin and histamine after tactile like stimulus. Unpaired t-test, ***p<0.001. Data represents the mean +/- SEM for 21 stimulations in 8 experiments from 3 patients.

This result highlights that in the presence of more serotonin and histamine (after mirtazapine incubation of ORS cells), the LTMR response was effectively halved.

Overall, this data suggests that serotonin and histamine being released from ORS cells after tactile stimulus can modulate LTMR intracellular calcium concentration by 5HT2, 5HT3 and H1 receptors activation. Thus, serotonin and histamine can be signalling molecules of tactile stimulus between epithelial tissue and LTMRs in the human HF. In the next section we will discuss about the beforementioned findings, their fit in the current literature and the advances that provide to the field in understanding the human HF as a sensory organ.

4. DISCUSSION

In this thesis I set out to test the hypothesis that the human HF itself plays an important role in tactile perception. Within the results chapter, different experimental methods have shown that the human HF is highly innervated by LTMRs in the bulge region where ORS cells reside. In vitro, these cells show mechanosensitive properties using tactile related ion channels. Interestingly, these cells are able to release the neurotransmitters histamine and serotonin after tactile and pain like stimulus. In a co-culture model, ORS cells are able to associate and elicit calcium responses in neuronal cultures from mice expressing specific LTMRs markers. This response is impaired when serotonin and histamine receptors on the LTMRs are blocked.

4.1 Human HF innervation

Human anagen HFs are highly innervated skin appendages. Whereas the whole follicle has axon wrapped around it, as revealed by pan-neuronal markers such PGP9.5, diverse LTMRs innervating the bulge and the upper bulge region express specific neuronal markers also found in murine hairy skin[68]. Although previous research has found that human HFs are highly innervated structures, our results show for first time that anagen human HFs are innervated by 5 different types of mechanoreceptors: 4 LTMRs and a HTMR[148–150]. As explained in the introduction, the different types of LTMRs are associated with different types of murine hairs follicles, however, our results suggest that terminal hairs in humans are innervated by all these sensory neurons.

Although the physiology of these sensory neurons has not been directly tested, the circumferential and longitudinal morphology of their endings and the expression of specific molecular markers is sufficient to characterize these neurons as LTMRs and HTMR.

Another aspect which supports the identity of this sensory neurons is the localization within the follicle. Although finding the specific follicular region which these LTMR innervate has not been possible in human follicles, the innervation niche is close to the K15 ORS cell region. These findings show that there is a phylogenetical continuum between murine and human innervating LTMRs and helps to explain why the HF is such a sensitive organ. Each of the LTMRs and HTMRs innervating the follicles are involved in processing certain types of stimuli. Therefore, the HF could be considered as a multi-unit sensory system where different types of sensory neurons convey together to process tactile information.

Although the main component of this multi-sensory system are the LTMRs and HTMRs which are the only cell types able to send tactile information towards the brain, other cell types in the follicle are important in modulating how LTMRs responds after tactile stimulus. The most prominent example is the interplay between Merkel cells and Aβ-LTMRs. The main 2 features which permit the communication of tactile stimulus from Merkel cells to LTMRs are their close proximity and then the mechanosensitive properties of Merkel cells[38,114].

The whole mount immunolabelling has revealed that the LTMR axons wrap around the follicle ORS cells. These cell, which are of epithelial origin, and their skin equivalent, keratinocytes, have been shown to be able to respond to tactile stimulus.[140]

4.2 ORS as a novel mechanosensitive cell in the human HF.

Once ORS cells were cultured from human HF explants and stimulated, the cells responded with by increasing their intracellular calcium concentration.

Using pharmacology, ORS cells were found to show increase their intracellular calcium concentration using extracellular supply suggesting that these cells have mechanosensitive

ion channels in their membrane which permit the influx of extracellular calcium. These findings were also supported by immunostaining using Piezo2 antibodies showing localization in ORS cells.

Thus, in ORS cells tactile stimulation opens mechanosensitive channels in the cell membrane which triggers an increase in calcium concentration inside the cell. The ORS could therefore be considered as touch receptors, however, as said before, the only cell type in the follicle capable of sending tactile information towards the brain are LTMRs. If ORS are true tactile receptors, they should be able to communicate with associated LTMRs after tactile like stimulus.

4.3 Novel interaction between ORS-LTMRs for tactile stimuli

To test the idea of a novel neuroepithelial interaction in the human HF between ORS cells and LTMRs, a co-culture was established between murine LTMRs and human ORS cells. After tactile like stimulus, ORS cells are able to trigger an increase of intracellular calcium to surrounding LTMRs which is totally blocked by bafilomycin and partially blocked by apyrase. The first experiment with bafilomycin confirms that a molecule being released by ORS cells triggers the increase in intracellular calcium concentration in LTMRs, whereas the second experiment with apyrase suggests that ATP is involved in partially mediating the calcium increase in LTMRs. These findings are in line with previous research that showed that ATP being release from epithelial tissue can initiate a neuronal responses[137,143,185]. These findings however have been conducted in interfollicular skin and not in HF epithelium, therefore the results in this thesis describe a novel neuroepithelial signalling between LTMRs and ORS cells in the human HF.

Interestingly, after apyrase incubation some LTMRs still responding, suggesting be that another molecule could be released by ORS cells after tactile like stimulus. In the Merkel cell neurite complex, research has shown that Merkel cells can release serotonin and adrenaline to activate the associate LTMRs. Using FSCV, we found that ORS cells can release both serotonin and histamine in response to mechanical stimulation in a frequency dependent manner, while comparatively interfollicular skin KC release significant more levels of histamine but negligible levels of serotonin. Lastly, blocking of serotonin and histamine receptors on LTMRs dampened their ability to respond to excitatory stimuli, released from ORS cells in response to tactile stimulus. Collectively, these results show that the HF ORS and LTMRs associated with the follicle form a neuroepithelial unit. Our finding that ORS cells, but not KC from interfollicular skin, release serotonin suggests a novel signalling mechanism for tactile stimulus in the human HF.

4.4 Considerations for pleasant touch and serotonin release

It is worth considering the physiological relevance of this data as it was generated in an in vitro set up. The interaction between the bulge and the sensory neurons innervating the follicle has been previously reported.

Taking into account the release of serotonin, is interesting to mention that C-LTMRs which innervate just HFs are activated by repeated and slow touch, when repeatedly stroking of the skin is <5cm/seconds[8,186–188]. This C-LTMRs have been linked to pleasure and emotional interactions and recent research in animal models has postulated that this LTMRs are the cellular receptor for social touch. The variations in tactile-like stimulus frequency and intensity in the FSCV experiments suggest that ORS cells can release different level of neurotransmitters. Interestingly, with 3 poke stimuli, ORS cells release more serotonins

compare to skin KC, Therefore, under repeated stimulus which can mimics repeated skin stroking, ORS cells, which are located close to C-LTMRs in the follicle start to release serotonin which activate C-LTMRs modulated the pleasure component of its activation. Thus, I speculate that serotonin release from HFs is a mediator molecule of C-LTMR activation for pleasant touch.

While the release of serotonin from ORS is unique compared to KC, is it worth remembering that ORS also communicate with LTMRs by the release of ATP and histamine and perhaps these molecules are employs to signalling different types of tactile stimulus such as pain, sustained deflection of the follicle etc.

Collectively, this data suggests that human HF ORS cells together with LTMRs form a neuroepithelial unit which we postulate facilitates decoding and translation of tactile stimulus. These findings lay the foundation for future studies to both evaluate if ORS cells have an excitatory capacity for C-LTMR activation, and to assess the role of the HF in pleasant or affective touch.

5. FUTURE DIRECTIONS

The findings in this thesis open several questions not answered in my research. One of the open questions regards to how serotonin release from ORS cells can modulate the firing rates and the electrical properties of the LTMRs. We aimed to perform patch clamp in our co-cultured model to investigate how tactile activated ORS cells can modulate the firing rates and the electrical properties of LTMRs, but time limitations and uncontrollable events such COVID-19 have made not possible to progress in such experiments. Due to the early stage of these experiments, I decided that is it not worthy to add them on this PhD thesis.

Another open question would be to ask if the serotonin release by ORS cells target specific types of LTMRs such as C-LTMRs. Answering this question would help to understand if ORS can release serotonin to modulate the pleasant touch signalling from C-LTMRs. Finally, studies in vivo using animal models will help to understand if ORS cells tactile activation can initiate behavioural response.

6. REFERENCES

1. Koch, S. L., Tridico, S. R., Bernard, B. A., Shriver, M. D. & Jablonski, N. G. The biology of human hair: A multidisciplinary review. *Am. J. Hum. Biol.* **32**, 1–17 (2020).
2. Pergament, D. & Davis, A. Chicago-Kent Law Review It ' s Not Just Hair : Historical and Cultural Considerations for an Emerging Technology CONSIDERATIONS FOR AN EMERGING TECHNOLOGY " Afro " hairstyles of prominent African-American radical activists. **75**, (1999).
3. RALF P AUS , M.D., AND G EORGE C OTSARELIS, M. D. & H. T He B Iology of H Air F Ollicles. *New Engl. J. Med. Fig.* **341**, 491–497 (2004).
4. Schneider, M. R., Schmidt-Ullrich, R. & Paus, R. The Hair Follicle as a Dynamic Miniorgan. *Curr. Biol.* **19**, R132–R142 (2009).
5. Maria, L. & Flecha-garcía, M. L. Proceedings of the Annual Meeting of the Cognitive Science Non-verbal Communication in Dialogue : Alignment between Eyebrow Raises and Pitch Accents in English. (2007).
6. Lumpkin, E. A., Marshall, K. L. & Nelson, A. M. The cell biology of touch. *J. Cell Biol.* **191**, 237–248 (2010).
7. Pickles, A., Sharp, H., Hellier, J. & Hill, J. Prenatal anxiety, maternal stroking in infancy, and symptoms of emotional and behavioral disorders at 3.5 years. *Eur. Child Adolesc. Psychiatry* **26**, 325–334 (2017).
8. McGlone, F., Wessberg, J. & Olausson, H. Discriminative and Affective Touch: Sensing and Feeling. *Neuron* **82**, 737–755 (2014).
9. Lauria, G. *et al.* European Federation of Neurological Societies/Peripheral Nerve Society Guideline on the use of skin biopsy in the diagnosis of small fiber neuropathy. *Eur. J. Neurol.* **17**, 903–12, e44-9 (2010).

10. Zimmerman, A., Bai, L. & Ginty, D. D. The gentle touch receptors of mammalian skin. *Science (80-.).* **346**, 950–954 (2014).

11. Schneider, M. R., Schmidt-Ullrich, R. & Paus, R. The Hair Follicle as a Dynamic Miniorgan. *Curr. Biol.* **19**, R132–R142 (2009).

12. Moore, K. A. & Lemischka, I. R. Stem cells and their niches. *Science (80-.).* **311**, 1880–1885 (2006).

13. Randall, V. A. Androgens and hair growth. *Dermatol. Ther.* **21**, 314–328 (2008).

14. Vidal, V. P. I. *et al.* Sox9 is essential for outer root sheath differentiation and the formation of the hair stem cell compartment. *Curr. Biol.* **15**, 1340–1351 (2005).

15. Kramer, E. & Peters, J. 416854a. **416**, (2002).

16. Daszczuk, P. *et al.* An Intrinsic Oscillation of Gene Networks Inside Hair Follicle Stem Cells: An Additional Layer That Can Modulate Hair Stem Cell Activities. *Front. Cell Dev. Biol.* **8**, 1–21 (2020).

17. Higgins, C. A., Westgate, G. E. & Jahoda, C. A. B. From telogen to exogen: Mechanisms underlying formation and subsequent loss of the hair club fiber. *J. Invest. Dermatol.* **129**, 2100–2108 (2009).

18. Peters, E. M. J., Botchkarev, V. A., Botchkareva, N. V., Tobin, D. J. & Paus, R. Hair-cycle-associated remodeling of the peptidergic innervation of murine skin, and hair growth modulation by neuropeptides. *J. Invest. Dermatol.* **116**, 236–245 (2001).

19. Botchkarev, V. A., Peters, E. M. J., Botchkareva, N. V., Maurer, M. & Paus, R. Hair cycle-dependent changes in adrenergic skin innervation, and hair growth modulation by adrenergic drugs. *J. Invest. Dermatol.* **113**, 878–887 (1999).

20. Botchkarev, V. A., Eichmüller, S., Johansson, O. & Paus, R. Hair cycle-dependent plasticity of skin and hair follicle innervation in normal murine skin. *J. Comp. Neurol.* **386**, 379–395 (1997).

21. Kandel, S. *Principles neural sciences 5th Edition*.

22. Jenkins, B. A. & Lumpkin, E. A. Developing a sense of touch. *Dev.* **144**, 4048–4090 (2017).

23. Lin, Y. T. & Chen, J. C. Dorsal Root Ganglia Isolation and Primary Culture to Study Neurotransmitter Release. *J. Vis. Exp.* 1–7 (2018). doi:10.3791/57569

24. Sharma, N. *et al.* The emergence of transcriptional identity in somatosensory neurons. *Nature* **577**, 392–398 (2020).

25. Luria, V. & Laufer, E. Lateral motor column axons execute a ternary trajectory choice between limb and body tissues. *Neural Dev.* **2**, 1–23 (2007).

26. de Moraes, E. R., Kushmerick, C. & Naves, L. A. Morphological and functional diversity of first-order somatosensory neurons. *Biophys. Rev.* **9**, 847–856 (2017).

27. Uddenberg, N. Functional organization of long, second-order afferents in the dorsal funiculus. *Exp. Brain Res.* **4**, 377–382 (1968).

28. Marin, E. C. *et al.* Connectomics Analysis Reveals First-, Second-, and Third-Order Thermosensory and Hygrosensory Neurons in the Adult Drosophila Brain. *Curr. Biol.* **30**, 3167-3182.e4 (2020).

29. Kuehn, E. D., Meltzer, S., Abraira, V. E., Ho, C. Y. & Ginty, D. D. Tiling and somatotopic alignment of mammalian low-threshold mechanoreceptors. *Proc. Natl. Acad. Sci. U. S. A.* **116**, 9168–9177 (2019).

30. Bourane, S. *et al.* Identification of a spinal circuit for light touch and fine motor control. *Cell* **160**, 503–515 (2015).

31. Watanabe, M. *et al.* The Cellular and Synaptic Architecture of the Mechanosensory Dorsal Horn. *Cell* **168**, 295-310.e19 (2017).

32. Parvizi-Fard, A., Amiri, M., Kumar, D., Iskarous, M. M. & Thakor, N. V. A functional spiking neuronal network for tactile sensing pathway to process edge orientation. *Sci.*

Rep. **11**, 1–16 (2021).

33. Jörntell, H. *et al.* Segregation of tactile input features in neurons of the cuneate nucleus. *Neuron* **83**, 1444–1452 (2014).
34. Abraira, V. E. & Ginty, D. D. The sensory neurons of touch. *Neuron* **79**, 618–639 (2013).
35. Tyll, S., Budinger, E. & Noesselt, T. Thalamic influences on multisensory integration. *Commun. Integr. Biol.* **4**, 378–381 (2011).
36. Wahlbom, A., Enander, J. M. D. & Jörntell, H. Widespread Decoding of Tactile Input Patterns Among Thalamic Neurons. *Front. Syst. Neurosci.* **15**, 1–12 (2021).
37. Boyle, K. A. *et al.* Defining a Spinal Microcircuit that Gates Myelinated Afferent Input: Implications for Tactile Allodynia. *Cell Rep.* **28**, 526-540.e6 (2019).
38. Handler, A. & Ginty, D. D. The mechanosensory neurons of touch and their mechanisms of activation. *Nat. Rev. Neurosci.* **22**, 521–537 (2021).
39. Rossant, C. *et al.* Spike sorting for large, dense electrode arrays. *Nat. Neurosci.* **19**, 634–641 (2016).
40. Johnson, K. O. The roles and functions of cutaneous mechanoreceptors. *Curr. Opin. Neurobiol.* **11**, 455–461 (2001).
41. Emanuel, A. J., Lehnert, B. P., Panzeri, S., Harvey, C. D. & Ginty, D. D. Cortical responses to touch reflect subcortical integration of LTMR signals. *Nature* **1**, 1–6 (2021).
42. Kell, C. A., Von Kriegstein, K., Rösler, A., Kleinschmidt, A. & Laufs, H. The sensory cortical representation of the human penis: Revisiting somatotopy in the male homunculus. *J. Neurosci.* **25**, 5984–5987 (2005).
43. Proulx, M. J., Todorov, O. S., Aiken, A. T. & de Sousa, A. A. Where am I? Who am I? The relation between spatial cognition, social cognition and individual differences in

the built environment. *Front. Psychol.* **7**, (2016).

44. He, J. L. *et al.* Disorder-specific alterations of tactile sensitivity in neurodevelopmental disorders. *Commun. Biol.* **4**, 1–15 (2021).
45. Fayaz, A., Croft, P., Langford, R. M., Donaldson, L. J. & Jones, G. T. Prevalence of chronic pain in the UK: A systematic review and meta-analysis of population studies. *BMJ Open* **6**, (2016).
46. Finnerup, N. B., Kuner, R. & Jensen, T. S. Neuropathic pain: Frommechanisms to treatment. *Physiol. Rev.* **101**, 259–301 (2021).
47. Lolignier, S., Eijkelkamp, N. & Wood, J. N. Mechanical allodynia. *Pflugers Arch. Eur. J. Physiol.* **467**, 133–139 (2014).
48. Colloca, L. *et al.* Neuropathic pain. *Nat. Rev. Dis. Prim.* **3**, 1–20 (2017).
49. Jensen, T. S. & Finnerup, N. B. Allodynia and hyperalgesia in neuropathic pain: Clinical manifestations and mechanisms. *Lancet Neurol.* **13**, 924–935 (2014).
50. Treede, R. D., Meyer, R. A., Raja, S. N. & Campbell, J. N. Peripheral and central mechanisms of cutaneous hyperalgesia. *Prog. Neurobiol.* **38**, 397–421 (1992).
51. Habig, K. *et al.* Low threshold unmyelinated mechanoafferents can modulate pain. *BMC Neurol.* **17**, 1–11 (2017).
52. Dhandapani, R. *et al.* Control of mechanical pain hypersensitivity in mice through ligand-targeted photoablation of TrkB-positive sensory neurons. *Nat. Commun.* **9**, (2018).
53. Lord, C. *et al.* Autism spectrum disorder. *Nat. Rev. Dis. Prim.* **6**, (2020).
54. Schaffler, M. D., Middleton, L. J. & Abdus-Saboor, I. Mechanisms of Tactile Sensory Phenotypes in Autism: Current Understanding and Future Directions for Research. *Curr. Psychiatry Rep.* **21**, (2019).
55. Orefice, L. L. L. *et al.* Peripheral Mechanosensory Neuron Dysfunction Underlies

Tactile and Behavioral Deficits in Mouse Models of ASDs. *Cell* **166**, 299–313 (2016).

56. Fonctionnelle, I. D. G. & Cedex, C. The impact of C-Tactile Low threshold mechanoreceptors on affective touch and social interactions in mice. (2021).

57. McGlone, F. & Reilly, D. The cutaneous sensory system. *Neurosci. Biobehav. Rev.* **34**, 148–159 (2010).

58. Taub, A. & Bishop, P. O. The spinocervical tract: Dorsal column linkage, conduction velocity, primary afferent spectrum. *Exp. Neurol.* **13**, 1–21 (1965).

59. García-Mesa, Y. *et al.* Merkel cells and Meissner's corpuscles in human digital skin display Piezo2 immunoreactivity. *J. Anat.* **231**, 978–989 (2017).

60. Harper, A. A. & Lawson, S. N. Electrical properties of rat dorsal root ganglion neurones with different peripheral nerve conduction velocities. *J. Physiol.* **359**, 47–63 (1985).

61. Bautista, D. M. & Lumpkin, E. A. Probing mammalian touch transduction. *J. Gen. Physiol.* **138**, 291–301 (2011).

62. Wellnitz, S. A., Lesniak, D. R., Gerling, G. J. & Lumpkin, E. A. The regularity of sustained firing reveals two populations of slowly adapting touch receptors in mouse hairy skin. *J. Neurophysiol.* **103**, 3378–3388 (2010).

63. Koltzenburg, M., Stucky, C. L. & Lewin, G. R. Receptive properties of mouse sensory neurons innervating hairy skin. *J. Neurophysiol.* **78**, 1841–1850 (1997).

64. Luo, W. *et al.* A Hierarchical NGF Signaling Cascade Controls Ret-Dependent and Ret-Independent Events during Development of Nonpeptidergic DRG Neurons. *Neuron* **54**, 739–754 (2007).

65. Olson, W., Dong, P., Fleming, M. & Luo, W. The specification and wiring of mammalian cutaneous low-threshold mechanoreceptors. *Wiley Interdiscip. Rev. Dev. Biol.* **5**, 389–404 (2016).

66. Roudaut, Y. *et al.* Touch sense: functional organization and molecular determinants of mechanosensitive receptors. *Channels (Austin).* **6**, 234–245 (2012).

67. Li, L. *et al.* The functional organization of cutaneous low-threshold mechanosensory neurons. *Cell* **147**, 1615–1627 (2011).

68. Handler, A. & Ginty, D. D. The mechanosensory neurons of touch and their mechanisms of activation. *Nat. Rev. Neurosci.* **22**, 521–537 (2021).

69. Narisawa, Y., Hashimoto, K. & Kohda, H. Merkel cells of the terminal hair follicle of the adult human scalp. *J. Invest. Dermatol.* **102**, 506–510 (1994).

70. Fr. Merkel. Tastzellen und Tastkbrperchen bei den Hausthieren u n d b e h n Menschen .

71. Woo, S. H., Lumpkin, E. A. & Patapoutian, A. Merkel cells and neurons keep in touch. *Trends Cell Biol.* **25**, 74–81 (2015).

72. Nikolaev, Y. A. *et al.* Lamellar cells in Pacinian and Meissner corpuscles are touch sensors. *Sci. Adv.* **6**, 1–10 (2020).

73. Neubarth, N. L. *et al.* Meissner corpuscles and their spatially intermingled afferents underlie gentle touch perception. *Science (80-.).* **368**, (2020).

74. Andres, K. H. C. THE STRUCTURE AND FUNCTION OF THE SLOWLY ADAPTING TYPE II MECHANORECEPTOR IN HAIRY SKIN. By. 417–445 (1972).

75. Rasmusson, D. D. & Turnbull, B. G. Sensory innervation of the raccoon forepaw: 2. Response properties and classification of slowly adapting fibers. *Somatosens. Mot. Res.* **4**, 63–75 (1986).

76. Johansson, R. S. & Vallbo, A. B. Tactile sensibility in the human hand: relative and absolute densities of four types of mechanoreceptive units in glabrous skin. *J. Physiol.* **286**, 283–300 (1979).

77. Takahashi-Iwanaga, H., Nio-Kobayashi, J., Habara, Y. & Furuya, K. A dual system of

intercellular calcium signaling in glial nets associated with lanceolate sensory endings in rat vibrissae. *J. Comp. Neurol.* **510**, 68–78 (2008).

78. Li, L. & Ginty, D. D. The structure and organization of lanceolate mechanosensory complexes at mouse hair follicles. *Elife* **3**, 1–24 (2014).

79. Brown, B. Y. A. G. & Iggo, A. From the Department of Veterinary Physiology , University of Edinburgh. 707–733 (1967).

80. Bai, L. *et al.* Genetic Identification of an Expansive Mechanoreceptor Sensitive to Skin Stroking. *Cell* **163**, 1783–1795 (2015).

81. Rutlin, M. *et al.* The cellular and molecular basis of direction selectivity of Aδ-LTMRs. *Cell* **159**, 1640–1651 (2014).

82. Seal, R. P. *et al.* Injury-induced mechanical hypersensitivity requires C-low threshold mechanoreceptors. *Nature* **462**, 651–655 (2009).

83. Alamri, A. S., Wood, R. J., Ivanusic, J. J. & Brock, J. A. The neurochemistry and morphology of functionally identified corneal polymodal nociceptors and cold thermoreceptors. *PLoS One* **13**, 1–15 (2018).

84. Ghitani, N. *et al.* Specialized Mechanosensory Nociceptors Mediating Rapid Responses to Hair Pull. *Neuron* **95**, 944-954.e4 (2017).

85. Dubin, A. E. & Patapoutian, A. Nociceptors: The sensors of the pain pathway. *J. Clin. Invest.* **120**, 3760–3772 (2010).

86. Altier, C. Spicing up the sensation of stretch: TRPV1 controls mechanosensitive piezo channels. *Sci. Signal.* **8**, 8–10 (2015).

87. Vandewauw, I. *et al.* A TRP channel trio mediates acute noxious heat sensing. *Nature* **555**, 662–666 (2018).

88. Walder, R. Y. *et al.* TRPV1 is important for mechanical and heat sensitivity in uninjured animals and development of heat hypersensitivity after muscle

inflammation. *Pain* **153**, 1664–1672 (2012).

89. Woolf, C. J., Shortland, P. & Coggeshall, R. E. Peripheral nerve injury triggers central sprouting of myelinated afferents. *Nature* **355**, 75–78 (1992).

90. Cain, D. M., Khasabov, S. G. & Simone, D. A. Response properties of mechanoreceptors and nociceptors in mouse glabrous skin: An in vivo study. *J. Neurophysiol.* **85**, 1561–1574 (2001).

91. Baron, R. Mechanisms of disease: Neuropathic pain - A clinical perspective. *Nat. Clin. Pract. Neurol.* **2**, 95–106 (2006).

92. Zylka, M. J. Nonpeptidergic circuits feel your pain. *Neuron* **47**, 771–772 (2005).

93. Braz, J. M., Nassar, M. A., Wood, J. N. & Basbaum, A. I. Parallel 'pain' pathways arise from subpopulations of primary afferent nociceptor. *Neuron* **47**, 787–793 (2005).

94. Bourane, S. *et al.* Low-Threshold Mechanoreceptor Subtypes Selectively Express MafA and Are Specified by Ret Signaling. *Neuron* **64**, 857–870 (2009).

95. Boulais, N. & Misery, L. The epidermis: A sensory tissue. *Eur. J. Dermatology* **18**, 119–127 (2008).

96. Poole, K., Moroni, M. & Lewin, G. R. Sensory mechanotransduction at membrane-matrix interfaces. *Pflugers Arch. Eur. J. Physiol.* **467**, 121–132 (2014).

97. Nowak, J. A., Polak, L., Pasolli, H. A. & Fuchs, E. Hair follicle stem cells are specified and function in early skin morphogenesis. *Cell Stem Cell* **3**, 33–43 (2008).

98. Cheng, C. C. *et al.* Hair follicle epidermal stem cells define a niche for tactile sensation. *Elife* **7**, 1–29 (2018).

99. Zhang, B. *et al.* Hyperactivation of sympathetic nerves drives depletion of melanocyte stem cells. *Nature* **577**, 676–681 (2020).

100. Chao, M. V. Neurotrophins and their receptors: A convergence point for many signalling pathways. *Nat. Rev. Neurosci.* **4**, 299–309 (2003).

101. Reichardt, L. F. Neurotrophin-regulated signalling pathways. *Philos. Trans. R. Soc. B Biol. Sci.* **361**, 1545–1564 (2006).

102. Peters, E. M. J. *et al.* Control of human hair growth by neurotrophins: Brain-derived neurotrophic factor inhibits hair shaft elongation, induces catagen, and stimulates follicular transforming growth factor β2 expression. *J. Invest. Dermatol.* **124**, 675–685 (2005).

103. Botchkarev, V. A. *et al.* Neurotrophin-3 involvement in the regulation of hair follicle morphogenesis. *J. Invest. Dermatol.* **111**, 279–285 (1998).

104. Stucky, C. L., Dechiara, T., Lindsay, R. M., Yancopoulos, G. D. & Koltzenburg, M. Neurotropin is requiresd for the survival of a subclllllass of hair follocle receptors.pdf. **18**, 7040–7046 (1998).

105. Carroll, P., Lewin, G. R., Koltzenburg, M., Toyka, K. V. & Thoenen, H. A role for BDNF in mechanosensation. *Nat. Neurosci.* **1**, 42–46 (1998).

106. Fujiwara, H. *et al.* The basement membrane of hair follicle stem cells is a muscle cell niche. *Cell* **144**, 577–589 (2011).

107. Shwartz, Y. *et al.* Cell Types Promoting Goosebumps Form a Niche to Regulate Hair Follicle Stem Cells. *Cell* **182**, 578-593.e19 (2020).

108. Zhang, B. *et al.* Hyperactivation of sympathetic nerves drives depletion of melanocyte stem cells. *Nature* **577**, 676–681 (2020).

109. Mammoto, T., Mammoto, A. & Ingber, D. E. Mechanobiology and Developmental Control. *Annu. Rev. Cell Dev. Biol.* **29**, 27–61 (2013).

110. Vogel, V. & Sheetz, M. Local force and geometry sensing regulate cell functions. *Nat. Rev. Mol. Cell Biol.* **7**, 265–275 (2006).

111. Wang, N., Butler, J. P. & Ingber, D. E. Mechanotransduction across the cell surface and through the cytoskeleton. *Science (80-.).* **260**, 1124–1127 (1993).

112. Emtage, L., Gu, G., Hartwieg, E. & Chalfie, M. Extracellular proteins organize the mechanosensory channel complex in C. elegans touch receptor neurons. *Neuron* **44**, 795–807 (2004).

113. Kim, S. E., Coste, B., Chadha, A., Cook, B. & Patapoutian, A. The role of Drosophila Piezo in mechanical nociception. *Nature* **483**, 209–212 (2012).

114. Walsh, C. M., Bautista, D. M. & Lumpkin, E. A. Mammalian touch catches up. *Curr. Opin. Neurobiol.* **34**, 133–139 (2015).

115. Lin, S. Y. & Corey, D. P. TRP channels in mechanosensation. *Curr. Opin. Neurobiol.* **15**, 350–357 (2005).

116. Vandewauw, I. *et al.* A TRP channel trio mediates acute noxious heat sensing. *Nature* **555**, 662–666 (2018).

117. Shin, K. C. *et al.* The Piezo2 ion channel is mechanically activated by low-threshold positive pressure. *Sci. Rep.* **9**, 1–9 (2019).

118. Parpaite, T. & Coste, B. Piezo channels. *Curr. Biol.* **27**, R250–R252 (2017).

119. Coste, B. *et al.* Piezo1 and Piezo2 are essential components of distinct mechanically activated cation channels. *Science (80-.).* **330**, 55–60 (2010).

120. Poole, K., Herget, R., Lapatsina, L., Ngo, H. D. & Lewin, G. R. Tuning Piezo ion channels to detect molecular-scale movements relevant for fine touch. *Nat. Commun.* **5**, 1–14 (2014).

121. Guo, Y. R. & MacKinnon, R. Structure-based membrane dome mechanism for piezo mechanosensitivity. *Elife* **6**, 1–19 (2017).

122. Coste, B. *et al.* Activated Cation Channels. *Science* **330**, 7–12 (2010).

123. Woo, S. *et al.* Piezo2 is required for Merkel-cell mechanotransduction. *Nature* **509**, 622–626 (2014).

124. Ranade, S. S. *et al.* Piezo2 is the major transducer of mechanical forces for touch

sensation in mice. *Nature* **516**, 121–125 (2014).

125. Chesler, A. T. *et al.* The role of PIEZO2 in human mechanosensation. *N. Engl. J. Med.* **375**, 1355–1364 (2016).
126. Szczot, M. *et al.* PIEZO2 mediates injury-induced tactile pain in mice and humans. *Sci. Transl. Med.* **10**, 1–10 (2018).
127. Marshall, K. L. *et al.* PIEZO2 in sensory neurons and urothelial cells coordinates urination. *Nature* **588**, 290–295 (2020).
128. Lacroix, J. J., Botello-Smith, W. M. & Luo, Y. Probing the gating mechanism of the mechanosensitive channel Piezo1 with the small molecule Yoda. *Nat. Commun.* **9**, (2018).
129. Geng, J. *et al.* A Plug-and-Latch Mechanism for Gating the Mechanosensitive Piezo Channel. *Neuron* **106**, 438-451.e6 (2020).
130. Ikeda, R., Ling, J., Cha, M. & Gu, J. G. In Situ Patch-Clamp Recordings from Merkel Cells in Rat Whisker Hair Follicles, an Experimental Protocol for Studying Tactile Transduction in Tactile-End Organs. *Mol. Pain* **11**, (2015).
131. Parpaite, T. & Coste, B. Piezo channels. *Curr. Biol.* **27**, R250–R252 (2017).
132. Maksimovic, S. *et al.* Epidermal Merkel cells are mechanosensory cells that tune mammalian touch receptors. *Nature* **509**, 617–621 (2014).
133. Maricich, S. M., Morrison, K. M., Mathes, E. L. & Brewer, B. M. Rodents rely on Merkel cells for texture discrimination tasks. *J. Neurosci.* **32**, 3296–3300 (2012).
134. Chang, W. *et al.* Merkel disc is a serotonergic synapse in the epidermis for transmitting tactile signals in mammals. *Proc. Natl. Acad. Sci. U. S. A.* **113**, E5491–E5500 (2016).
135. Hoffman, B. U. *et al.* Merkel Cells Activate Sensory Neural Pathways through Adrenergic Synapses. *Neuron* **100**, 1401-1413.e6 (2018).

136. Sonekatsu, M., Gu, S. L., Kanda, H. & Gu, J. G. Effects of norepinephrine and β2 receptor antagonist ICI 118,551 on whisker hair follicle mechanoreceptors dissatisfy Merkel discs being adrenergic synapses. *Mol. Brain* **12**, 10–13 (2019).

137. Koizumi, S. *et al.* Ca2+ waves in keratinocytes are transmitted to sensory neurons: The involvement of extracellular ATP and P2Y2 receptor activation. *Biochem. J.* **380**, 329–338 (2004).

138. Baumbauer, K. M. *et al.* Keratinocytes can modulate and directly initiate nociceptive responses. *Elife* **4**, 1–14 (2015).

139. Tsutsumi, M. *et al.* Mechanical-stimulation-evoked calcium waves in proliferating and differentiated human keratinocytes. *Cell Tissue Res.* **338**, 99–106 (2009).

140. Moehring, F. *et al.* Keratinocytes mediate innocuous and noxious touch via ATP-P2X4 signaling. *Elife* **7**, 1–35 (2018).

141. Sadler, K. E., Moehring, F. & Stucky, C. L. Keratinocytes are required for normal cold and heat sensation. 1–14 (2020).

142. Bjaelde, R. G., Arnadottir, S. S., Overgaard, M. T., Leipziger, J. & Praetorius, H. A. Renal epithelial cells can release ATP by vesicular fusion. *Front. Physiol.* **4 SEP**, (2013).

143. Verkhratsky, A. & Krishtal, O. Adenosine Triphosphate (ATP) as a Neurotransmitter. *Encycl. Neurosci.* **1**, 115–123 (2009).

144. Talagas, M. *et al.* Keratinocytes communicate with sensory neurons via synaptic-like contacts. *Ann. Neurol.* 1–15 (2020). doi:10.1002/ana.25912

145. Hashimoto, K. Fine structure of perifollicular nerve endings in human hair. *J. Invest. Dermatol.* **59**, 432–441 (1972).

146. MONTAGNA, W. & ELLIS, R. A. Histology and cytochemistry of human skin. XII. Cholinesterases in the hair follicles of the scalp. *J. Invest. Dermatol.* **29**, 151–157

(1957).

147. Doppler, K., Werner, C., Henneges, C. & Sommer, C. Analysis of myelinated fibers in human skin biopsies of patients with neuropathies. *J. Neurol.* **259**, 1879–1887 (2012).

148. Nolano, M. *et al.* Cutaneous innervation of the human face as assessed by skin biopsy. *J. Anat.* **222**, 161–169 (2013).

149. Provitera, V. *et al.* Myelinated nerve endings in human skin. *Muscle and Nerve* **35**, 767–775 (2007).

150. Truini, A. *et al.* Differential myelinated and unmyelinated sensory and autonomic skin nerve fiber involvement in patients with ophthalmic postherpetic neuralgia. *Front. Neuroanat.* **9**, 1–7 (2015).

151. Grimalt, R. *et al.* World Congress Hair Research. (2019).

152. Otberg, N. *et al.* Variations of Hair Follicle Size and Distribution in Different Body Sites. *J. Invest. Dermatol.* **122**, 14–19 (2004).

153. Poblet, E., Ortega, F. & Jiménez, F. The arrector pili muscle and the follicular unit of the scalp: A microscopic anatomy study. *Dermatologic Surg.* **28**, 800–803 (2002).

154. Torkamani, N., Rufaut, N. W., Jones, L. & Sinclair, R. D. Beyond goosebumps: Does the arrector pili muscle have a role in hair loss? *Int. J. Trichology* **6**, 88–94 (2014).

155. Purba, T. S. *et al.* Human epithelial hair follicle stem cells and their progeny: Current state of knowledge, the widening gap in translational research and future challenges. *BioEssays* **36**, 513–525 (2014).

156. Renier, N. *et al.* IDISCO: A simple, rapid method to immunolabel large tissue samples for volume imaging, Cell, Supplemental Information. *Cell* **159**, (2014).

157. Kim, S. W., Roh, J. & Park, C. S. Immunohistochemistry for pathologists: Protocols, pitfalls, and tips. *J. Pathol. Transl. Med.* **50**, 411–418 (2016).

158. Renier, N. *et al.* IDISCO: A simple, rapid method to immunolabel large tissue samples

for volume imaging. *Cell* **159**, 896–910 (2014).

159. Azaripour, A. *et al.* A survey of clearing techniques for 3D imaging of tissues with special reference to connective tissue. *Prog. Histochem. Cytochem.* **51**, 9–23 (2016).

160. Wang, J. T., Medress, Z. A. & Barres, B. A. Axon degeneration: Molecular mechanisms of a self-destruction pathway. *J. Cell Biol.* **196**, 7–18 (2012).

161. Canty, A. J. *et al.* In vivo imaging of injured cortical axons reveals a rapid onset form of Wallerian degeneration. *BMC Biol.* **18**, 1–17 (2020).

162. Moll, I. Merkel cell distribution in human hair follicles of the fetal and adult scalp. *Cell Tissue Res.* **277**, 131–138 (1994).

163. Fradette, J., Godbout, M. J., Michel, M. & Germain, L. Localization of Merkel cells at hairless and hairy human skin sites using keratin 18. *Biochem. Cell Biol.* **73**, 635–639 (1995).

164. Kong, Y., Liu, Y., Pan, L., Cheng, B. & Liu, H. Norepinephrine regulates keratinocyte proliferation to promote the growth of hair follicles. *Cells Tissues Organs* **201**, 423–435 (2016).

165. Fan, S. M. Y. *et al.* External light activates hair follicle stem cells through eyes via an ipRGC–SCN–sympathetic neural pathway. *Proc. Natl. Acad. Sci. U. S. A.* **115**, E6880–E6889 (2018).

166. Weddell, G. The pattern of cutaneous innervation in relation to cutaneous sensibility. *J. Anat.* **75**, 346–34667 (1941).

167. English for Writing Research Papers Useful Phrases. 9–16 (2016).

168. Cotsarelis, G., Kaur, P., Dhouailly, D., Hengge, U. & Bickenbach, J. R. Epithelial stem cells in the skin: Definition, markers, localization and functions. *Exp. Dermatol.* **8**, 80–88 (1999).

169. Klusch, A. *et al.* Coculture model of sensory neurites and keratinocytes to investigate

functional interaction: Chemical stimulation and atomic force microscope-transmitted mechanical stimulation combined with live-cell imaging. *J. Invest. Dermatol.* **133**, 1387–1390 (2013).

170. Brownell, I., Guevara, E., Bai, C. B., Loomis, C. A. & Joyner, A. L. Nerve-derived sonic hedgehog defines a niche for hair follicle stem cells capable of becoming epidermal stem cells. *Cell Stem Cell* **8**, 552–565 (2011).

171. Sakaue, M. & Sieber-Blum, M. Human epidermal neural crest stem cells as a source of schwann cells. *Dev.* **142**, 3188–3197 (2015).

172. Marshall, I. C. B. *et al.* Activation of vanilloid receptor 1 by resiniferatoxin mobilizes calcium from inositol 1,4,5-trisphosphate-sensitive stores. *Br. J. Pharmacol.* **138**, 172–176 (2003).

173. Lacroix, J. J., Botello-Smith, W. M. & Luo, Y. Probing the gating mechanism of the mechanosensitive channel Piezo1 with the small molecule Yoda. *Nat. Commun.* **9**, (2018).

174. Gnanasambandam, R. *et al.* GsMTx4: Mechanism of Inhibiting Mechanosensitive Ion Channels. *Biophys. J.* **112**, 31–45 (2017).

175. Lopes, D. M., Denk, F. & McMahon, S. B. The molecular fingerprint of dorsal root and trigeminal ganglion neurons. *Front. Mol. Neurosci.* **10**, 1–11 (2017).

176. Mauvezin, C. & Neufeld, T. P. Bafilomycin A1 disrupts autophagic flux by inhibiting both V-ATPase-dependent acidification and Ca-P60A/SERCA-dependent autophagosome-lysosome fusion. *Autophagy* **11**, 1437–1438 (2015).

177. Villarroya-Beltri, C. *et al.* ISGylation controls exosome secretion by promoting lysosomal degradation of MVB proteins. *Nat. Commun.* **7**, (2016).

178. Cordeiro, J. M., Gonçalves, P. P. & Dunant, Y. Synaptic vesicles control the time course of neurotransmitter secretion via a Ca2+/H+ antiport. *J. Physiol.* **589**, 149–167

(2011).

179. Komoszynski, M. & Wojtczak, A. Apyrases: function and relationshipt o ATPases. **1310**, 233–241 (1996).

180. Kumamoto, J., Goto, M., Nagayama, M. & Denda, M. Real-time imaging of human epidermal calcium dynamics in response to point laser stimulation. *J. Dermatol. Sci.* **86**, 13–20 (2017).

181. Kumar, P. *et al.* Transvascular delivery of small interfering RNA to the central nervous system. *Nature* **448**, 39–43 (2007).

182. Reynders, A. *et al.* Transcriptional Profiling of Cutaneous MRGPRD Free Nerve Endings and C-LTMRs. *Cell Rep.* **10**, 1007–1019 (2015).

183. Ray, P. *et al.* Comparative transcriptome profiling of the human and mouse dorsal root ganglia: An RNA-seq-based resource for pain and sensory neuroscience research. *Pain* **159**, 1325–1345 (2018).

184. Disner, S. G., Beevers, C. G., Haigh, E. A. P. & Beck, A. T. Neural mechanisms of the cognitive model of depression. *Nat. Rev. Neurosci.* **12**, 467–477 (2011).

185. Nakamura, F. & Strittmatter, S. M. P2Y1 purinergic receptors in sensory neurons: Contribution to touch-induced impulse generation. *Proc. Natl. Acad. Sci. U. S. A.* **93**, 10465–10470 (1996).

186. Nagi, S. S. *et al.* An ultrafast system for signaling mechanical pain in human skin. *Sci. Adv.* **5**, 1–11 (2019).

187. Löken, L. S., Wessberg, J., Morrison, I., McGlone, F. & Olausson, H. Coding of pleasant touch by unmyelinated afferents in humans. *Nat. Neurosci.* **12**, 547–548 (2009).

188. Liljencrantz, J. & Olausson, H. Tactile C fibers and their contributions to pleasant sensations and to tactile allodynia. *Front. Behav. Neurosci.* **8**, 6–11 (2014).

189. Fleming, M. S. *et al.* A RET-ER81-NRG1 signaling pathway drives the development of pacinian corpuscles. *J. Neurosci.* **36**, 10337–10355 (2016).

190. Guinard, D., Usson, Y., Guillermet, C. & Saxod, R. PS-100 and NF 70-200 double immunolabeling for human digital skin meissner corpuscle 3D imaging. *J. Histochem. Cytochem.* **48**, 295–302 (2000).

7. APPENDIX

Figure A1. Examples of follicular units obtained with the follicular unit extraction method (FUE) for whole mount immunolabelling. Scale bars

